Developmental Transitions of the Germ Cell Lineage of the Mouse

by

Andrew Edmund Baltus

B.S. Genetics
University of Wisconsin – Madison, 2000

SUBMITTED TO THE DEPARTMENT OF BIOLOGY IN PARTIAL FULFILLMENT OF THE REQIUREMENTS FOR THE DEGREE OF

DOCTOR OF PHILOSOPHY IN BIOLOGY
AT THE
MASSACHUSETTS INSTITUTE OF TECHNOLOGY

SEPTEMBER 2006

Signature of Author _____
Department of Biology
August 31, 2006

Certified by _____
David C. Page
Professor of Biology
Howard Hughes Medical Institute
Thesis Supervisor

Accepted by _____
Steve Bell
Biology Graduate Student Committee

Developmental Transitions of the Germ Cell Lineage of the Mouse

by

Andrew E. Baltus

Submitted to the Department of Biology on August 31, 2006
in Partial Fulfillment of the Requirements for the Degree
of Doctor of Philosophy in Biology

Abstract

Mammalian germ cells arise during early embryogenesis and migrate to the developing gonad where, under the direction of the somatic environment, they initiate distinct sex-specific developmental programs resulting in the production of egg or sperm. Our understanding of the molecular mechanisms governing many stages of germ cell development has advanced greatly in recent years. However, many aspects of germ cell development remain entirely uncharacterized at the molecular level. In this thesis I will present projects utilizing forward and reverse genetics that generate new points of entry into poorly understood transitions during germ cell development.

The X and Y chromosome do not have pairing partners during male meiosis. As a result they become silenced during this time. One mechanism that has been proposed to compensate for inactive X-linked housekeeping genes during male meiosis is X-to-autosome retropositions. We have identified a mutation within an X-to-autosome retrogene in the mouse spermatogenic mutant *jsd/jsd* that provides the first supporting evidence for this model. Evolutionary analysis indicates that since the X and Y chromosome evolved from a pair of autosomes, retroposition of this gene occurred and was maintained independently in several different mammalian lineages, demonstrating a positive selective pressure for this event.

Through targeted disruption of the vertebrate-specific *Stra8* gene, we have generated a point of entry into the study of meiotic initiation in mammals. *Stra8*, which is expressed exclusively in premeiotic germ cells, is required for the initiation of meiosis in mice. In female mice *Stra8* is required after the last mitotic division, but prior to meiotic DNA replication. In *Stra8*-deficient male mice, germ cells arrest at the onset of meiosis, but in a less stringent manner than observed in female germ cells.

Additionally, *Stra8* appears to be required for proper regulation of spermatogonial stem cells, as *Stra8*-deficient male mice undergo gradual germ cell depletion, followed by a high frequency of testicular germ cell tumor formation. Gaining a better understanding of these events in the *Stra8*-deficient mice will provide insight into the regulation of spermatogonial stem cell activity.

Thesis Supervisor: David C. Page
Title: Professor of Biology, Howard Hughes Medical Institute

Acknowledgements

My time at MIT has been a fantastic experience, which I attribute largely to my classmates (many of which have become great friends) and to the people that I have been lucky enough to work with inside and outside of the Page lab. David Page's enthusiasm is what drew me to the Page lab in the first place and is one of the many things that helped keep me motivated throughout the last several years. The Page lab has been an excellent environment during this time and I would like to specifically thank several individuals who had the greatest impact on me. Jeremy Wang and Alex Bortvin provided invaluable guidance while I was getting started. Julie Bradley and Doug Menke began projects that my work continued and their excitement for their own research helped propel my interests. Beyond this the lab was filled with incredibly helpful and friendly individuals too numerous to name, but to whom I am thankful I got to spend the last several years. I will always look fondly on my time at MIT and in the Page lab. Lastly, I would like to thank my wife, Gretchen, whose constant support made even the hardest times of graduate school easy to endure.

Table of Contents

Chapter 1: Introduction	5
Chapter 2: An X-to-autosome retrogene is required for spermatogenesis in mice	58
Chapter 3: A Vertebrate-specific Gene Required for the Initiation of Meiosis in Mice	69
Chapter 4: Spermatogonial Depletion and Testicular Germ Cell Tumor Formation in *Stra8*-deficient Mice	103
Chapter 5: Discussion	135
Appendix 1: Generation and Initial Characterization of a Doxycycline-inducible *Stra8* Mouse	148
Appendix 2: Follicle Formation and Oocyte Growth Occur Independently of Meiotic Progression?	162

Chapter 1

Introduction

In each generation, one cell lineage, the germline, carries with it the DNA that will be passed on to the next generation. This germ lineage must be specified in the early embryo, be prevented from responding to the many surrounding signals that drive somatic differentiation, migrate into the developing gonads, and in a developmentally regulated manner, undergo sex-specific gametogenesis ultimately giving rise to eggs and sperm in female and male animals respectively. During the sex-specific differentiation of gametes, germ cells of both sexes must initiate and properly undergo meiosis, the evolutionarily conserved process that underlies sexual reproduction, even while undergoing very distinct cellular morphogenesis. Our understanding of the molecular processes driving these developmental stages of germ cell biology has grown substantially in recent years, and yet many key events in germ cell development remain poorly understood.

The origin of the germline

For all organisms studied, a small number of cells are specified as primordial germ cells (PGCs) during early embryogenesis. These cells give rise exclusively to germ line cells by clonal mitotic divisions. To date, two distinct methods for germ cell specification have been determined. The first occurs when maternally inherited cytoplasmic determinants become sequestered within a small number of cells of the early embryo, and drive their differentiation into PGCs. The second occurs when the PGCs are specified as the result of inductive signals from their surroundings.

Many of the earliest observations of germ cell specification occurred in species in which the germ line is specified by maternal factors. Studies of frog eggs and early embryos resulted in the identification of cytoplasmic aggregates rich in mitochondria, protein and RNA. These cytoplasmic aggregates were observed to segregate into the PGC precursors during early embryogenesis, and were termed germ plasm (Mahowald and Hennen, 1971). Study of *Drosophila* pole cells, the first cells to be formed in the embryo and located at its posterior pole, contained unique cytoplasmic components rich in germ cell determinants (pole plasm) initially found localized at the posterior pole of the unfertilized egg (Illmensee and Mahowald, 1974). The pole cells are the PGC precursor cells in *Drosophila* and their ability to generate germ cells has been shown to require pole plasm. Similarly, study of the *C. elegans* germ cell lineage demonstrated that cytoplasmic granules (P granules) found in the unfertilized egg were asymmetrically distributed during early embryonic cleavage divisions, such that they became concentrated within the P4 cells which give rise to all PGCs (Strome and Wood, 1982). Additionally, although not as well characterized, the presence of germ cell determinant-rich germ plasm has been indicated in both zebrafish and chicken embryos (Knaut et al., 2000; Tsunekawa et al., 2000). These studies gave rise to the common belief that, for all organisms, germ cells are specified by the localization of maternally inherited cytoplasmic germ cell determinants.

After many years of study, no cytoplasmic aggregate resembling germ plasm could be identified in mice. It was finally demonstrated that mammalian PGCs are specified as the result of inductive signals from surrounding cells(McLaren, 2003). In mice, germ-line-restricted cells (approximately 20-50 cells) can be detected around day 7

of embryonic development (E7) by expression of several germ line specific genes and by alkaline phosphatase (AP) activity (Ginsburg et al., 1990). Although AP is not required for mammalian germ cell development (MacGregor et al., 1995), they maintain a high level of AP activity from the time of their specification until several days after entry into the developing gonad. This AP activity allowed some of the earliest work on murine germ cell specification and migration (Mintz and Russell, 1957; Ozdzenski, 1967). Because AP was not originally detectable until around E8.5, at which time the germ cells predominantly reside in the extraembryonic endoderm, a longstanding misconception arose that the germ cells were specified in this extraembryonic location. Although a more sensitive whole-mount approach later resulted in the detection of AP-positive PGCs within the proximal epiblast as early as E7.25 (Ginsburg et al., 1990), it was not until the mid 90s that the injection of fluorescent dye into single cells from the E6-6.5 epiblast demonstrated that the ancestors of PGCs were derived from the proximal epiblast (Lawson and Hage, 1994). None of the labeled lineages exclusively contained PGCs, as the allantois was also labeled, indicating that the PGC precursors are not yet germ lineage-restricted at E6.5. Although it was clear at this point that PGCs arose from the proximal epiblast, it was not yet clear why only a subset of cells from this region of the epiblast are capable of forming PGCs. Cell transplant experiments demonstrated that environmental factors within the proximal epiblast influenced the fate of these cells (Tam and Zhou, 1996). When clumps of cells from the distal epiblast were transplanted into the proximal epiblast those cells committed to the lineages of the proximal epiblast, including differentiation into PGCs.

In the last several years a greater understanding of the molecular events of mammalian PGC specification has began to come into focus (Figure 1). The observation that mice deficient for *bone morphogenic protein 4* (*Bmp4*) lacked PGCs revealed that BMP signaling is required for germ cell specification (Lawson et al., 1999). It was later demonstrated that the BMP signaling originated from the extraembryonic ectoderm (Yoshimizu et al., 2001). When epiblast explants were cultured adjacent to extraembryonic ectoderm, PGCs were formed, which did not occur in the absence of the extraembryonic ectoderm. Additionally, it was shown that the addition of BMP4 to the culture was sufficient to compensate for the absence of extraembryonic ectoderm (Pesce et al., 2002). We now know that, in addition to *Bmp4*, extraembryonic ectodermal expression of *Bmp8b* also acts on the epiblast during the induction PGCs (Ying et al., 2001). Additionally, activation of ALK2, a type I BMP receptor in the visceral endoderm, by BMP signaling from the extraembryonic ectoderm generates additional signal(s) required for PGC specification (de Sousa Lopes et al., 2004). Targeted disruption of either *Smad1* or *Smad5*, both previously shown to be intracellular transducers of BMP signaling (Heldin et al., 1997; Massague and Chen, 2000; Massague and Wotton, 2000) and expressed by cells of the epiblast at the time of BMP responsiveness, results in impaired PGC formation (Chang and Matzuk, 2001; Tremblay et al., 2001). Interestingly, only a small portion of proximal epiblast cells express both *Smad1* and *Smad5*, and thus may represent the true PGC precursors (Hayashi et al., 2002). In addition to BMP signaling, several genes with germ cell specific expression have been identified. The Pou family transcription factor *Oct4* (also known as *Pou5f1* or *Oct3/4*), which is expressed throughout the epiblast around the time of germ cell specification,

Figure 1: Induction and localization of the PGC precursors in mice. (A) Signals from the extraembryonic ectoderm (green) induce a subset of cell within the epiblast (blue) to become PGC precursors. (B) The PGC precursors, which also differentiate into allantois, upon induction migrate and cluster within the extraembryonic mesoderm. From this cluster lineage-restricted PGCs will emerge by E7.25. (modified from Matsui and Okamura, 2005)

A

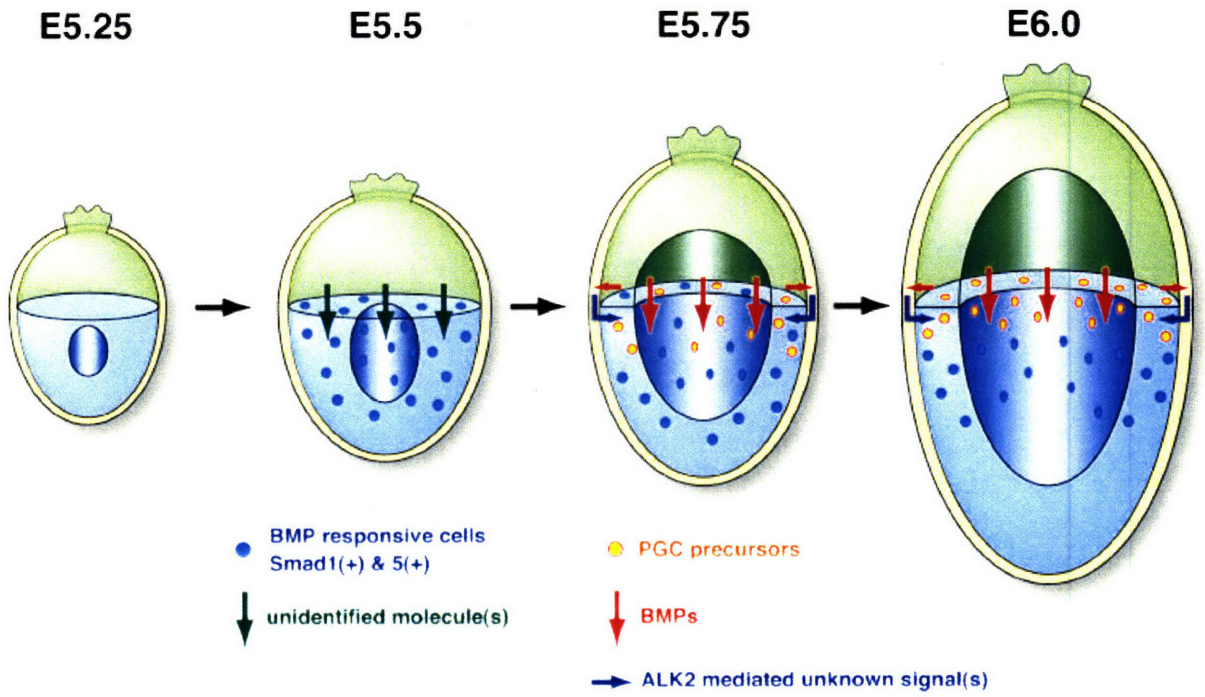
E5.25
E5.5
E5.75
E6.0
BMP responsive cells
Smad1(+) & 5(+)
unidentified molecule(s)
PGC precursors
BMPs
ALK2 mediated unknown signal(s)

B

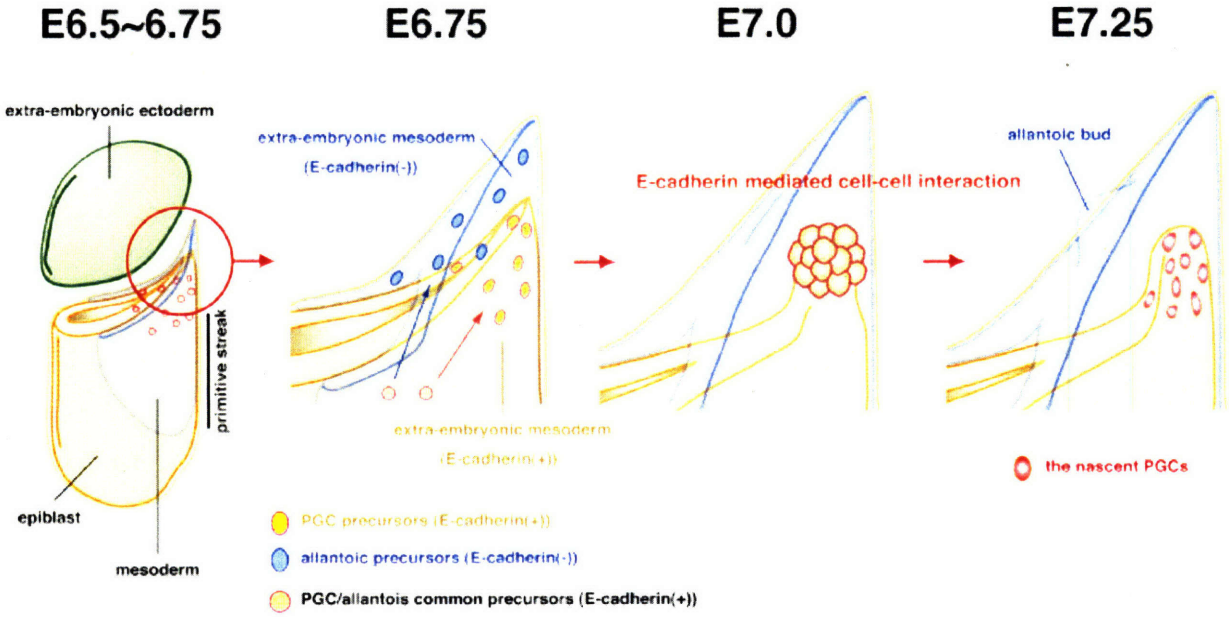
E6.5~6.75
E6.75
E7.0
E7.25
extra-embryonic ectoderm
primitive streak
epiblast
mesoderm
extra-embryonic mesoderm
(E-cadherin(-))
extra-embryonic mesoderm
(E-cadherin(+))
E-cadherin mediated cell-cell interaction
allantoic bud
the nascent PGCs
PGC precursors (E-cadherin(+))
allantoic precursors (E-cadherin(-))
PGC/allantois common precursors (E-cadherin(+))

becomes germ line restricted by E8 (Scholer et al., 1990; Yoshimizu et al., 2001). Additionally, gene expression analysis of PGC precursors and early PGCs has resulted in the identification of two genes with interesting germ-cell-related expression, *Ifitm3* (also known as *Fragilis* and *mil-1*) and *Pgc7* (also known as *Dppa3* and *Stella*) (Saitou et al., 2002; Sato et al., 2002; Tanaka and Matsui, 2002). *Ifitm3* can first be detected in proximal epiblast cells at E6.25 and then becomes restricted to the extraembryonic region, where AP-positive PGCs are found, between E6.5 and E7.2. *Pgc7* is first detected within this *Ifitm3* cluster at E7.2 and appears restricted to the PGCs.

Culture experiments demonstrating the ability of E6.5 but not E6.75 epiblast to generate PGCs and the ability of extraembryonic mesoderm to do so at E6.75 lends further support to the model that upon induction the PGC precursors migrate from the epiblast into the extraembryonic mesoderm where a subset will become germ lineage restricted by E7.2 (Okamura et al., 2003; Yoshimisu et al., 2001). It is possible that the cell-cell interactions that occur within this *Ifitm3*/AP/*Oct4*-positive cluster of extraembryonic PGC precursors results in the final lineage-restriction of PGCs, likely the 40-45 *Pgc7*-positive cells found within the cluster. This model is supported by experiments showing that inactivation of the cell adhesion molecule *E-cadherin,* by culture with an *E-cadherin* specific blocking monoclonal antibody ECCD-1, inhibits the differentiation of PGC precursors into PGCs(Okamura et al., 2003).

Studies of germ cell development in *C. elegans* and *Drosophila* have demonstrated a key role for transcriptional repression in PGC specification and maintenance. In these organisms, general transcription levels are lower in the PGC founder cells, but more specifically, the molecular programs that drive differentiation of

the surrounding somatic cells are repressed (Lamb and Laird, 1976; Seydoux and Fire, 1994; Seydoux et al., 1996; Zalokar, 1976). As the stem cell-like properties of PGCs need to be maintained for them to function properly, it is important that they not be induced to differentiate into somatic lineages. In fact, in mutants that lack this transcriptional repression, the PGCs adopt somatic fates (Seydoux et al., 1996). It has been recently observed in mice that PGC founder cells repress several region-specific homeobox genes, including *Hoxa1*, *Hoxb1*, *Lim1* and *Evx1*, which are highly expressed by the surrounding somatic cells (Saitou et al., 2002). Within the last year a previously characterized transcriptional repressor, *B-lymphocyte-induced maturation protein 1* (*Blimp1*, also known as *Prdm1*), has been shown to be required for this repression in mice (Ohinata et al., 2005; Vincent et al., 2005). 20-25 *Blimp1* positive cells are found within the *Ifitm3* population of PGC precursors at E7.25, and *Blimp1* expression is observed to precede *Pgc7* expression. Targeted disruption of *Blimp1* results in loss of over 90% of PGCs, with the remaining PGCs having clearly aberrant transcriptional profiles. These *Pgc7*-positive, *Blimp1*-deficient PGCs exhibit defects in repression of *Hoxa1* and *Hoxb1*. Some lack expression of other PGC markers such as *Sox2* and *Nanos3*, and more surprisingly, some co-express the usually suppressed Hox genes and the PGC specific transcripts, indicating that *Blimp1* may act to block the inductive signals that drive the differentiation of the somatic cells, which surround the PGCs. Additionally, the fact that mice heterozygous for the *Blimp1* mutation have reduced PGC numbers suggests that PGCs are very sensitive to *Blimp1* levels.

Germ cells actively migrate to the embryonic gonad

In all organisms studied, PGCs are derived from different cell lineages and embryonic locations than the somatic component of the gonad, thus requiring PGCs to migrate to the developing somatic gonad later in embryogenesis (Figure 2) (Nieuwkoop and Sutasurya, 1976; Starz-Gaiano and Lehmann, 2001). One explanation is that the need to limit the number of cell divisions in the germ line requires specification (and often segregation) within the early embryo, while gonad development needs to occur along with the rest of embryonic development.

It has recently been shown that even before PGC specification, attractive and repulsive forces, translated through the interferon-induced transmembrane proteins IFITM1 and IFITM3, result in the migration of the PGC precursors from the epiblast to the extraembryonic mesoderm and also maintain their localization within a small cluster from which lineage-restricted PGCs emerge by E7.25 (Tanaka et al., 2005). This may be in large part because IFITM proteins are part of protein complexes involved in homotypic adhesion (Evans et al., 1990; Deblandre et al., 1995). As mentioned above, the entire epiblast expresses *Ifitm3* beginning around E6.25 with its expression gradually becoming restricted to the PGC precursor cells, which might directly account for the clustering of the PGC precursors in the posterior tip of the proximal epiblast. The PGC precursors within the epiblast begin to express *Ifitm1* at E6.75, as does the proximal epiblast and posterior mesoderm (Tanaka et al., 2005). Subsequent loss of *Ifitm1* expression by PGCs (around E7.5, after PGC specification has occurred) is required for the PGCs to move beyond the *Ifitm1*-expressing primitive streak and mesoderm to the *Ifitm1*-negative posterior endoderm that will give rise to the hindgut by E9.0 (Tanaka et al., 2005; Tam

Figure 2: Germ cell migration in the mouse. (A) After specification the PGCs are found within the extraembryonic mesoderm, near the allantois. During gastrulation the PGCs migrate through the primitive streak and mesoderm into the posterior endoderm where they become incorporated into the hindgut (B). (C) By E9 the PGCs are confined to the hindgut as embryogenesis brings it within closer proximity of the developing gonads. (D) At E9.5 the PGCs begin their migration from the hindgut towards the developing gonads, direction of the white arrows. (E) The PGCs begin to cluster as they approach and colonize the embryonic gonads. Abbreviations: al, allantois; ht, heart; nt, neural tube. (modified from Molyneaux and Wylie, 2004).

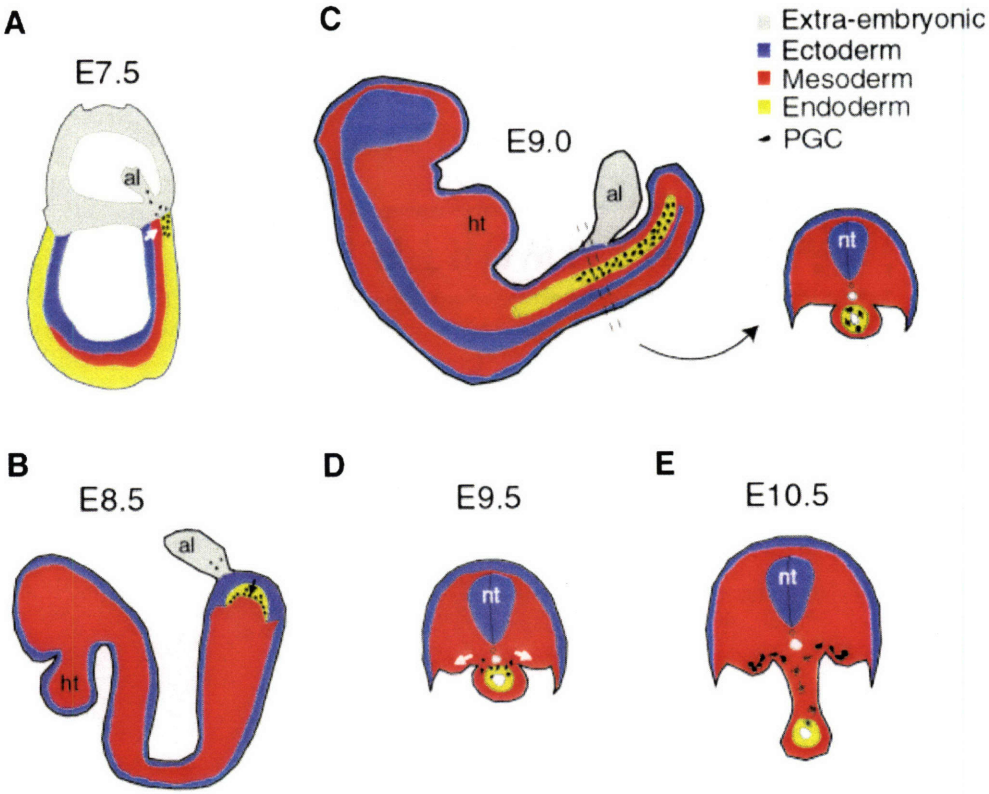
A
E7.5
al
C
E9.0
al
ht
nt
Extra-embryonic
Ectoderm
Mesoderm
Endoderm
PGC
B
E8.5
al
ht
D
E9.5
nt
E
E10.5
nt

and Snow, 1981) (Figure 2A,B). The PGCs then remain restricted to the *Ifitm1*-negative hindgut by the surrounding *Ifitm1*-positive tissues, while embryonic development brings this region into closer proximity of the developing embryonic gonads (Figure 2C) (Tanaka et al., 2005; Tam and Snow, 1981). These data are supported by earlier reports that PGCs at this time can be observed, by time-lapse movie, to be highly motile, but unable to escape the hindgut (Molyneaux et al., 2001). Additionally, the finding that hindgut cells express the adhesion molecule *E-cadherin,* while the PGCs lose *E-cadherin* expression when in the hindgut, explains why they may be observed to move freely within the hindgut, though unable to leave due to the *Ifitm1* repulsion of the surrounding tissue (Bendel-Stenzel et al., 2000).

In addition to the above evidence that may explain the movement and localization of the PGCs within the hindgut, the tyrosine-kinase receptor, *Kit* and its membrane-bound ligand, *Steel Factor* have been shown to be required for PGC survival in the hindgut (Besmer et al., 1993). Mutation of either *Kit*, expressed by PGCs, or *Steel Factor*, expressed by the hindgut, result in dramatic loss of PGCs by E9.5, suggesting a role for *Kit-Steel* interaction in PGC survival. However, abnormal localization of PGCs within the hindgut of a milder *Kit* mutant (W^e/W^e) indicates a possible role for *Kit-Steel* in PGC migration as well as survival (Buehr et al., 1993). In addition to *Kit-Steel* interactions, FGF signaling has been implicated in germ cell development (Matsui et al., 1992; Resnick et al., 1998). Targeted mutagenesis of FGFR2-IIIb has clearly demonstrated that FGF signaling is required to maintain PGC motility and survival of PGCs during migration (Takeuchi et al., 2005).

Around E9.5 the PGCs exit the hindgut, separate into two populations and migrate towards the developing embryonic gonads (Figure 2D). This final migration of the PGCs from the hindgut to the embryonic gonads is completed between E10.5 and E11.5 (Tam and Snow, 1981). The directed migration of the PGCs from the hindgut appears to be the result of secretion of chemotropic factors by the genital ridge (gonads and connected mesonephroi). *In vitro* culture experiments have clearly demonstrated that genital ridge conditioned media, as well as *transforming growth factor beta* (TGFβ) and *stromal derived factor 1* (SDF-1) can act as chemoattractants for PGCs (Godin et al., 1990; Godin et. Al., 1991; Molyneaux et al., 2003). The evidence for SDF-1 is currently the strongest in support of it being a chemoattractant factor governing this migration *in vivo*. The addition of SDF-1 to cultured embryo slices blocks the hindgut to gonadal migration of the PGCs. Additionally, implantation of SDF-1 coated beads into embryo slices results in accumulation of PGCs to the site of insertion (Molyneaux et al., 2003). Mice with mutations in either SDF-1 or its receptor CXCR4 have substantially reduced numbers of PGCs successfully completing the migration into the embryonic gonads (Ara et al., 2003; Molyneaux et al., 2003). The fact that SDF-1 acts in many embryonic locations at this time provides suggestion that a similar caging to that by which *Ifitm1* keeps PGCs in the hindgut may limit the migratory path to the genital ridge (Molyneaux and Wylie 2004).

Upon exit from the hindgut, where the PGCs are not observed to associate with each other, the PGCs are found to connect to each other by thin processes and begin to form clusters of cells by the end of the migration (Gomperts et al., 1994). This clustering has been shown to be *E-cadherin*-dependent (Bendel-Stenzel et al., 2000), suggesting that although PGCs are *E-cadherin*-negative while in the hindgut, they require *E-cadherin* for

proper interaction within the gonad. Further support of the necessity for intracellular communication between PGCs comes from the fact that PGC colonization of the embryonic gonad is impaired in mice lacking the gap-junction protein *Cx43* (Juneja et al., 1999). Although the mechanism remains uncharacterized, PGCs become non-motile upon colonization of the gonad, a process that may be related to the greater PGC-PGC interaction that occurs at this time (Figure 2E).

Development of the somatic gonad

The urogenital system (kidneys, gonads and their duct systems) of mammals arises from the intermediate mesoderm. The genital ridge, a thickening of the ventral surface of the mesonephros, can first be identified starting about E10, shortly before the arrival of the PGCs (Byskov and Hoyer, 1994). This initial development of the gonad is known to require several transcription factors including *Wilms tumor 1* (*Wt1*), *Steroidogenic factor 1* (*Sf1*), *Emx2* and *Lhx9*. Disruption of any of these transcription factors results in degeneration of the gonads in both sexes (Kreidberg et al., 1993; Luo et al., 1994; Miyamoto et al., 1997; Birk et al., 2000). Although initially only a few cell layers thick, the gonad has grown substantially by E11.5, at which time nearly all PGCs have reached and appear to randomly distribute throughout the gonad (Molyneaux et al., 2001). Male and female gonads remain histologically indistinguishable at this time. These bipotential gonads develop normally in germ-cell-depleted mice, indicating that germ cells are not required for this early development of the gonad (Merchant, 1975). During the next few days (E11.5-13.5) no obvious morphological changes occur in the female gonads. During the same time period, the somatic cells of the male gonad initiate

a massive reorganization in which the germ cells are enclosed within testicular cords. The formation of testicular cords provides the first morphologically observable difference between male and female gonads (testis and ovary respectively). The cords contain the germ cells as well as Sertoli cells, which act as supporting cells for the germ cells throughout spermatogenesis, after initiating testis development.

Beginning around E10.5, the Y-linked gene *Sry* is expressed by a subset of cells within the XY genital ridges (Gubbay et al., 1990; Koopman et al., 1990; Sinclair et al., 1990). These *Sry*-positive cells have since been definitively shown to be the Sertoli cells (Albrecht and Eicher, 2001). Expression of *Sry* sets in motion the masculinization of the bipotential gonad, thus resulting in the formation of testes in XY mammals. Conversely, feminization of the XX gonad is often referred to as the default pathway, as it only occurs in the absence of *Sry*. In fact, observed expression of an *Sry* promoter-driven GFP transgene in a subset of cells within XX embryonic gonads (presumably the same cells that would become Sertoli cells in the presence of *Sry*) demonstrated that mechanisms that initiate *Sry* expression are independent of chromosomal sex (Albrecht and Eicher, 2001). Several genes, including *Dax1*, *Foxl2* and *Wnt4*, have been suggested as candidate *Sry*-like "master regulator" of ovarian development, however, null mutations of any of these genes in mice do not cause female to male sex-reversal (Yu et al., 1998; Vainio et al., 1999; Schmidt et al., 2004; Uda et al., 2004). It is interesting to note here that although it has been known for decades that the Y chromosome generates a dominant testis-determining function (i.e., *Sry* expression), the mechanisms governing *Sry* expression as well as those governing ovarian development remain completely unknown,

and in fact it remains unclear exactly how *Sry* and its downstream effectors function to drive testis development.

Testis development, including expression of *Sry* and testicular cord formation, does not require the presence of germ cells (Handel and Eppig, 1979; Mintz and Russell, 1957). In germ-cell-deficient mice, testis differentiation proceeds with only a slight delay, generating adult testes that can function as recipients for wild-type spermatogonial stem cells by transplantation, fully supporting spermatogenesis (Brinster and Avarbock, 1994). It has been hypothesized that XY gonads need to block germ cells from initiating meiosis as meiotic germ cells have been shown to antagonize testicular development. Testis-specific developmental processes including mesonephric cell migration and testis cord formation can be induced in XX gonads prior to, but not after, germ cells enter meiosis (Tilmann and Capel, 1999; Yao et al., 2003).

Histologically, embryonic ovaries do not undergo obvious structural organization until late embryogenesis. Around birth, granulosa cells organize around and become tightly associated with individual oocytes, forming follicles. The follicles form the predominant structural feature of the ovary, similar to the cords of the testis. Although *Sry* can act dominantly to induce testis development of an XX gonad, it has been suggested that ovarian development also must be an active process (Eicher and Washburn, 1986). The molecular trigger for ovarian development has not yet been identified, but several ovary-expressed genes have been shown to antagonize testicular development (reviewed in Brennan and Capel, 2004). The expression of two female-specific genes, *Bmp2* (Yao et al., 2004) and *Follistatin* (*Fst*, Menke and Page, 2002) is absent in XX gonads deficient for another female-specific gene, *Wnt4*. *Wnt4* has been

shown to have anti-testis activities. XX gonads deficient for *Wnt4* lose their germ cells, followed by expression of male markers and development of cord-like structures (Vainio et al., 1999). Additionally, *Wnt4*-deficient XX gonads develop the testis-specific coelomic vessel, which can be disrupted in XY gonads by ectopic expression of *Wnt4* (Jeays-Ward et al., 2003; Jordan et al., 2003).

Unlike what is seen for testis development in male mice, in germ-cell-deficient female mice, follicles do not form and instead of an ovary the gonad becomes what is referred to as a "streak gonad" predominantly composed of fibrous connective tissue (McLaren, 1984). Additionally, if germ cells are lost after follicles form, the follicles rapidly degenerate (Behringer et al., 1990; Couse et al., 1999). This demonstrates that ovarian development is dependent upon the presence of germ cells, and possibly specifically upon the presence of meiotic germ cells (oocytes).

Germ cell entry into the embryonic gonad

During their migration from the proximal epiblast to the embryonic gonads mammalian PGCs are proliferative, increasing in number from approximately 10-100 and ending with greater than 1500 PGCs entering each gonad (reviewed by McLaren, 1981). The PGCs continue to proliferate upon entering the gonad until around E13.5. During this time male and female PGCs remain morphologically indistinguishable (McLaren and Southee, 1997). Upon entry of the PGCs into the embryonic gonad they begin to express several germ-cell-specific genes. These include *germ cell nuclear antigen 1* (*Gcna1*), *mouse vasa homolog* (*Mvh*) and *germ cell-less* (*Gcl*) (Enders and May, 1994; Toyooka et al., 2000; Kimura et al., 1999). The gene coding for *Gcna1* has not yet been identified;

Mvh and *Gcl* have been knocked out with no apparent phenotype in embryonic germ cells (Tanaka et al., 2000; Kimura et al., 2003). At this same time the gene *deleted in azoospermia-like* (*Dazl*) becomes expressed in both male and female PGCs (Seligman and Page, 1998), and is required for survival of male and female germ cells embryonically (Cooke 1996; Lin and Page, 2005; Lin, personal communication). *Dazl* will be discussed more in later discussions of germ cell sex determination.

In addition to these sex non-specific changes in motility, morphology and gene expression upon gonadal entry, several epigenetic changes take place in the PGCs at this time. Coincident with entry into the gonad, methylation marking maternally and paternally imprinted genes is actively removed (Hajkova et al., 2002). Later during gametogenesis sex-specific epigenetic patterns are re-established. This re-establishment occurs prior to meiosis in male germ cells, and during late stages of oocyte development in females (Hajkova et al., 2002; Coffigny et al., 1999). It is currently unknown if this sex-specific timing of re-methylation plays a developmentally important role. It is however known that the patterns of methylation are distinct between the male and female gametes. This epigenetic reprogramming, unique to the germ cells, acts to remove previous maternal and paternal imprinting so that the generated gametes (ova and sperm) will possess only their properly associated sex-specific imprints, which is thought to be required for totipotency of the preimplantation embryo. Recent work has demonstrated that this imprinting is also required to prevent parthenogenesis (the development of the ova into a new individual without fertilization by a sperm), thus acting as a key component to developmental regulation (Kono et al., 2004). Additionally, this reprogramming would serve to remove any epimutations that have arisen prior to this

time in germ cell development. A recent study has demonstrated that inheritance of uncorrected epimutations in mice can result in specific disease phenotypes or susceptibilities (Rakyan et al., 2001).

In addition to the removal of epigenetic modifications, it is also important that the inactive X-chromosome, in XX PGCs, be reactivated at this time. Like somatic cells, XX PGCs establish an inactive X-chromosome during early embryogenesis (McMahon et al., 1981), however both X chromosomes are active during oogenesis due to reactivation of the inactive X upon entry into the gonad (McLaren and Monk, 1981; Tam et al., 1994; Nesterova et al., 2002). This X-reactivation is only logistically sex-specific as XXY germ cells undergo reactivation of their inactive X-chromosome upon entry into an embryonic testis (Mroz et al., 1999).

Germ cell sex is determined by cellular environment

In mammals, germ cell sex has been defined operationally, with no understanding of the molecular processes regulating this developmental decision (Figure 3). PGCs in embryonic testis are considered to become male-sex-determined when they enter a G_0/G_1 cell cycle arrest around E13.5, which they maintain until after birth when they return to a proliferative state, become spermatogonial stem cells and begin populating the testis in preparation for spermatogenesis. PGCs in embryonic ovaries are considered to become female-sex-determined when they enter prophase of meiosis I. Germ cell sex is not determined by sex chromosome constitution but rather by the germ cell microenvironment. Several lines of evidence, including study of ectopic germ cells, XX/XY chimeric mice and *in vitro* tissue co-culture support this conclusion. Primordial

Figure 3: Cartoon depicting early male and female sexual dimorphism in gonad development beginning around the time that PGCs enter the bi-potential gonad.

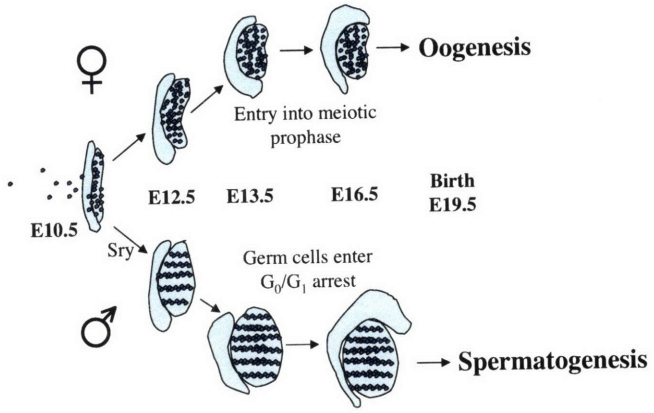
♀
Oogenesis
Entry into meiotic prophase
E10.5
E12.5
E13.5
E16.5
Birth
E19.5
Sry
Germ cells enter
G_0/G_1 arrest
♂
Spermatogenesis

germ cells that fail to migrate into the gonad are referred to as ectopic germ cells. Ectopic XY germ cells found in the adrenal glands have been observed to enter meiosis and develop into oocytes, on a similar timeline to XX germ cells in embryonic ovaries (Zamboni and Upadhyay, 1983), indicating that they are not predetermined to become male gametes. These findings have been furthered by *in vitro* co-culture experiments in which XX or XY germ cells from E11.5 embryonic gonads co-cultured with embryonic lung tissue enter meiosis (McLaren and Southee, 1997). Interestingly, however, XY germ cells isolated from E12.5 (or later) embryonic testis developed as prospermatogonia while XX germ cells isolated from embryonic ovaries of the same ages enter meiosis. Likewise, if XY germ cells are isolated from embryonic testis at E12.5 (or later) and placed into reconstituted embryonic ovarian tissue or grown on a monolayer of feeder cells they develop as prospermatogonia (Adams and McLaren, 2002; Nakatsuji and Chuma, 2001) and thus have lost the potential to be feminized. Similar experiments designed to test the ability of embryonic testes to masculinize XX germ cells demonstrated that E11.5 and E12.5 XX germ cells would develop as male prospermatogonia if placed into reconstituted embryonic testes (Adams and McLaren, 2002). However, by E13.5 the majority of XX germ cells are unable to be masculinized by a testicular environment, presumably since they have committed to meiosis by this time. Together these data indicate that germ cells in the embryonic testis are male-sex-determined by E12.5 and germ cells in the embryonic ovary are female-sex-determined by E13.5. Studies of XX/XY chimeric mice support these conclusions. XX germ cells that are found in a testicular environment develop as prospermatogonia (Palmer and Burgoyne, 1991). Additionally, although unable to complete spermatogenesis due to the

requirement for Y chromosome genes (Mazeyrat et al., 2001), XX germ cells in XX sex-reversed mice initiate male development (McLaren, 1981). In studies of XX-XY chimeras in which XY germ cells are found in the embryonic ovaries, they enter meiosis and develop as oocytes (McLaren, 1984). This ability of XY germ cells to undergo oogenesis is also observed in models of XY sex-reversal (Taketo-Hosotani et al., 1989). The conclusion from these studies is that between E12.5 and E13.5 most germ cells within an ovarian environment become female-sex-determined and those within a testicular cord become male-sex-determined.

To date, there is no molecular definition germ cell sex determination, other than to say that they no longer can be coaxed to undergo sex-reversal. As stated above, the hallmark used to define this sexual commitment event is the initiation of meiosis in the female and the onset of the G_0/G_1 arrest as prospermatogonia in males. It is important to acknowledge here that there must be a decision point prior to the observation of either of these sexually committed states during which the germ cells respond to their environment, and currently no data exist to address this issue. In fact, it is commonly believed that the initiation of meiosis occurs based upon a clock mechanism within the germ cells, and that there is a factor generated by the testis that overrides this clock, resulting in the observed mitotic arrest (reviewed by McLaren, 2000). Recent work in our lab, which builds upon work I will present in this thesis and which will be described in the discussion, has now provided molecular evidence that begins to address how this germ cell sexual commitment occurs in male and female mice (Koubova et al., 2006).

Stra8 is the earliest identified marker of female germ cell sex determination

The *stimulated by retinoic acid gene 8* (*Stra8*) has recently been established as a molecular marker of female germ cell sex differentiation (Menke et al., 2003) and is, to date, the earliest such example. *Stra8* is expressed by PGCs within an ovary but not a testis beginning at E12.5, approximately one day before they are observed histologically to be in meiosis and about the time that they begin to lose the ability to undergo female-to-male sex reversal if placed in a testicular environment (McLaren and Southee, 1997). *Stra8* expression is germ-cell-specific and appears in an anterior to posterior wave beginning at E12.5 and ending around E16.5, which encompasses the E13.5-15.5 window during which female germ cells are observed histologically to have entered meiotic prophase (Peters, 1970; Peters et al., 1962). Since this observation, it has been shown that several meiotic markers including the synaptonemal complex protein, *Scp3*, a marker of DNA double strand break formation, gamma-H2AX, and the meiosis-specific recombinational repair protein, *Dmc1* all appear in a germ-cell-specific anterior-to-posterior wave similar to that of *Stra8*, but beginning at least a day later (Menke et al., 2003; Yao et al., 2003; Bullejos and Koopman, 2004). In addition to *Stra8* being an ideal candidate for further study of female germ cell sex determination, the observed anterior-to-posterior wave of meiotic markers is at odds with the previous model that meiotic initiation occurs cell autonomously around this time. It has been observed that PGCs enter the embryonic gonads in a random manner, and rapidly become non-motile, suggesting that this anterior-posterior wave could not be established by the order in which the germ cells enter the gonad (Molyneaux et al., 2001). Although the predominant model is one in which a meiosis-inhibiting substance blocks the initiation of meiosis by testicular germ cells (McLaren and Southee, 1997), it has been suggested that

embryonic ovaries possess a meiosis-stimulating activity (Byskov and Saxen, 1976). However, due to the identification of meiotic germ cells in ectopic locations such as the embryonic adrenal gland and the mesonephros as well as those observed in lung reaggregates in culture, acceptance of a meiosis-inducing substance requires the presence of this substance in these diverse locations as well (McLaren, 1984; McLaren and Southee, 1997; Zamboni and Upadhyay, 1983). My data combined with other recent observations from our lab has begun to shine some light on this topic, which will be addressed in later chapters of this thesis.

The PGCs enter the embryonic gonads while still expressing several genes commonly used as markers of pluripotency. These include *Oct3/4*, *Nanos*, and *Dppa3/Stella* (Saitou et al., 2002;Bowles et al., 2003). When observed by whole-mount *in situ* hybridization it has become clear that expression of several of these markers is lost in a similar anterior-to-posterior wave to that of *Stra8* and the other meiotic markers (Menke et al., 2003; Bellejos et al., 2004). Interestingly, the expression of these pluripotency markers is retained by male germ cells throughout embryonic development and is maintained in the premeiotic cells of the adult testis (Lin and Page, 2005).

Male and female germ cell sex determination and *Stra8* expression requires *Dazl*

As mentioned above, *Dazl* becomes expressed sex-non-specifically by the germ cells shortly after entry into the embryonic gonads (Lin and Page, 2005; Lin, personal communication). Initial characterizations of *Dazl*-deficient mixed background mice resulted in little characterization of the role for *Dazl* in embryonic germ cells (Ruggiu et al., 1997; Schrans-Stassen., 2001; Saunders et al., 2003). More recently the *Dazl*

deficiency allele has been backcrossed onto a C57BL/6 background. This pure strain background reveals an earlier requirement for *Dazl* in germ cells than had previously been reported. Both ovarian and testicular germ cells undergo a developmental arrest around E12.5, the time at which the germ cells undergo sexual determination. In fact, germ cells in *Dazl* mutant C57BL/6 mice appear to arrest in a sexually undifferentiated state indicated by their nuclear morphology and lack of male or female sexual differentiation (Lim and Page, 2005; Lim, personal communication). Ovarian germ cells deficient for *Dazl* do not down-regulate markers of pluripotency (*Oct4* and *Dppa3/Stella*) or up-regulate *Stra8* or markers of meiosis (*Dmc1*, γH2AX and SCP3). *Dazl*-deficient ovaries become germ-cell-depleted around the time of birth. Testicular *Dazl*-deficient germ cells are not observed to initiate the male-specific G_0/G_1 arrest (based on nuclear morphology) but are observed to undergo apoptosis prior to birth. These observations indicate that *Dazl* is required for male and female germ cell sexual differentiation. Microarray analysis comparing *Dazl*-deficient ovaries to wild-type littermates confirms that *Dazl* is required upstream of meiosis and for the down-regulation of many pluripotency markers in female germ cells (Gill, personal communication). Several genes have been identified by this analysis that do not fit either of these categories and they are currently being analyzed with the hope of gaining a better understanding of the role that *Dazl* plays during female germ cell sex determination. Although similar analysis has not been performed on the *Dazl*-deficient embryonic testes, it is known that *Dazl*-deficient testicular germ cells fail to undergo the embryonic *de novo* methylation required as part of the epigenetic reprogramming discussed earlier (Hu, personal communication).

Meiotic initiation and prophase progression

Nearly all eukaryotic organisms, from yeast to humans, reproduce sexually. The cornerstone of sexual reproduction is the ability of a diploid cell to produce haploid gametes (or spores) that have exchanged genetic material between homologous chromosomes. It is during meiosis, a highly specialized cell cycle found in all sexually reproducing organisms, that these events occur. Meiosis differs most notably from mitosis due to consecutive divisions without an intervening S-phase, resulting in the reduction of diploid chromosome content to haploid, thus compensating for the genome doubling that occurs at fertilization. Molecular events of the first meiotic prophase ensure that the chromosomes are properly segregated during the proceeding meiotic divisions, and that genetic material is exchanged between homologous chromosomes. For meiosis to succeed the genome needs to be replicated, homologous chromosomes must find each other, align along their length, initiate DNA double strand breaks (DSB), form synaptonemal complexes (synapse), and complete recombination all during the prophase of meiosis I and all while the chromosomes are becoming progressively more condensed. An overview of cohesin and synaptonemal complex formation is presented in Figure 4. The flawless completion of these events is vital to meiotic progression and fertility for all sexually reproducing organisms

The molecular mechanisms governing meiotic initiation have been characterized in both *S. cerevisiae* and *C. elegans* (Figure 5). In *S. cerevisiae* nutrient starvation results in the activation of the transcription factor *IME1* and the protein kinase *IME2*, which together induce meiotic initiation (reviewed(Honigberg and Purnapatre, 2003)). In *C.*

Figure 4: (A) Cartoon of cohesion and synaptonemal complex formation during premeiotic S-phase and the early stages of prophase of meiosis I. (B) Photomicrographs of cohesin and synaptonemal complex formation in oocytes as they progress into meiotic prophase (modified from *Chromosome Research* **12**: 197-213, 2004)

A

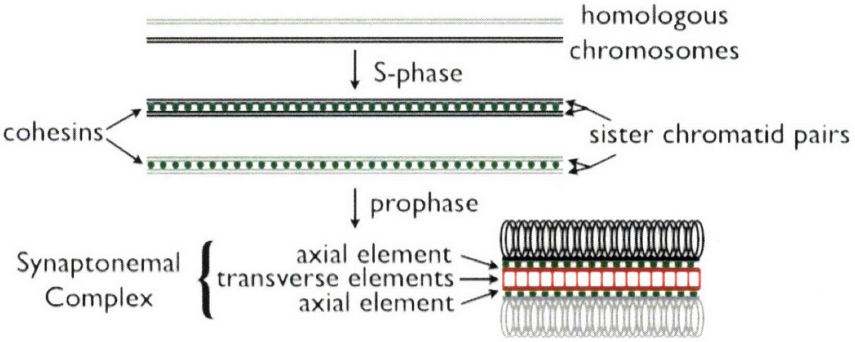
homologous
chromosomes
S-phase
cohesins
sister chromatid pairs
prophase
Synaptonemal
Complex
axial element
transverse elements
axial element

B

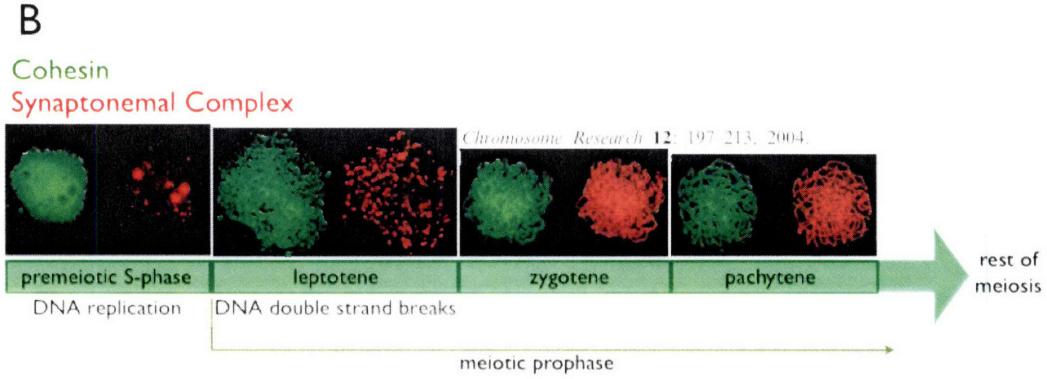
Cohesin
Synaptonemal Complex
premeiotic S-phase
leptotene
zygotene
pachytene
rest of
meiosis
DNA replication
DNA double strand breaks
meiotic prophase

Figure 5: Cartoon of the cell cycle as it relates to the transition from mitosis to meiosis. Below is listed the pathway regulating the initiation of meiosis in budding (*S. cerevisiae*) and fission yeast (*S. pombe*).

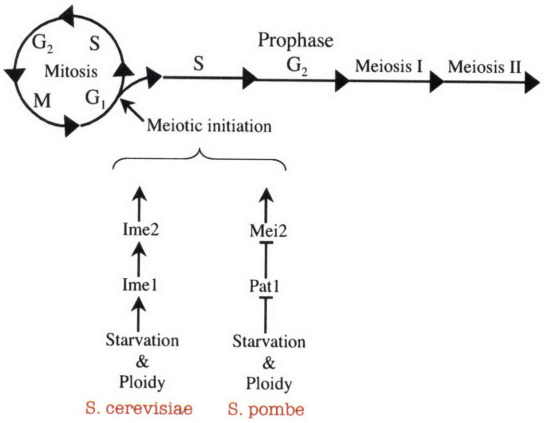
G2
S
Mitosis
M
G1
S
Prophase
G2
Meiosis I
Meiosis II
Meiotic initiation
Ime2
Ime1
Starvation
&
Ploidy
S. cerevisiae
Mei2
Pat1
Starvation
&
Ploidy
S. pombe

elegans the transition from mitosis to meiosis is regulated by the somatic distal tip cell (DTC), which produces the LAG-2 ligand that binds the GLP-1 receptor on germ cells continuing mitotic proliferation. When the GLP-1/Notch signaling pathway is not activated (LAG-2 is not detected), GLD-1 and GLD-2 accumulate, driving entry into the meiotic cell cycle (reviewed(Hansen et al., 2004)). Although both the IME1/IME2 and GLP-1/Notch pathways are well understood in yeast and nematodes respectively, the mechanisms regulating this transition have not been elucidated for any vertebrate species. There does not appear to be a single evolutionarily conserved mechanism for regulating the early meiotic events for sexually reproducing organisms. In fact, the unique tissue environment and developmental state during which germ cells initiate meiosis in each organism would be consistent with highly divergent mechanisms regulating this transition. Therefore, to gain an understanding of how mammalian germ cells initiate the transition from mitosis to meiosis, we will need to characterize genes and mechanisms that have evolved along with the unique environment of mammalian meiosis.

In mammals, the timing of meiotic initiation differs greatly between the sexes. Female germ cells initiate meiosis embryonically, arresting near the end of meiotic prophase and finally completing gametogenesis in the adult ovary. At the same time in gestation that female germ cells initiate meiosis, male germ cells enter a G_0/G_1 cell cycle arrest, which is maintained until after birth. Shortly after birth, the male germ cells are released from this arrest and become a spermatogonial stem cell population. These spermatogonial stem cells, through multiple rounds of mitotic division, give rise to a population of spermatocytes, which undergo meiosis. Additionally, the process of spermatogenesis results in constant production of spermatocytes such that cells entering

meiosis can be found at any time during the reproductive life of the male. The striking differences in gonad structure and timing of meiotic initiation between female and male mammals raises a question as to whether a unique mechanism would be required to regulate this transition for each sex.

Spermatogenesis

As mentioned above, male germ cells become sex determined around E13.5 when they are observed to undergo a G_0/G_1 arrest, at which time they are referred to as prospermatogonia. Although they remain arrested until birth, we know that during this time they are actively methylating their DNA to establish the male-specific imprinting that is required for embryonic development (reviewed in Allegrucci et al., 2005). Around the time of birth the prospermatogonia will return to a proliferative state and will transition into A_s (A-single) spermatogonia, the testicular stem cells that maintain spermatogenesis throughout the reproductive life of the animal. All non-stem cell progeny from a single A_s division remain connected to each other by cytoplasmic bridges throughout their development, thus progressing as a synchronized population of cells. Spermatogenesis is a tightly regulated process, which has been very well characterized in the mouse (Bellve et al., 1977; Eddy et al., 1991). Even though a cross section of any given testicular tubule will have many stages of spermatogenic cells in it, the same stage cells will always be found together. This allows the definition of each stage of tubule cross-section. Spermatogenic cells have been classified into four categories; spermatogonia, spermatocytes, spermatids and spermatozoa. All pre-meiotic cells are called spermatogonia; these include the stem cells as well as those that have become

committed to terminal differentiation. Upon the initiation of meiosis, testicular germ cells are called spermatocytes, and the post-meiotic haploid cells are called spermatids. Finally, the mature gametes are called spermatozoa or sperm. The stages of spermatogenesis in the mouse were originally described by Oakberg (1956a; 1956b) (Figure 6). Around birth, the testis contains only undifferentiated type A_s spermatogonia, which in addition to repopulating themselves, give rise to A_{pr} (A-paired) spermatogonia which then divide 1-3 times to give rise to A_{al} (A-aligned$_{4\text{-}16}$) spermatogonia. These early spermatogonial divisions can occur in any stage tubule, and are likely regulated by cell density within the tubules. In a stage-specific manner A_{al}, in chains of 4 to 16, transition into A_1 spermatogonia, which undergo a series of highly reproducible mitotic divisions resulting in the formation of A_2, A_3, A_4, A_{im} (A-intermediate) and finally B spermatogonia. The B spermatogonia divide to produce preleptotene (or premeiotic) spermatocytes for the first time about 7-8 days after birth. These spermatocytes rapidly progress into the leptotene stage of meiotic prophase I (Nebel et al., 1961). The earliest postmeiotic cells, round spermatids, are first observed about 20 days after birth (Nebel et al., 1961). During the next 2 weeks, the round spermatids differentiate into elongating spermatids in which the sperm tail forms and the nucleus condenses. At the end of this process, morphologically mature sperm are released into the fluid-filled lumen of the tubule.

Oogenesis

Around E12.5 the oogonia (premeiotic germ cells within the embryonic ovary) have undergone their last mitotic division. At this point, the female has all of the oogonia that

Figure 6: (Top) Cartoon showing division and amplification of spermatogenic cell types including the premeiotic spermatogonia, the meiotic spermatocytes and the post-meiotic spermatids. (Bottom) Photomicrographs of Hematoxylin and Eosin stained testicular tubule with various spermatogenic stages highlighted in different colors.

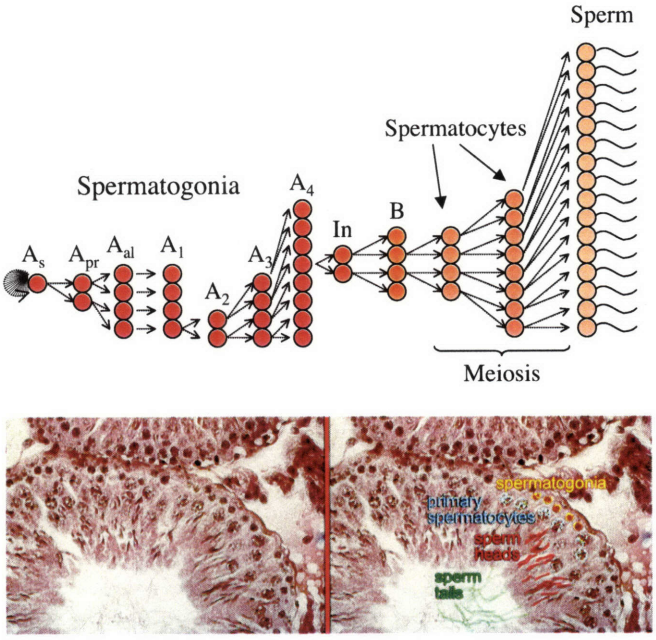
Sperm
Spermatocytes
Spermatogonia
A_4
B
In
A_s
A_{pr}
A_{al}
A_1
A_2
A_3
Meiosis
spermatogonia
primary spermatocytes
sperm heads
sperm tails

she will ever have; the total number is somewhere between 30,000 and 75,000 in mice (reviewed by McLaren, 2000). All of the oogonia progress into meiosis over the next few days, and around birth will all have reached the diplotene stage of prophase of meiosis I. At this point, the oocytes become arrested and remain quiescent until sexual maturation. Beginning shortly before birth, granulosa cells begin to organize around the oocytes. The granulosa-encircled oocyte is referred to as a primordial follicle. The organization of granulosa cells around the oocyte requires expression of the helix-loop-helix transcription factor *Figα* (also called *Figla*) by the oocyte (Soyal et al., 2000). Although it is clear that *Figα* is required for this initial follicle formation, it remains unknown by what mechanism *Figα* functions in the recruitment of granulosa cells.

With the onset of puberty, the ovaries become activated by hormone stimulation, and every 4 days, a new group of primordial follicles (6-16 in mice, depending on strain) are stimulated to proceed toward ovulation. This cohort of primordial follicles become primary follicles, which are marked by the granulosa cells becoming cuboidal, and become committed to the subsequent stages of follicle development. The mechanism for selecting and activating primordial follicles is not known, but it likely requires a fine balance between inhibitory and stimulatory factors as it is important to stimulate enough follicles to ensure fertility, but few enough that the female remains fertile for a substantial percentage of her life.

Unlike in the male, where there is little or no evidence that the germ cells have any effect on somatic development, the oocytes both initiate follicle formation and play an active role in follicle maintenance and maturation throughout oogenesis. Follicles require expression of the oocyte-specific gene *growth differentiation factor 9* (*Gdf9*), a member

of the TGFβ family, to mature beyond the primary follicle stage. Targeted disruption of *Gdf9* results in the somatic follicle cells being unable to mature beyond the primary follicle stage, but has no effect on the recruitment of primordial follicles to become primary follicles (Dong et al., 1996). In addition to *Gdf9*, the cross-talk between the oocyte and the somatic follicle cells utilizes the *Kit-Steel* interaction mentioned previously. The oocytes express the receptor *Kit*, while the follicle cells express the ligand *Steel Factor*. Further evidence for oocyte-granulosa communication comes from data that the oocyte can directly effect the levels of *Steel Factor* produced by the granulosa cells, likely through *Gdf9* (reviewed Eppig, 2001). Although other factors, known and unknown, play a role in the complex interactions of the maturing oocyte/follicle complex, it is important to note here that the oocyte itself is directly involved in the entire process.

During the primary follicle stage, the granulosa cells begin to proliferate, and once two or more layers of granulosa cells surround the oocyte the follicle becomes preantral. At this stage, the oocyte begins an extensive growth phase coincident with a dramatic increase in RNA and protein synthesis as well as an increase in the number of ribosomes, mitochondria and other cellular organelles. Also during this stage, the granulosa cells become highly proliferative and a layer of theca cells develops around the follicle. The zona pellucida, a protective coat that forms around the plasma membrane of the oocyte and is required for oocyte survival and fertilization, forms during this stage (Oehninger, 2003). *Figα* is directly required for expression of the zona pellucida genes encoding the glycoproteins ZP1, ZP2 and ZP3. The granulosa cells form gap junctions with the oocyte via processes that pass through the zona pellucida (Anderson and Albertini, 1976).

Connexin proteins form these gap junctions, including *Connexin-37* that is expressed specifically by the oocyte (Goodenough et al., 1999; Amleh and Dean, 2002). The formation of a fluid filled cavity (antrum) within the follicle marks the transition from preantral to antral follicle. During this transition the oocyte gains the competence to resume meiosis (Hecht, 1998). It is also at this time that the epigenetic reprogramming mentioned earlier is completed by the methylation of DNA in a female-specific pattern (Hiura et al., 2006).

Growth and development of antral follicles requires follicle-stimulating hormone (FSH) as well as the zona pellucida proteins ZP2 and ZP3 (Kumar et al., 1997; Dierich et al., 1998; Zhao and Dean, 2002). The follicle's dependence on FSH begins when it reaches a certain size (preovulatory follicle); this marks the beginning of a feedback loop required for selection of a limited number of the most advanced oocytes for ovulation. The increase in theca cell numbers, as the antral follicle grows in response to FSH, results in increased levels of estrogen (theca-derived androgen is converted into estrogen by the granulosa cells). In response to the increased estrogen, the theca cells make more LH receptors. As the theca cells become more sensitive to the LH they generate more androgen, which results in increased estrogen, which in turn results in reduced FSH levels. This positive feedback loop causes LH to spike sharply, and causes all but the largest preovulatory follicles to undergo atresia. This LH surge releases the oocytes within remaining dominant follicles from their prophase I arrest and induces ovulation. The first meiotic division, which results in formation of the first polar body, occurs just prior to release from the ovary. Meiosis II begins immediately but arrests at metaphase until fertilization, which triggers completion of the second meiotic division and the

formation of the second polar body. During each cycle, another cohort of primordial follicles is stimulated to undergo maturation and ovulation.

Points of entry into the study of germ cell development

Much of our knowledge of mammalian germ cell development has come from histological and morphological observations. Molecular study of germ cell development in mammals has been largely limited due to a small number of identified points of entry. A predominant source of such entry points has come from analysis of genes in mammals whose importance had been documented in more genetically tractable organisms (such as yeast, worms and flies). This approach has proven useful for gene families that are highly conserved in either sequence or structure throughout eukaryotic evolution and has proven particularly useful, for instance, in characterizing the meiotic machinery. More recently, comparative gene expression approaches have begun to generate lists of genes with interesting expression patterns during specific stages of germ cell development. These varying approaches have dramatically increased the number of stages of germ cell development for which we now have markers and candidate genes, however there remain many stages about which we know little or nothing.

References

Adams, I. R., and McLaren, A. (2002). Sexually dimorphic development of mouse primordial germ cells: switching from oogenesis to spermatogenesis. Development 129, 1155-1164.

Albrecht, K. H., and Eicher, E. M. (2001). Evidence that Sry is expressed in pre-Sertoli cells and Sertoli and granulosa cells have a common precursor. Dev Biol 240, 92-107.

Allegrucci, C., Thurston, A., Lucas, E., and Young, L. (2005). Epigenetics and the germline. Reproduction 129, 137-149.

Amleh, A., and Dean, J. (2002). Mouse genetics provides insight into folliculogenesis, fertilization and early embryonic development. Hum Reprod Update 8, 395-403.

Anderson, E., and Albertini, D. F. (1976). Gap junctions between the oocyte and companion follicle cells in the mammalian ovary. J Cell Biol 71, 680-686.

Ara, T., Nakamura, Y., Egawa, T., Sugiyama, T., Abe, K., Kishimoto, T., Matsui, Y., and Nagasawa, T. (2003). Impaired colonization of the gonads by primordial germ cells in mice lacking a chemokine, stromal cell-derived factor-1 (SDF-1). Proc Natl Acad Sci U S A 100, 5319-5323.

Behringer, R. R., Cate, R. L., Froelick, G. J., Palmiter, R. D., and Brinster, R. L. (1990). Abnormal sexual development in transgenic mice chronically expressing mullerian inhibiting substance. Nature 345, 167-170.

Bellve, A. R., Cavicchia, J. C., Millette, C. F., O'Brien, D. A., Bhatnagar, Y. M., and Dym, M. (1977). Spermatogenic cells of the prepuberal mouse. Isolation and morphological characterization. J Cell Biol 74, 68-85.

Bellve, A. R., Millette, C. F., Bhatnagar, Y. M., and O'Brien, D. A. (1977). Dissociation of the mouse testis and characterization of isolated spermatogenic cells. J Histochem Cytochem 25, 480-494.

Bendel-Stenzel, M. R., Gomperts, M., Anderson, R., Heasman, J., and Wylie, C. (2000). The role of cadherins during primordial germ cell migration and early gonad formation in the mouse. Mech Dev 91, 143-152.

Besmer, P., Manova, K., Duttlinger, R., Huang, E. J., Packer, A., Gyssler, C., and Bachvarova, R. F. (1993). The kit-ligand (steel factor) and its receptor c-kit/W: pleiotropic roles in gametogenesis and melanogenesis. Dev Suppl, 125-137.

Birk, O. S., Casiano, D. E., Wassif, C. A., Cogliati, T., Zhao, L., Zhao, Y., Grinberg, A., Huang, S., Kreidberg, J. A., Parker, K. L., et al. (2000). The LIM homeobox gene Lhx9 is essential for mouse gonad formation. Nature 403, 909-913.

Bowles, J., Teasdale, R. P., James, K., and Koopman, P. (2003). Dppa3 is a marker of pluripotency and has a human homologue that is expressed in germ cell tumours. Cytogenet Genome Res 101, 261-265.

Brennan, J., and Capel, B. (2004). One tissue, two fates: molecular genetic events that underlie testis versus ovary development. Nat Rev Genet 5, 509-521.

Brinster, R. L., and Avarbock, M. R. (1994). Germline transmission of donor haplotype following spermatogonial transplantation. Proc Natl Acad Sci U S A 91, 11303-11307.

Buehr, M., McLaren, A., Bartley, A., and Darling, S. (1993). Proliferation and migration of primordial germ cells in We/We mouse embryos. Dev Dyn 198, 182-189.

Bullejos, M., and Koopman, P. (2004). Germ cells enter meiosis in a rostro-caudal wave during development of the mouse ovary. Mol Reprod Dev 68, 422-428.

Byskov, A. G., and Hoyer, P. E. (1994). Embryology of mammalian gonads and ducts. In The Physiology of Reproduction, E. Knobil, and J. Neill, eds. (New York, Raven Press), pp. 487-540.

Byskov, A. G., and Saxen, L. (1976). Induction of meiosis in fetal mouse testis in vitro. Dev Biol 52, 193-200.

Chang, H., and Matzuk, M. M. (2001). Smad5 is required for mouse primordial germ cell development. Mech Dev 104, 61-67.

Coffigny, H., Bourgeois, C., Ricoul, M., Bernardino, J., Vilain, A., Niveleau, A., Malfoy, B., and Dutrillaux, B. (1999). Alterations of DNA methylation patterns in germ cells and Sertoli cells from developing mouse testis. Cytogenet Cell Genet 87, 175-181.

Cooke, H. J., Lee, M., Kerr, S., and Ruggiu, M. (1996). A murine homologue of the human DAZ gene is autosomal and expressed only in male and female gonads. Hum Mol Genet 5, 513-516.

Couse, J. F., Hewitt, S. C., Bunch, D. O., Sar, M., Walker, V. R., Davis, B. J., and Korach, K. S. (1999). Postnatal sex reversal of the ovaries in mice lacking estrogen receptors alpha and beta. Science 286, 2328-2331.

de Sousa Lopes, S. M., Roelen, B. A., Monteiro, R. M., Emmens, R., Lin, H. Y., Li, E., Lawson, K. A., and Mummery, C. L. (2004). BMP signaling mediated by ALK2 in the visceral endoderm is necessary for the generation of primordial germ cells in the mouse embryo. Genes Dev 18, 1838-1849.

Deblandre, G. A., Marinx, O. P., Evans, S. S., Majjaj, S., Leo, O., Caput, D., Huez, G. A., and Wathelet, M. G. (1995). Expression cloning of an interferon-inducible 17-kDa membrane protein implicated in the control of cell growth. J Biol Chem 270, 23860-23866.

Dierich, A., Sairam, M. R., Monaco, L., Fimia, G. M., Gansmuller, A., LeMeur, M., and Sassone-Corsi, P. (1998). Impairing follicle-stimulating hormone (FSH) signaling in vivo: targeted disruption of the FSH receptor leads to aberrant gametogenesis and hormonal imbalance. Proc Natl Acad Sci U S A 95, 13612-13617.

Dong, J., Albertini, D. F., Nishimori, K., Kumar, T. R., Lu, N., and Matzuk, M. M. (1996). Growth differentiation factor-9 is required during early ovarian folliculogenesis. Nature 383, 531-535.

Eddy, E. M., O'Brien, D. A., Fenderson, B. A., and Welch, J. E. (1991). Intermediate filament--like proteins in the fibrous sheath of the mouse sperm flagellum. Ann N Y Acad Sci 637, 224-239.

Eicher, E. M., and Washburn, L. L. (1986). Genetic control of primary sex determination in mice. Annu Rev Genet 20, 327-360.

Enders, G. C., and May, J. J., 2nd (1994). Developmentally regulated expression of a mouse germ cell nuclear antigen examined from embryonic day 11 to adult in male and female mice. Dev Biol 163, 331-340.

Eppig, J. J. (2001). Oocyte control of ovarian follicular development and function in mammals. Reproduction 122, 829-838.

Evans, S. S., Lee, D. B., Han, T., Tomasi, T. B., and Evans, R. L. (1990). Monoclonal antibody to the interferon-inducible protein Leu-13 triggers aggregation and inhibits proliferation of leukemic B cells. Blood 76, 2583-2593.

Extavour, C. G., and Akam, M. (2003). Mechanisms of germ cell specification across the metazoans: epigenesis and preformation. Development 130, 5869-5884.

Ginsburg, M., Snow, M. H., and McLaren, A. (1990). Primordial germ cells in the mouse embryo during gastrulation. Development 110, 521-528.

Godin, I., Deed, R., Cooke, J., Zsebo, K., Dexter, M., and Wylie, C. C. (1991). Effects of the steel gene product on mouse primordial germ cells in culture. Nature 352, 807-809.

Godin, I., Wylie, C., and Heasman, J. (1990). Genital ridges exert long-range effects on mouse primordial germ cell numbers and direction of migration in culture. Development 108, 357-363.

Gomperts, M., Garcia-Castro, M., Wylie, C., and Heasman, J. (1994). Interactions between primordial germ cells play a role in their migration in mouse embryos. Development 120, 135-141.

Goodenough, D. A., Simon, A. M., and Paul, D. L. (1999). Gap junctional intercellular communication in the mouse ovarian follicle. Novartis Found Symp 219, 226-235; discussion 235-240.

Gubbay, J., Collignon, J., Koopman, P., Capel, B., Economou, A., Munsterberg, A., Vivian, N., Goodfellow, P., and Lovell-Badge, R. (1990). A gene mapping to the sex-determining region of the mouse Y chromosome is a member of a novel family of embryonically expressed genes. Nature 346, 245-250.

Hajkova, P., Erhardt, S., Lane, N., Haaf, T., El-Maarri, O., Reik, W., Walter, J., and Surani, M. A. (2002). Epigenetic reprogramming in mouse primordial germ cells. Mech Dev 117, 15-23.

Handel, M. A., and Eppig, J. J. (1979). Sertoli cell differentiation in the testes of mice genetically deficient in germ cells. Biol Reprod 20, 1031-1038.

Hansen, D., Hubbard, E. J., and Schedl, T. (2004). Multi-pathway control of the proliferation versus meiotic development decision in the Caenorhabditis elegans germline. Dev Biol 268, 342-357.

Hansen, D., Wilson-Berry, L., Dang, T., and Schedl, T. (2004). Control of the proliferation versus meiotic development decision in the C. elegans germline through regulation of GLD-1 protein accumulation. Development 131, 93-104.

Hayashi, K., Kobayashi, T., Umino, T., Goitsuka, R., Matsui, Y., and Kitamura, D. (2002). SMAD1 signaling is critical for initial commitment of germ cell lineage from mouse epiblast. Mech Dev 118, 99-109.

Hecht, N. B. (1998). Molecular mechanisms of male germ cell differentiation. Bioessays 20, 555-561.

Heldin, C. H., Miyazono, K., and ten Dijke, P. (1997). TGF-beta signalling from cell membrane to nucleus through SMAD proteins. Nature 390, 465-471.

Hiura, H., Obata, Y., Komiyama, J., Shirai, M., and Kono, T. (2006). Oocyte growth-dependent progression of maternal imprinting in mice. Genes Cells 11, 353-361.

Honigberg, S. M., and Purnapatre, K. (2003). Signal pathway integration in the switch from the mitotic cell cycle to meiosis in yeast. J Cell Sci 116, 2137-2147.

Illmensee, K., and Mahowald, A. P. (1974). Transplantation of posterior polar plasm in Drosophila. Induction of germ cells at the anterior pole of the egg. Proc Natl Acad Sci U S A 71, 1016-1020.

Jeays-Ward, K., Hoyle, C., Brennan, J., Dandonneau, M., Alldus, G., Capel, B., and Swain, A. (2003). Endothelial and steroidogenic cell migration are regulated by WNT4 in the developing mammalian gonad. Development 130, 3663-3670.

Jordan, B. K., Shen, J. H., Olaso, R., Ingraham, H. A., and Vilain, E. (2003). Wnt4 overexpression disrupts normal testicular vasculature and inhibits testosterone synthesis by repressing steroidogenic factor 1/beta-catenin synergy. Proc Natl Acad Sci U S A 100, 10866-10871.

Juneja, S. C., Barr, K. J., Enders, G. C., and Kidder, G. M. (1999). Defects in the germ line and gonads of mice lacking connexin43. Biol Reprod 60, 1263-1270.

Kimura, T., Ito, C., Watanabe, S., Takahashi, T., Ikawa, M., Yomogida, K., Fujita, Y., Ikeuchi, M., Asada, N., Matsumiya, K., et al. (2003). Mouse germ cell-less as an essential component for nuclear integrity. Mol Cell Biol 23, 1304-1315.

Kimura, T., Yomogida, K., Iwai, N., Kato, Y., and Nakano, T. (1999). Molecular cloning and genomic organization of mouse homologue of Drosophila germ cell-less and its expression in germ lineage cells. Biochem Biophys Res Commun 262, 223-230.

Knaut, H., Pelegri, F., Bohmann, K., Schwarz, H., and Nusslein-Volhard, C. (2000). Zebrafish vasa RNA but not its protein is a component of the germ plasm and segregates asymmetrically before germline specification. J Cell Biol 149, 875-888.

Kono, T., Obata, Y., Wu, Q., Niwa, K., Ono, Y., Yamamoto, Y., Park, E. S., Seo, J. S., and Ogawa, H. (2004). Birth of parthenogenetic mice that can develop to adulthood. Nature 428, 860-864.

Koopman, P., Munsterberg, A., Capel, B., Vivian, N., and Lovell-Badge, R. (1990). Expression of a candidate sex-determining gene during mouse testis differentiation. Nature 348, 450-452.

Koubova, J., Menke, D. B., Zhou, Q., Capel, B., Griswold, M. D., and Page, D. C. (2006). Retinoic acid regulates sex-specific timing of meiotic initiation in mice. Proc Natl Acad Sci U S A.

Kreidberg, J. A., Sariola, H., Loring, J. M., Maeda, M., Pelletier, J., Housman, D., and Jaenisch, R. (1993). WT-1 is required for early kidney development. Cell 74, 679-691.

Kumar, T. C. (1997). Development of immunocontraceptives: an introduction. Hum Reprod Update 3, 299-300.

Lamb, M. M., and Laird, C. D. (1976). Increase in nuclear poly(A)-containing RNA at syncytial blastoderm in Drosophila melanogaster embryos. Dev Biol 52, 31-42.

Lawson, K. A., Dunn, N. R., Roelen, B. A., Zeinstra, L. M., Davis, A. M., Wright, C. V., Korving, J. P., and Hogan, B. L. (1999). Bmp4 is required for the generation of primordial germ cells in the mouse embryo. Genes Dev 13, 424-436.

Lawson, K. A., and Hage, W. J. (1994). Clonal analysis of the origin of primordial germ cells in the mouse. Ciba Found Symp 182, 68-84; discussion 84-91.

Lin, Y., and Page, D. C. (2005). Dazl deficiency leads to embryonic arrest of germ cell development in XY C57BL/6 mice. Dev Biol 288, 309-316.

Luo, X., Ikeda, Y., and Parker, K. L. (1994). A cell-specific nuclear receptor is essential for adrenal and gonadal development and sexual differentiation. Cell 77, 481-490.

MacGregor, G. R., Zambrowicz, B. P., and Soriano, P. (1995). Tissue non-specific alkaline phosphatase is expressed in both embryonic and extraembryonic lineages during mouse embryogenesis but is not required for migration of primordial germ cells. Development 121, 1487-1496.

Mahowald, A. P., and Hennen, S. (1971). Ultrastructure of the "germ plasm" in eggs and embryos of Rana pipiens. Dev Biol 24, 37-53.

Massague, J., and Chen, Y. G. (2000). Controlling TGF-beta signaling. Genes Dev 14, 627-644.

Massague, J., and Wotton, D. (2000). Transcriptional control by the TGF-beta/Smad signaling system. Embo J 19, 1745-1754.

Matsui, Y., Zsebo, K., and Hogan, B. L. (1992). Derivation of pluripotential embryonic stem cells from murine primordial germ cells in culture. Cell 70, 841-847.

Mazeyrat, S., Saut, N., Grigoriev, V., Mahadevaiah, S. K., Ojarikre, O. A., Rattigan, A., Bishop, C., Eicher, E. M., Mitchell, M. J., and Burgoyne, P. S. (2001). A Y-encoded subunit of the translation initiation factor Eif2 is essential for mouse spermatogenesis. Nat Genet 29, 49-53.

McLaren, A. (1984). Meiosis and differentiation of mouse germ cells. Symp Soc Exp Biol 38, 7-23.

McLaren, A. (2000). Germ and somatic cell lineages in the developing gonad. Mol Cell Endocrinol 163, 3-9.

McLaren, A. (2003). Primordial germ cells in the mouse. Dev Biol 262, 1-15.

McLaren, A., and Monk, M. (1981). X-chromosome activity in the germ cells of sex-reversed mouse embryos. J Reprod Fertil 63, 533-537.

McLaren, A., and Southee, D. (1997). Entry of mouse embryonic germ cells into meiosis. Dev Biol 187, 107-113.

McMahon, A., Fosten, M., and Monk, M. (1981). Random X-chromosome inactivation in female primordial germ cells in the mouse. J Embryol Exp Morphol 64, 251-258.

Menke, D. B., Koubova, J., and Page, D. C. (2003). Sexual differentiation of germ cells in XX mouse gonads occurs in an anterior-to-posterior wave. Dev Biol 262, 303-312.

Menke, D. B., and Page, D. C. (2002). Sexually dimorphic gene expression in the developing mouse gonad. Gene Expr Patterns 2, 359-367.

Merchant, H. (1975). Rat gonadal and ovarioan organogenesis with and without germ cells. An ultrastructural study. Dev Biol 44, 1-21.

Mintz, B., and Russell, E. S. (1957). Gene-induced embryological modifications of primordial germ cells in the mouse. J Exp Zool 134, 207-237.

Miyamoto, N., Yoshida, M., Kuratani, S., Matsuo, I., and Aizawa, S. (1997). Defects of urogenital development in mice lacking Emx2. Development 124, 1653-1664.

Molyneaux, K., and Wylie, C. (2004). Primordial germ cell migration. Int J Dev Biol 48, 537-544.

Molyneaux, K. A., Stallock, J., Schaible, K., and Wylie, C. (2001). Time-lapse analysis of living mouse germ cell migration. Dev Biol 240, 488-498.

Molyneaux, K. A., Wang, Y., Schaible, K., and Wylie, C. (2004). Transcriptional profiling identifies genes differentially expressed during and after migration in murine primordial germ cells. Gene Expr Patterns 4, 167-181.

Molyneaux, K. A., Zinszner, H., Kunwar, P. S., Schaible, K., Stebler, J., Sunshine, M. J., O'Brien, W., Raz, E., Littman, D., Wylie, C., and Lehmann, R. (2003). The chemokine SDF1/CXCL12 and its receptor CXCR4 regulate mouse germ cell migration and survival. Development 130, 4279-4286.

Mroz, K., Carrel, L., and Hunt, P. A. (1999). Germ cell development in the XXY mouse: evidence that X chromosome reactivation is independent of sexual differentiation. Dev Biol 207, 229-238.

Nakatsuji, N., and Chuma, S. (2001). Differentiation of mouse primordial germ cells into female or male germ cells. Int J Dev Biol 45, 541-548.

Nebel, B. R., Amarose, A. P., and Hacket, E. M. (1961). Calendar of gametogenic development in the prepuberal male mouse. Science 134, 832-833.

Nesterova, T. B., Mermoud, J. E., Hilton, K., Pehrson, J., Surani, M. A., McLaren, A., and Brockdorff, N. (2002). Xist expression and macroH2A1.2 localisation in mouse primordial and pluripotent embryonic germ cells. Differentiation 69, 216-225.

Nieuwkoop, P. D., and Sutasurya, L. A. (1976). Embryological evidence for a possible polyphyletic origin of the recent amphibians. J Embryol Exp Morphol 35, 159-167.

Oakberg, E. F. (1956). Duration of spermatogenesis in the mouse and timing of stages of the cycle of the seminiferous epithelium. Am J Anat 99, 507-516.

Oakberg, E. F. (1956). A description of spermiogenesis in the mouse and its use in analysis of the cycle of the seminiferous epithelium and germ cell renewal. Am J Anat 99, 391-413.

Oehninger, S. (2003). Biochemical and functional characterization of the human zona pellucida. Reprod Biomed Online 7, 641-648.

Ohinata, Y., Payer, B., O'Carroll, D., Ancelin, K., Ono, Y., Sano, M., Barton, S. C., Obukhanych, T., Nussenzweig, M., Tarakhovsky, A., et al. (2005). Blimp1 is a critical determinant of the germ cell lineage in mice. Nature 436, 207-213.

Okamura, D., Kimura, T., Nakano, T., and Matsui, Y. (2003). Cadherin-mediated cell interaction regulates germ cell determination in mice. Development 130, 6423-6430.

Ozdzenski, W. (1967). Observations on the origin of primordial germ cells in the mouse. Zoologica Pol 17, 367-379.

Palmer, S. J., and Burgoyne, P. S. (1991). In situ analysis of fetal, prepuberal and adult XX----XY chimaeric mouse testes: Sertoli cells are predominantly, but not exclusively, XY. Development 112, 265-268.

Pesce, M., Gioia Klinger, F., and De Felici, M. (2002). Derivation in culture of primordial germ cells from cells of the mouse epiblast: phenotypic induction and growth control by Bmp4 signalling. Mech Dev 112, 15-24.

Peters, H. (1970). Migration of gonocytes into the mammalian gonad and their differentiation. Philos Trans R Soc Lond B Biol Sci 259, 91-101.

Peters, H., Levy, E., and Crone, M. (1962). Deoxyribonucleic acid synthesis in oocytes of mouse embryos. Nature 195, 915-916.

Rakyan, V. K., Preis, J., Morgan, H. D., and Whitelaw, E. (2001). The marks, mechanisms and memory of epigenetic states in mammals. Biochem J 356, 1-10.

Resnick, J. L., Ortiz, M., Keller, J. R., and Donovan, P. J. (1998). Role of fibroblast growth factors and their receptors in mouse primordial germ cell growth. Biol Reprod 59, 1224-1229.

Ruggiu, M., Speed, R., Taggart, M., McKay, S. J., Kilanowski, F., Saunders, P., Dorin, J., and Cooke, H. J. (1997). The mouse Dazla gene encodes a cytoplasmic protein essential for gametogenesis. Nature 389, 73-77.

Saitou, M., Barton, S. C., and Surani, M. A. (2002). A molecular programme for the specification of germ cell fate in mice. Nature 418, 293-300.

Sato, M., Kimura, T., Kurokawa, K., Fujita, Y., Abe, K., Masuhara, M., Yasunaga, T., Ryo, A., Yamamoto, M., and Nakano, T. (2002). Identification of PGC7, a new gene expressed specifically in preimplantation embryos and germ cells. Mech Dev 113, 91-94.

Saunders, P. T., Turner, J. M., Ruggiu, M., Taggart, M., Burgoyne, P. S., Elliott, D., and Cooke, H. J. (2003). Absence of mDazl produces a final block on germ cell development at meiosis. Reproduction 126, 589-597.

Schmidt, D., Ovitt, C. E., Anlag, K., Fehsenfeld, S., Gredsted, L., Treier, A. C., and Treier, M. (2004). The murine winged-helix transcription factor Foxl2 is required for granulosa cell differentiation and ovary maintenance. Development 131, 933-942.

Scholer, H. R., Ruppert, S., Suzuki, N., Chowdhury, K., and Gruss, P. (1990). New type of POU domain in germ line-specific protein Oct-4. Nature 344, 435-439.

Schrans-Stassen, B. H., Saunders, P. T., Cooke, H. J., and de Rooij, D. G. (2001). Nature of the spermatogenic arrest in Dazl -/- mice. Biol Reprod 65, 771-776.

Seligman, J., and Page, D. C. (1998). The Dazh gene is expressed in male and female embryonic gonads before germ cell sex differentiation. Biochem Biophys Res Commun 245, 878-882.

Seydoux, G., and Fire, A. (1994). Soma-germline asymmetry in the distributions of embryonic RNAs in Caenorhabditis elegans. Development 120, 2823-2834.

Seydoux, G., Mello, C. C., Pettitt, J., Wood, W. B., Priess, J. R., and Fire, A. (1996). Repression of gene expression in the embryonic germ lineage of C. elegans. Nature 382, 713-716.

Sinclair, A. H., Berta, P., Palmer, M. S., Hawkins, J. R., Griffiths, B. L., Smith, M. J., Foster, J. W., Frischauf, A. M., Lovell-Badge, R., and Goodfellow, P. N. (1990). A gene from the human sex-determining region encodes a protein with homology to a conserved DNA-binding motif. Nature 346, 240-244.

Soyal, S. M., Amleh, A., and Dean, J. (2000). FIGalpha, a germ cell-specific transcription factor required for ovarian follicle formation. Development 127, 4645-4654.

Starz-Gaiano, M., and Lehmann, R. (2001). Moving towards the next generation. Mech Dev 105, 5-18.

Strome, S., and Wood, W. B. (1982). Immunofluorescence visualization of germ-line-specific cytoplasmic granules in embryos, larvae, and adults of Caenorhabditis elegans. Proc Natl Acad Sci U S A 79, 1558-1562.

Taketo-Hosotani, T., Nishioka, Y., Nagamine, C. M., Villalpando, I., and Merchant-Larios, H. (1989). Development and fertility of ovaries in the B6.YDOM sex-reversed female mouse. Development 107, 95-105.

Takeuchi, Y., Molyneaux, K., Runyan, C., Schaible, K., and Wylie, C. (2005). The roles of FGF signaling in germ cell migration in the mouse. Development 132, 5399-5409.

Tam, P. P., and Snow, M. H. (1981). Proliferation and migration of primordial germ cells during compensatory growth in mouse embryos. J Embryol Exp Morphol 64, 133-147.

Tam, P. P., and Zhou, S. X. (1996). The allocation of epiblast cells to ectodermal and germ-line lineages is influenced by the position of the cells in the gastrulating mouse embryo. Dev Biol 178, 124-132.

Tam, P. P., Zhou, S. X., and Tan, S. S. (1994). X-chromosome activity of the mouse primordial germ cells revealed by the expression of an X-linked lacZ transgene. Development 120, 2925-2932.

Tanaka, S. S., and Matsui, Y. (2002). Developmentally regulated expression of mil-1 and mil-2, mouse interferon-induced transmembrane protein like genes, during formation and differentiation of primordial germ cells. Gene Expr Patterns 2, 297-303.

Tanaka, S. S., Toyooka, Y., Akasu, R., Katoh-Fukui, Y., Nakahara, Y., Suzuki, R., Yokoyama, M., and Noce, T. (2000). The mouse homolog of Drosophila Vasa is required for the development of male germ cells. Genes Dev 14, 841-853.

Tanaka, S. S., Yamaguchi, Y. L., Tsoi, B., Lickert, H., and Tam, P. P. (2005). IFITM/Mil/fragilis family proteins IFITM1 and IFITM3 play distinct roles in mouse primordial germ cell homing and repulsion. Dev Cell 9, 745-756.

Tilmann, C., and Capel, B. (1999). Mesonephric cell migration induces testis cord formation and Sertoli cell differentiation in the mammalian gonad. Development 126, 2883-2890.

Toyooka, Y., Tsunekawa, N., Takahashi, Y., Matsui, Y., Satoh, M., and Noce, T. (2000). Expression and intracellular localization of mouse Vasa-homologue protein during germ cell development. Mech Dev 93, 139-149.

Tremblay, K. D., Dunn, N. R., and Robertson, E. J. (2001). Mouse embryos lacking Smad1 signals display defects in extra-embryonic tissues and germ cell formation. Development 128, 3609-3621.

Tsunekawa, N., Naito, M., Sakai, Y., Nishida, T., and Noce, T. (2000). Isolation of chicken vasa homolog gene and tracing the origin of primordial germ cells. Development 127, 2741-2750.

Uda, M., Ottolenghi, C., Crisponi, L., Garcia, J. E., Deiana, M., Kimber, W., Forabosco, A., Cao, A., Schlessinger, D., and Pilia, G. (2004). Foxl2 disruption causes mouse ovarian failure by pervasive blockage of follicle development. Hum Mol Genet 13, 1171-1181.

Vainio, S., Heikkila, M., Kispert, A., Chin, N., and McMahon, A. P. (1999). Female development in mammals is regulated by Wnt-4 signalling. Nature 397, 405-409.

Vincent, S. D., Dunn, N. R., Sciammas, R., Shapiro-Shalef, M., Davis, M. M., Calame, K., Bikoff, E. K., and Robertson, E. J. (2005). The zinc finger transcriptional repressor Blimp1/Prdm1 is dispensable for early axis formation but is required for specification of primordial germ cells in the mouse. Development 132, 1315-1325.

Yao, H. H., DiNapoli, L., and Capel, B. (2003). Meiotic germ cells antagonize mesonephric cell migration and testis cord formation in mouse gonads. Development 130, 5895-5902.

Yao, H. H., Matzuk, M. M., Jorgez, C. J., Menke, D. B., Page, D. C., Swain, A., and Capel, B. (2004). Follistatin operates downstream of Wnt4 in mammalian ovary organogenesis. Dev Dyn 230, 210-215.

Ying, Y., Qi, X., and Zhao, G. Q. (2001). Induction of primordial germ cells from murine epiblasts by synergistic action of BMP4 and BMP8B signaling pathways. Proc Natl Acad Sci U S A 98, 7858-7862.

Yoshimizu, T., Obinata, M., and Matsui, Y. (2001). Stage-specific tissue and cell interactions play key roles in mouse germ cell specification. Development 128, 481-490.

Yoshimizu, T., Sugiyama, N., De Felice, M., Yeom, Y. I., Ohbo, K., Masuko, K., Obinata, M., Abe, K., Scholer, H. R., and Matsui, Y. (1999). Germline-specific expression of the Oct-4/green fluorescent protein (GFP) transgene in mice. Dev Growth Differ 41, 675-684.

Yu, R. N., Ito, M., Saunders, T. L., Camper, S. A., and Jameson, J. L. (1998). Role of Ahch in gonadal development and gametogenesis. Nat Genet 20, 353-357.

Zalokar, M. (1976). Autoradiographic study of protein and RNA formation during early development of Drosophila eggs. Dev Biol 49, 425-437.

Zamboni, L., and Upadhyay, S. (1983). Germ cell differentiation in mouse adrenal glands. J Exp Zool 228, 173-193.

Zhao, M., and Dean, J. (2002). The zona pellucida in folliculogenesis, fertilization and early development. Rev Endocr Metab Disord 3, 19-26.

Chapter 2

An X-to-autosome retrogene is required for spermatogenesis in mice

Andrew E. Baltus, Julie Bradley, Helen Skaletsky,
Morgan Royce-Tolland, Ken Dewar and David C. Page

Author Contributions:
JB, HS, MR-T and KD performed the genetic mapping and sequencing of the critical region in the *jsd/jsd* and B6 mice. JB did the RT-PCR and northern-blot analysis. AEB and HS isolated the Utp14b cDNAs and performed the evolutionary analysis of the Utp14 retroposons. AEB, JB and DCP wrote the manuscript.

nature genetics

An X-to-autosome retrogene is required for spermatogenesis in mice

Julie Bradley[1,4], Andrew Baltus[1,4], Helen Skaletsky[1], Morgan Royce-Tolland[1], Ken Dewar[2,3] & David C Page[1]

We identified the gene carrying the juvenile spermatogonial depletion mutation (*jsd*), a recessive spermatogenic defect mapped to mouse chromosome 1 (refs. 1,2). We localized *jsd* to a 272-kb region and resequenced this area to identify the underlying mutation: a frameshift that severely truncates the predicted protein product of a 2.3-kb genomic open reading frame. This gene, *Utp14b*, evidently arose through reverse transcription of an mRNA from an X-linked gene and integration of the resulting cDNA into an intron of an autosomal gene, whose promoter and 5′ untranslated exons are shared with *Utp14b*. To our knowledge, *Utp14b* is the first protein-coding retrogene to be linked to a recessive mammalian phenotype. The X-linked progenitor of *Utp14b* is the mammalian ortholog of yeast Utp14, which encodes a protein required for processing of pre-rRNA[3] and hence for ribosome assembly. Our findings substantiate the hypothesis[4] that mammalian spermatogenesis is supported by autosomal retrogenes that evolved from X-linked housekeeping genes to compensate for silencing of the X chromosome during male meiosis[5–7]. We find that *Utp14b*-like retrogenes arose independently and were conserved during evolution in at least four mammalian lineages. This recurrence implies a strong selective pressure, perhaps to enable ribosome assembly in male meiotic cells.

The *jsd* mutation was previously mapped to a 0.4-cM region of mouse chromosome 1, spanning about 1.5 Mb[1,2]. By analyzing 4,826 meioses from two F_1 intercrosses (**Supplementary Fig. 1** online), we confirmed this localization and more precisely mapped *jsd* to a region of <0.1 cM (**Fig. 1a**). Sequencing of two wild-type BACs spanning the critical region showed that it measured ~272 kb.

The critical region contains only two genes that are conserved in mice and humans: *Acsl3* and *Kcne4*. (In humans, the genes *ACSL3* and *KCNE4* are also located adjacent to one another, on chromosome 2, in a region orthologous to mouse chromosome 1.) In addition, GenScan analysis of the critical region sequence identified a 2.3-kb open reading frame (ORF) in the second intron of *Acsl3* (**Fig. 1b**) that was absent from the homologous region of the human gene. We refer to this ORF as ORF2.3.

Using the wild-type BAC sequence as a reference, we resequenced the critical region in genomic DNA from *jsd/jsd* mice to identify any differences from the wild-type strain (C57BL/6) on which the mutation arose spontaneously (sequence available on our website; see URLs). We found a sequence difference in ORF2.3 at nucleotides 306–307, where the dinucleotide GG in the wild-type chromosome was replaced by the hexanucleotide CTTTTC in the *jsd* chromosome (**Fig. 1c**). This mutation in ORF2.3 shifts the reading frame and introduces a stop codon at nucleotide 312, severely truncating the predicted protein. This mutation in ORF2.3 was genetically inseparable from the *jsd* mutation in all 4,826 meioses examined (**Supplementary Fig. 1** online).

We found no other substantial sequence differences between *jsd* and wild-type chromosomes. We detected single-unit differences in the lengths of two microsatellite arrays, both located well away from coding sequences. The coding and 5′ upstream regions of *Acsl3* and *Kcne4* were identical on *jsd* and wild-type chromosomes. We were unable to completely resequence 13 microsatellite or other low-complexity arrays, but none of these fell in coding or putative regulatory regions. The absence of substantial sequence differences elsewhere in the critical region indicates that the GG→CTTTTC mutation in ORF2.3 causes the spermatogenic failure observed in *jsd/jsd* male mice.

We then tested whether ORF2.3 is transcribed and, if so, whether its expression pattern is consistent with its being the gene defective in *jsd/jsd* males. Transplantation of wild-type spermatogonia into testes of *jsd/jsd* mice rescues spermatogenesis, implying that *jsd* functions in testicular germ cells[8,9]. We found that ORF2.3 was transcribed in testes by sequencing of wild-type testis cDNA clones (**Fig. 1b**) and northern-blot analysis (**Fig. 2a**). ORF2.3 transcription did not differ significantly in testes of wild-type versus *jsd/jsd* mice, in keeping with it carrying a frameshift mutation. ORF2.3 seemed to be expressed in the spermatogenic cells themselves, as transcripts were not found in germ cell–deficient testes (from W^v/W^v mice; **Fig. 2d**) but were detected in purified spermatogonia, spermatocytes and spermatids (by RT-PCR; data not shown). ORF2.3 was also transcribed in brain (**Fig. 2a**). Published spermatogonial transplantation findings[8,9] are compatible with expression of the gene containing the *jsd* mutation not only in testes but also elsewhere in the body. Thus, the transcription pattern of ORF2.3 is consistent with previous findings for *jsd*.

[1]Howard Hughes Medical Institute, Whitehead Institute, and Department of Biology, Massachusetts Institute of Technology, Cambridge, Massachusetts 02142, USA. [2]Whitehead Institute/MIT Center for Genome Research, Cambridge, Massachusetts 02142, USA. [3]Present address: McGill University and Genome Quebec Innovation Centre, Montreal, Quebec H3A 1A4, Canada. [4]These authors contributed equally to this work. Correspondence should be addressed to D.C.P.

Published online 18 July 2004; doi:10.1038/ng1390

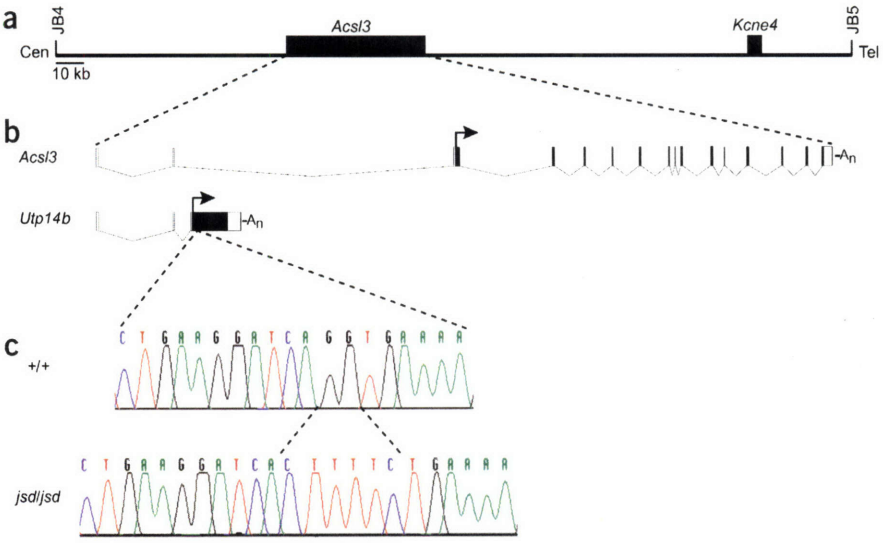

Figure 1 Insertion-deletion mutation in a transcribed ORF (ORF2.3) in the *jsd* critical region. (**a**) Sequence-based map of the *jsd* critical region, oriented with respect to the centromere (left) and telomere (right). The *jsd* mutation was mapped between genetic markers JB4 and JB5 (**Supplementary Fig. 1** online). Black boxes indicate the locations of two genes conserved between human and mouse. (**b**) *Acsl3* and *Utp14b* (ORF2.3) transcripts. Coding exons are shown in black, and translation start sites are indicated by arrows. A_n, poly-A tracts. (**c**) Sequence of nucleotides 295–313 of wild-type ORF2.3 and corresponding region of *jsd* chromosome.

Examination of the cDNA sequence containing ORF2.3, and comparison with the genomic DNA sequence, identified two 5′ untranslated exons, both of which also serve as 5′ untranslated exons in *Acsl3* (**Fig. 1b**). We called the gene that contains both ORF2.3 and its 5′ untranslated exons *Utp14b*. We conclude that *Acsl3* and *Utp14b* form a bicistronic unit with a shared promoter.

Because the *jsd* mutation falls in an intron of *Acsl3*, we considered the possibility that *Acsl3* itself, and not *Utp14b*, is the gene defective in *jsd/jsd* mice. If so, the mutation should disrupt transcription or splicing of *Acsl3*, as its coding sequence is unchanged. By northern-blot analysis, we observed a 3.5-kb *Acsl3* transcript in all tissues tested, with strongest expression in testis and brain (**Fig. 2b,c**). Thus, *Acsl3* was expressed in a wider range of tissues than *Utp14b*. Neither the size nor the abundance of this *Acsl3* transcript seemed to be altered in testes of *jsd/jsd* mice, suggesting that the mutation does not interfere with *Acsl3* transcription or splicing. We conclude that *Utp14b*, and not *Acsl3*, is the gene defective in *jsd/jsd* mice, and that truncation of the protein product of *Utp14b* causes spermatogenic failure.

At a molecular level, mouse *Utp14b* is atypical not only in that it forms part of a larger, bicistronic unit, which are rare in mammalian genomes[10], but also because it has no ortholog in the human genome, and its coding sequence is not interrupted by introns. Electronic searches of the mouse and human genomes showed that the X chromosome carries a widely expressed gene (*Utp14a*) whose coding sequence is homologous to that of mouse *Utp14b* but is interrupted by 14 introns (**Fig. 3** and **Supplementary Fig. 2** online)[11]. The existence of a conserved, intron-bearing homolog suggested a molecular evolutionary explanation for *Utp14b*. After the mouse lineage diverged from that of humans, a processed mRNA derived from the X-chromosomal gene *Utp14a* was probably reverse-transcribed. The resulting cDNA was integrated into an intron of the autosomal gene *Acsl3*, whose function was preserved despite the enlistment of its promoter and 5′ untranslated exons in the service of the newly created gene *Utp14b*.

Other testis-expressed autosomal retrogenes with X-linked progenitors have been reported in mammals[4,12–23]. In each case, as with *Utp14b*, the X-linked source gene is expressed widely, whereas the autosomal retrogene is expressed most prominently in testis. Mouse *Utp14b* is the first protein-coding retrogene in mammals to which a recessive phenotype has been ascribed. *Zfa*, an autosomal retrogene derived from the X-chromosomal gene *Zfx*[18,19], is the only other protein-coding retrogene in which a loss-of-function mutation has been

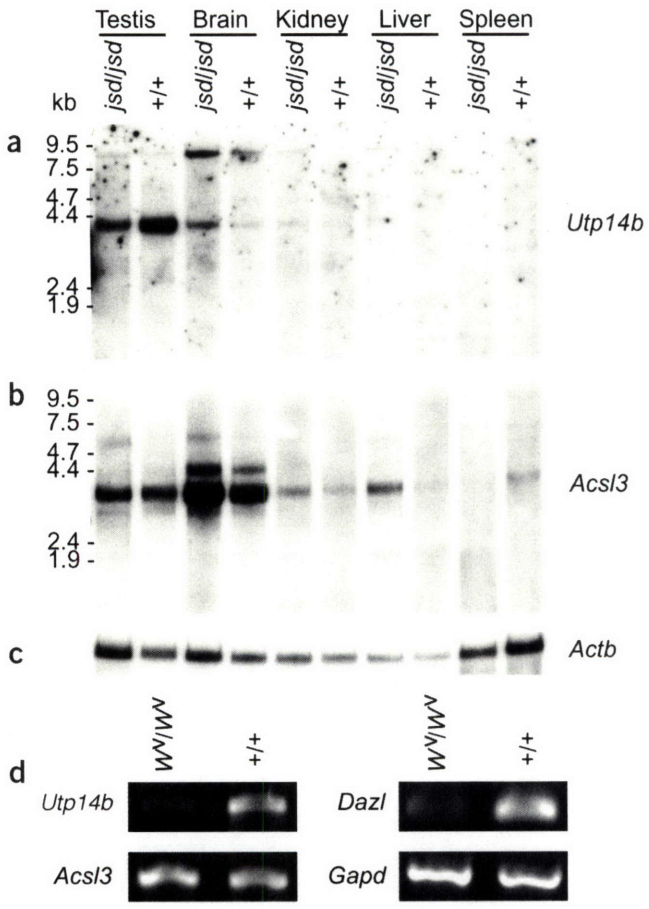

Figure 2 Transcription of *Utp14b* (ORF2.3) and *Acsl3*. (**a**) Northern-blot analysis of *Utp14b* (ORF2.3) in five tissues from *jsd/jsd* and wild-type 7-week-old male mice. (**b**) Hybridization of the same blot with an *Acsl3* probe. (**c**) Control hybridization of the same blot with an *Actb* probe. (**d**) RT-PCR analysis of poly(A)$^+$ RNA samples from testes of adult W^v/W^v (germ cell–depleted) and wild-type mice. *Dazl* (expressed only in germ cells) and *Gapd* (expressed ubiquitously) were used as controls.

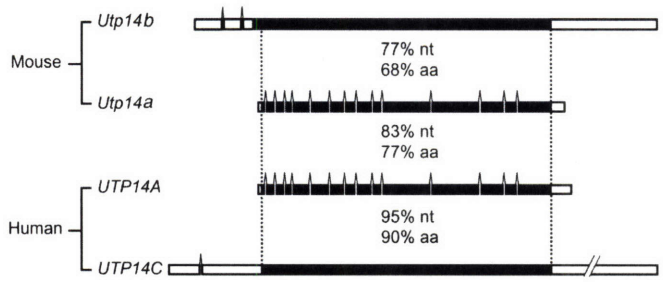

Figure 3 Schematic alignment of transcripts from mouse *Utp14b*, its X-linked homologs *Utp14a* and *UTP14A* in mouse and human, respectively, and its human autosomal homolog *UTP14C*. Coding regions are shown in black, and positions of introns are indicated. Percentage identities (nucleotide (nt) and amino acid (aa)) between coding sequences are given.

reported. Ablation of *Zfa* yielded no detectable phenotype[24]. To our knowledge, mouse *Utp14b* is also the first functional mammalian retrogene found to have parasitized an existing transcription unit.

Our findings substantiate the hypothesis[4] that mammalian spermatogenesis is dependent on autosomal retrogenes that evolved from X-linked progenitors to compensate for X-chromosome silencing during male meiosis. This hypothesis leads to three predictions regarding the *in vivo* function of X-to-autosome retrogenes, all of which are fulfilled by *Utp14b*. First, loss of retrogene function should perturb gametogenesis in males without otherwise affecting health or development in either sex. An early frameshift mutation in the *Utp14b* retrogene completely disrupts spermatogenesis. Second, retrogene function should be required only in the germ cells themselves, and not in the somatic cells of the testes. This is the case with *Utp14b*[8,9]. Third, retrogene function should be required only during meiosis; any spermatogenic defect should manifest at or after meiosis. As *jsd/jsd* XY mice age, premeiotic cell (spermatogonial) numbers and differentiation deteriorate, but this seems to be a secondary consequence of an altered hormonal environment in the testis, and not a direct result of the primary defect in the spermatogenic lineage[25]. The earliest defect observed in *jsd/jsd* deficient males is a marked reduction in the numbers of postmeiotic cells, or spermatids, at three weeks of age, during the first round of spermatogenesis[26]. This is consistent with the gene carrying the *jsd* mutation being required primarily, or exclusively, in meiotic cells.

Utp14a, the X-linked progenitor of *Utp14b*, encodes the mammalian ortholog of yeast Utp14, an essential protein required for processing of pre-rRNA (**Supplementary Fig. 3** online)[3]. X-to-autosome retrogenes are thought to serve essential housekeeping functions[4]. We postulate that this is the case for *Utp14b*, and specifically that it supports ribosome assembly and hence protein synthesis during male meiosis.

Utp14b exists in mice but not in humans. Might a similar but distinct functional retrogene exist in humans? This question is motivated by the facts that the X chromosome is inactivated during male meiosis in both humans and mice[5–7] and *Utp14a* is X-linked in both species. Electronic examination of the human genome identified a testis-transcribed gene, on chromosome 13, that shares the following properties with mouse *Utp14b*: an unmistakable similarity to the coding sequence of *Utp14a*, an intact and conserved ORF and an absence of coding-region introns (**Fig. 3** and ref. 27). This human retrogene, *UTP14C*, is not orthologous to mouse *Utp14b*. As indicated by comparison of mouse and human map locations (**Supplementary Fig. 4** online) and by phylogenetic sequence analysis (**Fig. 4**), the mouse *Utp14b* and human *UTP14C* retrogenes are products of two independent retroposition events.

We next searched for intronless derivatives of *Utp14a* in 16 other eutherian species. We carried out PCR on genomic DNAs from these 16 species using primers from regions of nucleotide-sequence conservation among the mouse and human *Utp14* genes. We identified a *Utp14a*-derived retrogene in 13 species, including such diverse eutherians as hamster, lemur, elephant and cow. In all 13 cases, we confirmed both strong coding-sequence similarity to *Utp14a* and the absence of coding-region introns by sequencing of PCR products. In every case, the sequenced region (at least 750 nucleotides, and typically >1,500 nucleotides) showed an intact, conserved ORF, with no frameshift mutations, no premature stop codons and a preponderance of silent nucleotide substitutions when compared with mouse or human *Utp14a*. These findings suggest that most eutherians possess a *Utp14a*-derived retrogene that encodes a functional protein subject to purifying selection. We did not find *Utp14a*-derived retrogenes in dog, horse or rabbit, but this negative evidence is inconclusive. Sequence divergence might account for the failure of our PCR primers to amplify a product in these species.

Finally, we carried out a sequence-based phylogenetic analysis of the known *Utp14a*-derived retrogenes to determine whether they could all be accounted for by the two retroposition events that gave rise to mouse *Utp14b* and human *UTP14C*. This analysis indicated that at least two (and perhaps three) additional, independent retroposition events are required to account for the array of *Utp14a*-derived retrogenes observed in eutheria (**Fig. 4** and **Supplementary Fig. 5** online). Thus, the retrogenesis and fixation of *Utp14b* during rodent evolution was reproduced,

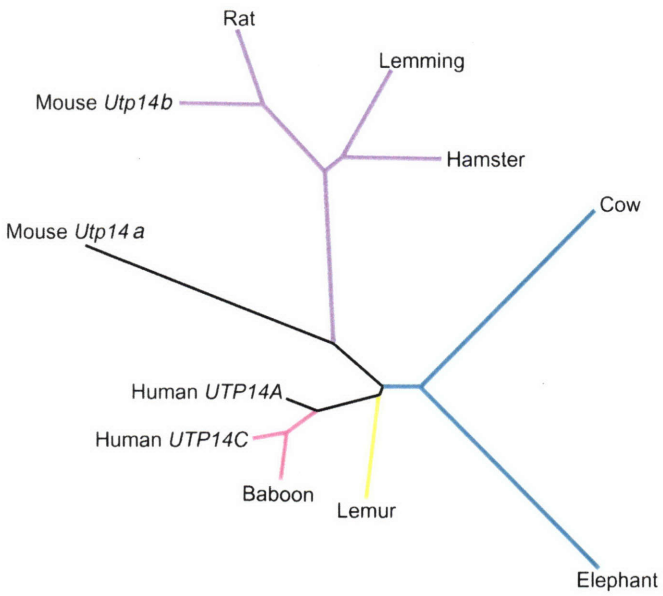

Figure 4 Phylogenetic comparison of *Utp14b* homologs in diverse eutherian mammals indicates that a minimum of four retroposition events (indicated by blue, red, yellow and green branches) occurred. This unrooted tree depicts phylogenetic relationships between the X-linked, intron-bearing *Utp14a* orthologs in mouse and human and their identified intronless derivatives in nine eutherians. Mouse *Utp14b* and its retrogene homologs in rodents seem to be orthologs, (*i.e.*, the result of a single retroposition event; blue branch). An independent event (red branch) accounts for the human and baboon retrogenes, which are orthologs. Another event (yellow branch, node well-separated from the human/baboon node, accounts for the lemur retrogene. At least one and perhaps two events (green branch) account for the cow and elephant retrogenes. The lengthy branches to the cow and elephant retrogenes indicate that the responsible event(s) occurred well before that responsible for the lemur retrogene, whose branch is relatively short.

presumably with independent sites of insertion, in other eutherian lineages. This is notable, as most retroposed copies of protein-coding genes identified to date in mammalian genomes are functionless pseudogenes[28,29]. We found no *Utp14a* pseudogenes in either mouse or human. Ironically, we did find a processed pseudogene of *Utp14b* in the mouse (**Supplementary Fig. 5** online). The fixation and maintenance of *Utp14a*-derived retrogenes in multiple eutherian lineages implies a persistent and widespread selective pressure. That selective pressure could arise from the need to assemble ribosomes and thereby support spermatogenesis in the face of meiotic X-chromosome inactivation.

METHODS

Mice. C57BL/6J *jsd*/+ male mice were a gift from W. Beamer (The Jackson Laboratory). We purchased C57BL/6J, DBA/2J, W^v/W^v and *Mus musculus castaneus*/Ei mice from The Jackson Laboratory.

Genetic mapping. We mated C57BL/6J *jsd*/*jsd* females with DBA/2J or *Mus musculus castaneus*/Ei males and intercrossed the offspring. We genotyped the resulting progeny for polymorphic DNA markers located on chromosome 1 and flanking *jsd*; see **Supplementary Table 1** for markers, PCR primers and assay conditions. We determined the *jsd* genotypes of critical recombinants (**Supplementary Fig. 1** online) by progeny testing, crossing to *jsd*/*jsd* or *jsd*/+ mice. We phenotyped adult males by dissecting out testes, which in *jsd*/*jsd* mice weighed no more than one-third as much as the testes of *jsd*/+ and +/+ littermates. These experiments were approved by the Committee on Animal Care at the Massachusetts Institute of Technology.

BAC sequencing and electronic gene prediction. We screened both the RPCI-22 and RPCI-23 libraries to construct a BAC contig of the *jsd* region of mouse chromosome 1. Two BACs spanning the critical *jsd* region, RPCI-22-292L24 and RPCI-23-395H12, were sequenced at the Whitehead Institute/MIT Center for Genome Research as described[30]. We searched for known and previously unidentified genes in the critical region by analyzing its sequence using RepeatMasker, GENSCAN and a BLAST search of the mouse and human expressed-sequence tag and nonredundant segments of GenBank.

Resequencing. We generated a series of overlapping fragments, each about 1 kb in length, that collectively span the 272-kb critical region (**Fig. 1**) by PCR using genomic DNA from C57BL/6J *jsd*/*jsd* mice as starting material. We selected PCR primers using Primer 3. We purified PCR products on Sephacryl-S300 columns and sequenced them using fluorescent-dye-terminator cycle sequencing protocols (BigDye kit, Amersham). Primers used in PCR generation of sequencing templates were also used as sequencing primers, and we selected additional sequencing primers at sites internal to the PCR-generated templates. Whenever the C57BL/6J *jsd*/*jsd* sequence differed from the BAC reference sequence, we resequenced C57BL/6J wild-type genomic DNA, which resolved all discrepancies except those described in the text.

cDNA and transcriptional analysis. We screened a mouse testis cDNA library (Stratagene) by hybridization using probes corresponding to 5′ and 3′ regions of ORF2.3. We subcloned two cDNA inserts into plasmids and sequenced them in their entirety. Both cDNA clones contained the 3′ untranslated region and were polyadenylated. The longer clone, pUtp14b3.5, included 5′ untranslated sequence and is depicted in **Figure 1**.

We isolated total RNAs from mouse tissues homogenized in TRIzol reagent (Gibco/BRL) and poly(A)$^+$ RNAs from total RNAs using the MicroPoly(A) Purist kit (Ambion). We prepared northern blots using 2 μg of purified poly(A)$^+$ RNA per lane and the NorthernMax-Gly (Ambion) glyoxal-based system. We hybridized northern-blot membranes to probes (radioactively labeled by random priming) in ExpressHyb (Clontech) hybridization solution at 68 °C, washed them with 2× saline sodium citrate and 0.1% SDS at room temperature and 0.2× saline sodium citrate and 0.1% SDS at 50 °C and exposed them to film at −80 °C for 12–48 h. Before hybridizations, we stripped northern-blot membranes in 1% SDS, 10 mM Tris and 1 mM EDTA for 15 min at 80 °C, equilibrated them in 2× saline sodium citrate and 0.1% SDS for 2 min and then exposed them to control film.

For RT-PCR, we used 1–5 μg of poly(A)$^+$ RNA in an oligo d(T)-primed first-strand cDNA synthesis reaction with Stratascript reverse transcriptase (Stratagene).

PCR amplification of homologs in diverse mammals. We chose primers from regions of at least 15 nucleotides of sequence identity among mouse *Utp14b*, mouse and human *UTP14A* and human *UTP14C*. We tested all primer pairs using mouse and human genomic DNAs as templates. We then applied satisfactory primer pairs to genomic DNAs from gorilla, chimpanzee, baboon, orangutan, rhesus monkey, squirrel monkey, lemur, cow, elephant, horse, dog, rabbit, guinea pig, hamster, lemming and rat. We purified and sequenced the resulting PCR products as described earlier. We obtained the sequences used in phylogenetic analysis (**Fig. 4** and **Supplementary Fig. 5** online) using species-specific primers to amplify and sequence a single PCR product from each species.

Phylogenetic analysis. We built phylogenetic trees using the neighbor-joining method with Kimura 2-parameter distance as implemented in PHYLIP software (version 3.5c).

URLs. RepeatMasker is available at http://www.repeatmasker.org/. GENSCAN is available at http://genes.mit.edu/GENSCAN.html. BLAST search is available at http://www.ncbi.nlm.nih.gov/BLAST/. Primer 3 is available at http://www.genome.wi.mit.edu/cgi-bin/primer/primer3_www.cgi/. PHYLIP software is available at http://evolution.genetics.washington.edu/phylip.html. The sequence of the *jsd* critical region is available at http://jura.wi.mit.edu/page.

GenBank accession numbers. *jsd* critical region BACs: RPCI-22-292L24, AC079222; RPCI-23-395H12, AC079134. Mouse *Utp14b* cDNAs, AY316161 and AY316162; mouse *Utp14a* cDNA, AY316163; human *UTP14A* cDNA, BC001149; human *UTP14C* cDNA (KIAA0266), D87455. Genomic sequence of *Utp14b*-like retrogenes: baboon, AY316164; chimpanzee, AY316165; cow, AY316166; elephant, AY316167; gorilla, AY316168; guinea pig, AY316169; hamster, AY316170; lemming, AY316171; lemur, AY316172; orangutan, AY316173; rat, AY316174; rhesus monkey, AY316175; squirrel monkey, AY316176. Genomic sequence of *Utp14b*-derived pseudogene in mouse, AY641472.

Note: Supplementary information is available on the Nature Genetics website.

ACKNOWLEDGMENTS

We thank W. Beamer for providing C57BL/6J *jsd*/+ mice; the Genome Sequencing group at the Whitehead/MIT Center for Genome Research for BAC sequencing; B. Birren and E.S. Lander for support; and A. Bortvin, J. Alfoldi, J. Koubova, J. Lange, J. Potash, J. Saionz, J. Wang, K. Kleene and S. Rozen for comments on the manuscript. This work was supported by the Howard Hughes Medical Institute.

COMPETING INTERESTS STATEMENT

The authors declare that they have no competing financial interests.

Received 3 February; accepted 3 June 2004
Published online at http://www.nature.com/naturegenetics/

1. Beamer, W.G., Cunliffe-Beamer, T.L., Shultz, K.L., Langley, S.H. & Roderick, T.H. *Juvenile spermatogonial depletion (jsd)*: a genetic defect of germ cell proliferation of male mice. *Biol. Reprod.* **38**, 899–908 (1988).
2. Boettger-Tong, H. *et al.* Identification and sequencing the juvenile spermatogonial depletion critical interval on mouse chromosome 1 reveals the presence of eight candidate genes. *Biochem. Biophys. Res. Commun.* **288**, 1129–1135 (2001).
3. Dragon, F. *et al.* A large nucleolar U3 ribonucleoprotein required for 18S ribosomal RNA biogenesis. *Nature* **417**, 967–970 (2002).
4. McCarrey, J.R. & Thomas, K. Human testis-specific *PGK* gene lacks introns and possesses characteristics of a processed gene. *Nature* **326**, 501–505 (1987).
5. Handel, M.A., Park, C. & Kot, M. Genetic control of sex-chromosome inactivation during male meiosis. *Cytogenet. Cell. Genet.* **66**, 83–88 (1994).
6. Solari, A.J. The behavior of the XY pair in mammals. *Int. Rev. Cytol.* **38**, 273–317 (1974).
7. Richler, C. *et al.* Splicing components are excluded from the transcriptionally inactive XY body in male meiotic nuclei. *Mol. Biol. Cell* **5**, 1341–1352 (1994).
8. Boettger-Tong, H.L., Johnston, D.S., Russell, L.D., Griswold, M.D. & Bishop, C.E. *Juvenile spermatogonial depletion (jsd)* mutant seminiferous tubules are capable of supporting transplanted spermatogenesis. *Biol. Reprod.* **63**, 1185–1191 (2000).
9. Ohta, H. *et al.* Defect in germ cells, not in supporting cells, is the cause of male infertility in the *jsd* mutant mouse: proliferation of spermatogonial stem cells without dif-

ferentiation. *Int. J. Androl.* **24**, 15–23 (2001).
10. Chen, H.H., Liu, T.Y., Li, H. & Choo, K.B. Use of a common promoter by two juxtaposed and intronless mouse early embryonic genes, *Rnf33* and *Rnf35*: implications in zygotic gene expression. *Genomics* **80**, 140–143 (2002).
11. Scanlan, M.J. *et al.* Humoral immunity to human breast cancer: antigen definition and quantitative analysis of mRNA expression. *Cancer Immun.* **1**, 4 (2001).
12. Dahl, H.-H.M., Brown, R.M., Hutchison, W.M., Maragos, C. & Brown, G.K. A testis-specific form of the human pyruvate dehydrogenase E1α subunit is coded for by an intronless gene on chromosome 4. *Genomics* **8**, 225–232 (1990).
13. Hendriksen, P.J.M. *et al.* Testis-specific expression of a functional retroposon encoding glucose-6-phosphate dehydrogenase in the mouse. *Genomics* **41**, 350–359 (1997).
14. Dass, B. *et al.* The gene for a variant form of the polyadenylation protein CstF-64 is on chromosome 19 and is expressed in pachytene spermatocytes in mice. *J. Biol. Chem.* **276**, 8044–8050 (2001).
15. Sargent, C.A., Young, C., Marsh, S., Ferguson-Smith, M.A. & Affara, N.A. The glycerol kinase gene family: structure of the Xp gene, and related intronless retroposons. *Hum. Mol. Genet.* **3**, 1317–1324 (1994).
16. Elliott, D.J. *et al.* An evolutionarily conserved germ cell-specific *hnRNP* is encoded by a retrotransposed gene. *Hum. Mol. Genet.* **9**, 2117–2124 (2000).
17. Sedlacek, Z. *et al.* Human and mouse *XAP-5* and *XAP-5-like* (*X5L*) genes: identification of an ancient functional retroposon differentially expressed in testis. *Genomics* **61**, 125–132 (1999).
18. Mardon, G. *et al.* Mouse *Zfx* protein is similar to *Zfy-2*: each contains an acidic activating domain and 13 zinc fingers. *Mol. Cell. Biol.* **10**, 681–688 (1990).
19. Ashworth, A., Skene, B., Swift, S. & Lovell-Badge, R. *Zfa* is an expressed retroposon derived from an alternative transcript of the *Zfx* gene. *EMBO J.* **9**, 1529–1534 (1990).
20. Boer, P.H., Adra, C.N., Lau, Y.F. & McBurney, M.W. The testis-specific phosphoglycerate kinase gene *pgk-2* is a recruited retroposon. *Mol. Cell. Biol.* **7**, 3107–3112 (1987).
21. Halford, S. *et al.* Characterization of a novel human opsin gene with wide tissue expression and identification of embedded and flanking genes on chromosome 1q43. *Genomics* **72**, 203–208 (2001).
22. Uechi, T., Maeda, N., Tanaka, T. & Kenmochi, N. Functional second genes generated by retrotransposition of the X-linked ribosomal protein genes. *Nucleic Acids Res.* **30**, 5369–5375 (2002).
23. Cremers, F.P. *et al.* An autosomal homologue of the choroideremia gene colocalizes with the Usher syndrome type II locus on the distal part of chromosome 1q. *Hum. Mol. Genet.* **1**, 71–75 (1992).
24. Banks, K.G. *et al.* Retroposon compensatory mechanism hypothesis not supported: *Zfa* knockout mice are fertile. *Genomics* **82**, 254–260 (2003).
25. Tohda, A. *et al.* Testosterone suppresses spermatogenesis in *juvenile spermatogonial depletion* (*jsd*) mice. *Biol. Reprod.* **65**, 532–537 (2001).
26. Kojima, Y. *et al.* Cessation of spermatogenesis in *juvenile spermatogonial depletion* (*jsd/jsd*) mice. *Int. J. Urol.* **4**, 500–507 (1997).
27. Nagase, T. *et al.* Prediction of the coding sequences of unidentified human genes. VI. The coding sequences of 80 new genes (KIAA0201-KIAA0280) deduced by analysis of cDNA clones from cell line KG-1 and brain. *DNA Res.* **3**, 321-329, 341–354 (1996).
28. Vanin, E.F. Processed pseudogenes. Characteristics and evolution. *Biochim. Biophys. Acta* **782**, 231–241 (1984).
29. Zhang, Z., Harrison, P.M., Liu, Y. & Gerstein, M. Millions of years of evolution preserved: a comprehensive catalog of the processed pseudogenes in the human genome. *Genome Res.* **13**, 2541–2558 (2003).
30. Lander, E.S. *et al.* Initial sequencing and analysis of the human genome. *Nature* **409**, 860–921 (2001).

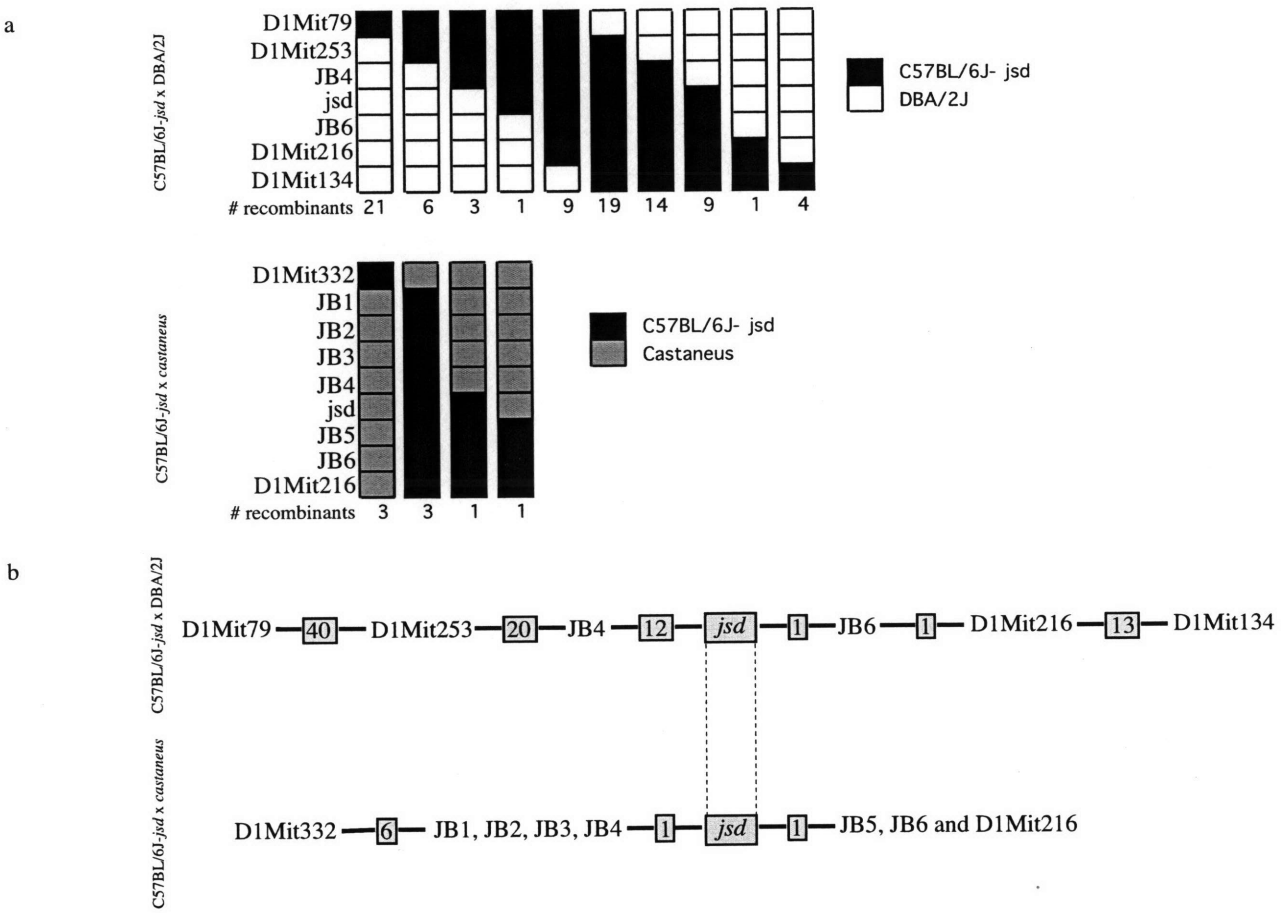

Supplementary Figure 1. Genetic linkage mapping of *jsd*. (**a**) Recombinant chromosomes identified among F2 progeny of C57BL/6J-jsd/jsd females mated with DBA/2J (above) or Mus musculus castaneus/Ei (below) males. For each of the two crosses, genetic markers are listed on the left from proximal (top) to distal (bottom). The columns represent the deduced genotypes of recombinant chromosomes; immediately below are indicated the numbers of each recombinant type observed. (**b**) Genetic maps emerging from the data presented in part (a). Genetic markers are listed from proximal (left) to distal (right). The numbers of cross-overs observed between markers are highlighted in yellow. Genetic markers that were recombinationally inseparable in the *M. m. castaneus* cross are grouped together there.

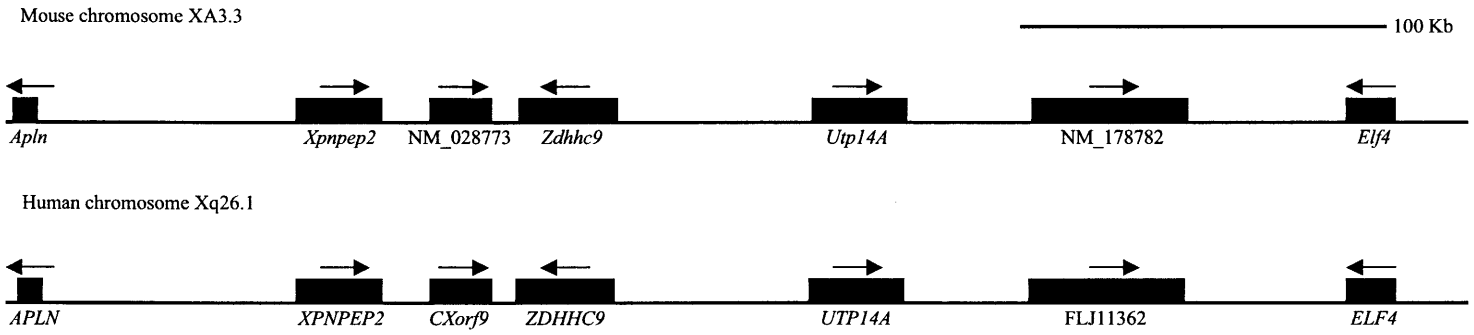

Supplementary Figure 2: Gene maps of the regions of the mouse and human X chromosomes that contain the *Utp14A/UTP14A* gene.

Supplementary Figure 3: Amino acid alignments of human and mouse proteins homologous to yeast Utp14.

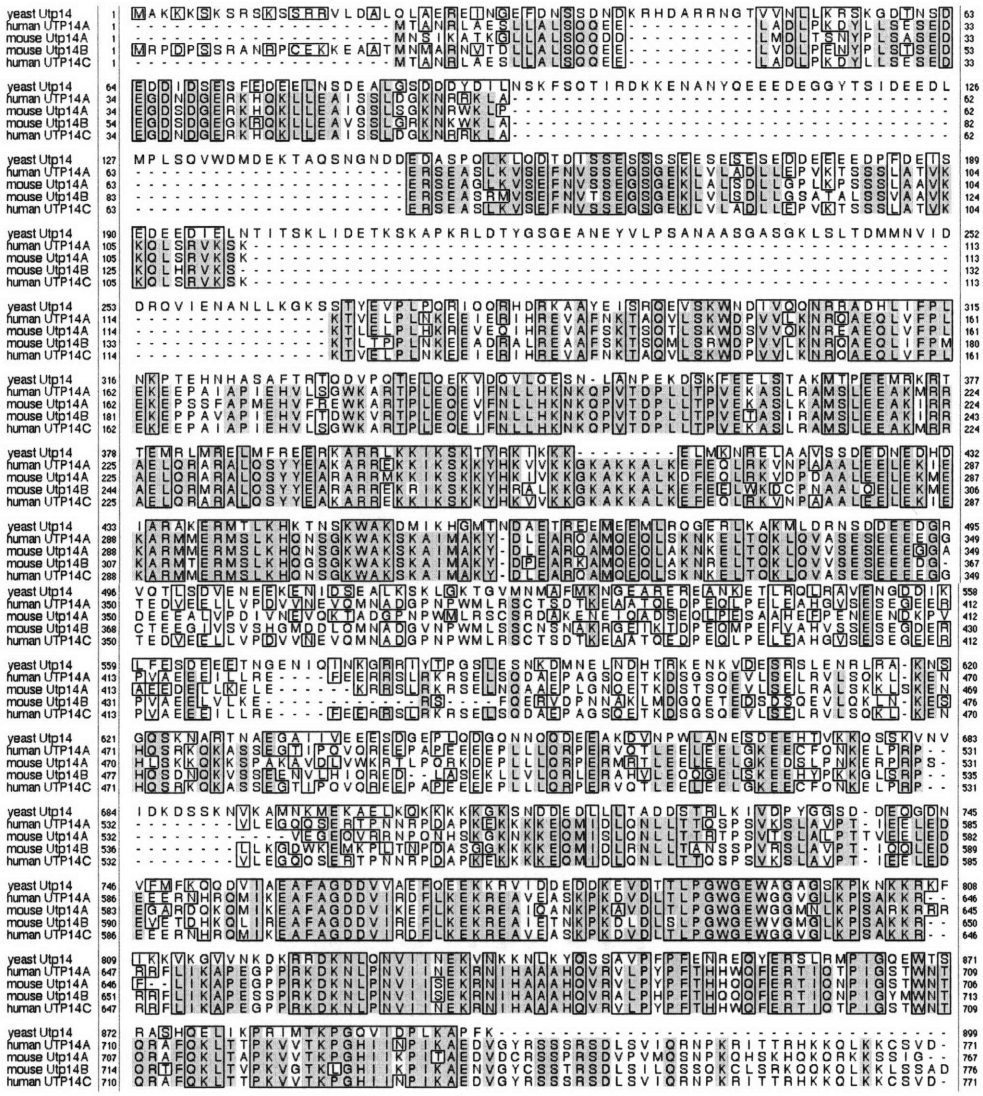

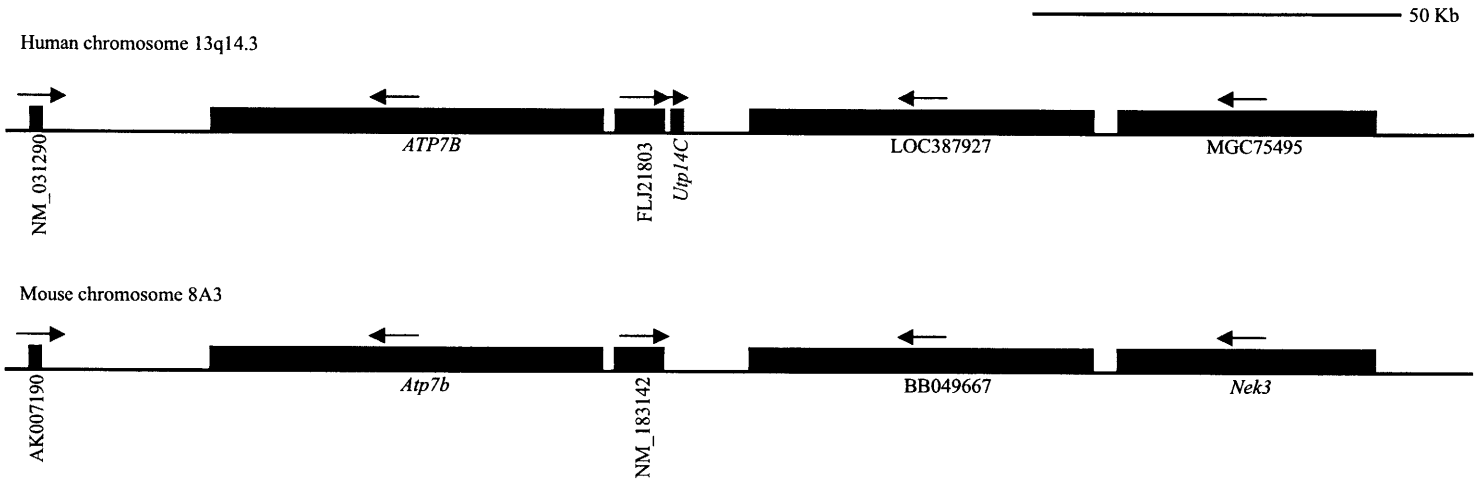

Supplementary Figure 4: Gene maps of the *Utp14C* insertion region on human chromosome 13 and the syntenic region of the mouse genome.

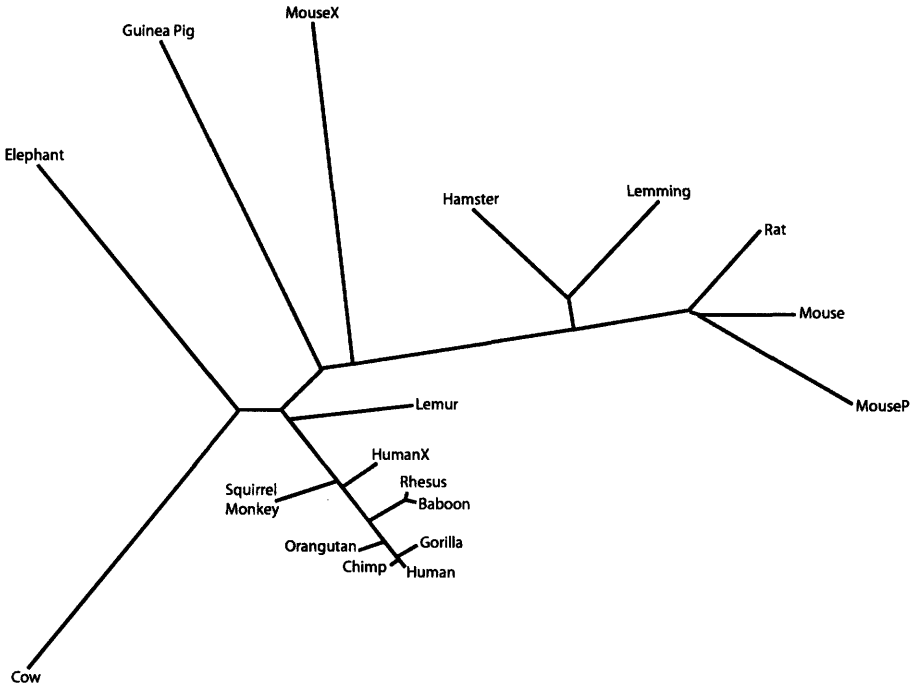

Supplementary Figure 5 : Phylogenetic tree of *jsd* sequences. Unrooted tree generated by neighbor-joining/UPGMA method version 3.572c. All *jsd* orthologs (processed pseudogenes) are represented by the name of the species that they were sequenced from, the X-linked progenitor genes are indicated by species name followed by an X, and the only identified pseudogene (found in mouse) is indicated by mouseP.

Chapter 3

The Vertebrate-specific Gene *Stra8* is Required for Meiotic Initiation in Mice

Andrew E. Baltus, Douglas B. Menke, Yueh-Chiang Hu, Mary L. Goodheart,

Anne E. Carpenter, Dirk G. de Rooij, and David C. Page

Author contributions:

DBM generated the *Stra8* knockout ES cells, MLG injected the ES cells into blastocyts, AEB conceived of and performed all further experiments with the follow support; Y-CH provided technical assistance during generation of ovarian single cell suspensions and subsequent antibody staining, AEC designed the software used to perform the DNA content analysis and DGD provided invaluable expertise on the morphological characterization of testicular germ cells.

Abstract

The transition from mitosis to meiosis is a defining juncture in the life cycle of sexually reproducing organisms. In mammals, molecular factors governing meiotic initiation have not been elucidated. Here we report that *Stra8*, a gene found only in vertebrates, is required for meiotic initiation in female and male mice, despite a marked difference in timing between the sexes. *Stra8*-deficient female germ cells fail to undergo meiotic DNA replication, chromosome condensation, cohesion, synapsis and recombination. *Stra8*-deficient male germ cells also have a premeiotic defect, resulting in arrest and apoptosis prior to meiotic prophase. Combined with other recent observations, our findings suggest a pivotal role for *Stra8* in sexually differential regulation of meiotic initiation.

Introduction

Meiosis is the keystone of sexual reproduction, enabling diploid organisms to produce haploid gametes. Mechanisms by which diploid cells transition from mitosis to meiosis have been studied intensely in some invertebrates, including *S. cerevisiae (Honigberg and Purnapatre, 2003)* and *C. elegans (Hansen et al., 2004).* In these two species, the molecular pathways governing meiotic initiation appear to be dissimilar (Kadyk and Kimble, 1998), and there is no evidence that either pathway is conserved to vertebrates, where mechanisms regulating the transition into meiosis have not been determined. However, one gene, *Stimulated by retinoic acid gene 8 (Stra8),* is known to be expressed exclusively in premeiotic germ cells in both sexes of mice. In females, *Stra8* is expressed in the embryonic ovary, in an anterior-to-posterior wave that precedes a similar wave of expression of early meiotic genes (Bullejos and Koopman, 2004; Menke et al., 2003; Yao et al., 2003). In males, *Stra8* is expressed in pubertal and adult testes, in premeiotic spermatogenic cells (Oulad-Abdelghani et al., 1996). Thus, *Stra8* might play a role early in meiosis, or perhaps in the transition from mitosis to meiosis, in both sexes.

Results

Stra8 is required for male and female fertility, but not viability

To explore the role of *Stra8* in germ cell development, we employed gene targeting to derive mice that lack *Stra8* function (Figure 1). We found that both female and male homozygotes for the targeted *Stra8* allele were infertile with no viability or observed non-gonadal defects. Heterozygotes were fertile. Inspection of the reproductive organs of *Stra8*-deficient adults revealed a marked reduction in the size of ovaries and testes (Figure 2A and 2B). While the ovaries of heterozygous females displayed a normal distribution of maturing ovarian follicles at 8 weeks of age (Figure 2C), the ovaries of *Stra8*-deficient females contained no oocytes or follicles (Figure 2D). While heterozygous males displayed normal spermatogenesis at 8 weeks of age, with a full range of premeiotic, meiotic, and postmeiotic cells (Figure 2E), the testicular germ cells of *Stra8*-deficient animals were severely reduced in number, and all appeared to be premeiotic (Figure 2F). This germ cell depletion would explain the observed reduction in testis weights.

Stra8-deficient female germ cells do not undergo meiotic chromosome condensation

Having found no oocytes in 8-week-old *Stra8*-deficient females, we compared histologically the gonadal germ cells of wild-type and *Stra8*-deficient female embryos. We observed no differences through embryonic day 13.5 (E13.5). In wild-type ovaries, germ cells proliferate mitotically until about E13.5, by which time they acquire a distinctive morphology, with patches of condensed chromatin at the periphery of the nucleus (Hartung and Stahl, 1977; McLaren and Southee, 1997) (Figure 3A). *Stra8*-

Figure 1. Targeted disruption of the *Stra8* locus. (**A**) A 7.8kb region of chromosome 6, containing exons 2-7 of the *Stra8* gene, was replaced with an *IRES-LacZ/PGK-Neo* selection cassette. E, EcoRV; B, BamHI. (**B**) Southern blot confirmation of correctly targeted ES cell clones using a BamHI/EcoRV (E/B) restriction digest and a probe 3' of the targeted region. The wild-type allele yields a 6.8kb E/B fragment, while the homologously targeted allele yields a 2.9kb E/B fragment. (**C**) Germline transmission of the targeted *Stra8* allele verified using a multiplex PCR assay (primers a, b and c indicated on panel A).

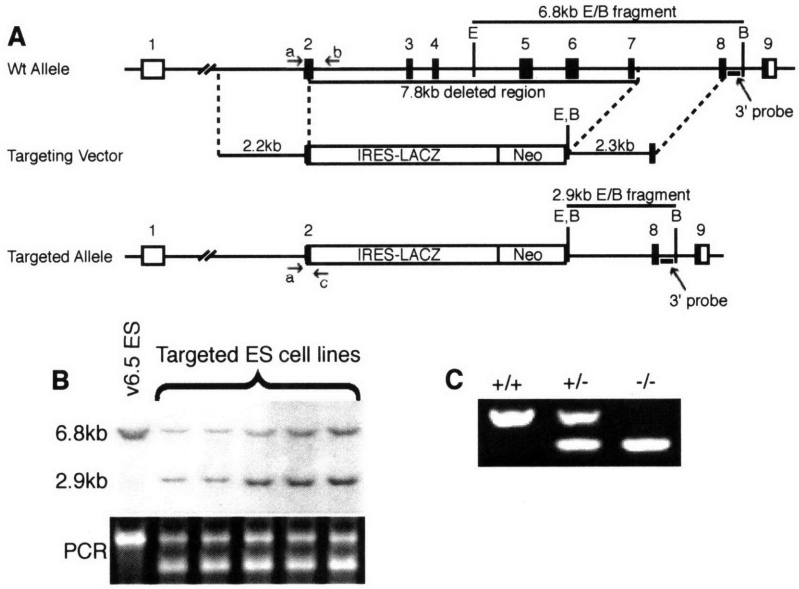
A
Wt Allele
6.8kb E/B fragment
E
B
1
2
3
4
5
6
7
8
9
a
b
7.8kb deleted region
3' probe
E,B
Targeting Vector
2.2kb
IRES-LACZ
Neo
2.3kb
2.9kb E/B fragment
Targeted Allele
c
B
v6.5 ES
Targeted ES cell lines
6.8kb
2.9kb
PCR
C
+/+
+/-
-/-

Figure 2. Germ cell loss and reduced gonadal size in *Stra8*-deficient mice. (**A**) Gross morphology of *Stra8*-deficient (right) and wild-type (left) ovaries from 8-week-old littermates. (**B**) Gross morphology of *Stra8*-deficient (right) and wild-type (left) testes from 8-week-old littermates. (**C** to **F**) Photomicrographs of hematoxylin and eosin-stained sections of gonads, all from 8-week-old animals: wild-type ovary (**C**), *Stra8*-deficient ovary (**D**), wild-type testis (**E**), and *Stra8*-deficient testis (**F**).

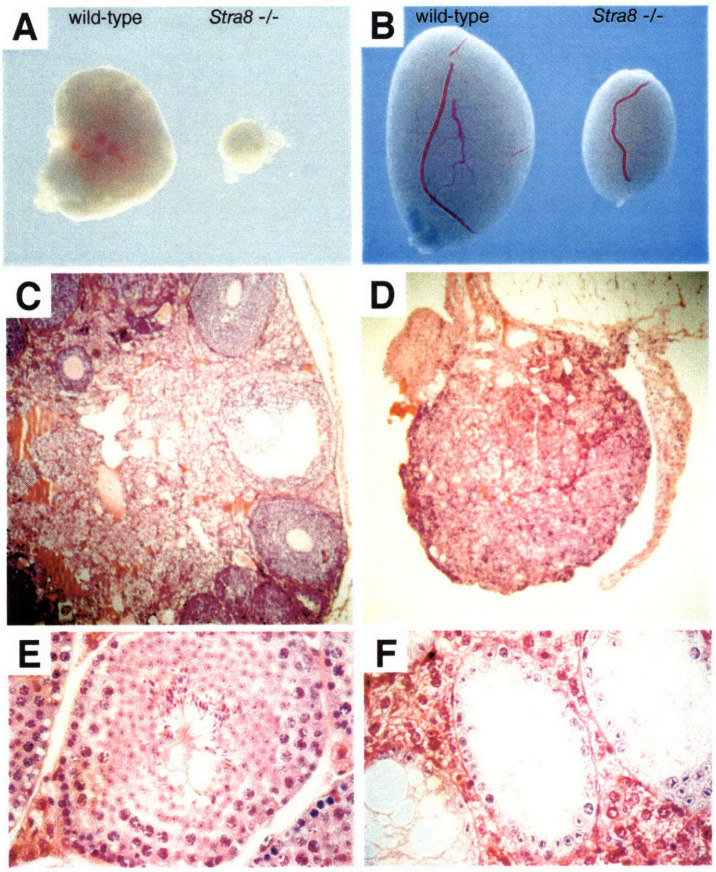
A
wild-type
Stra8 -/-
B
wild-type
Stra8 -/-
C
D
E
F

Figure 3. Photomicrographs of hematoxylin and eosin-stained ovarian sections from wild-type and *Stra8*-deficient littermate embryos at E13.5 (**A** and **B**), E14.5 (**C** and **D**), and E16.5 (**E** and **F**). Arrows indicate representative germ cells.

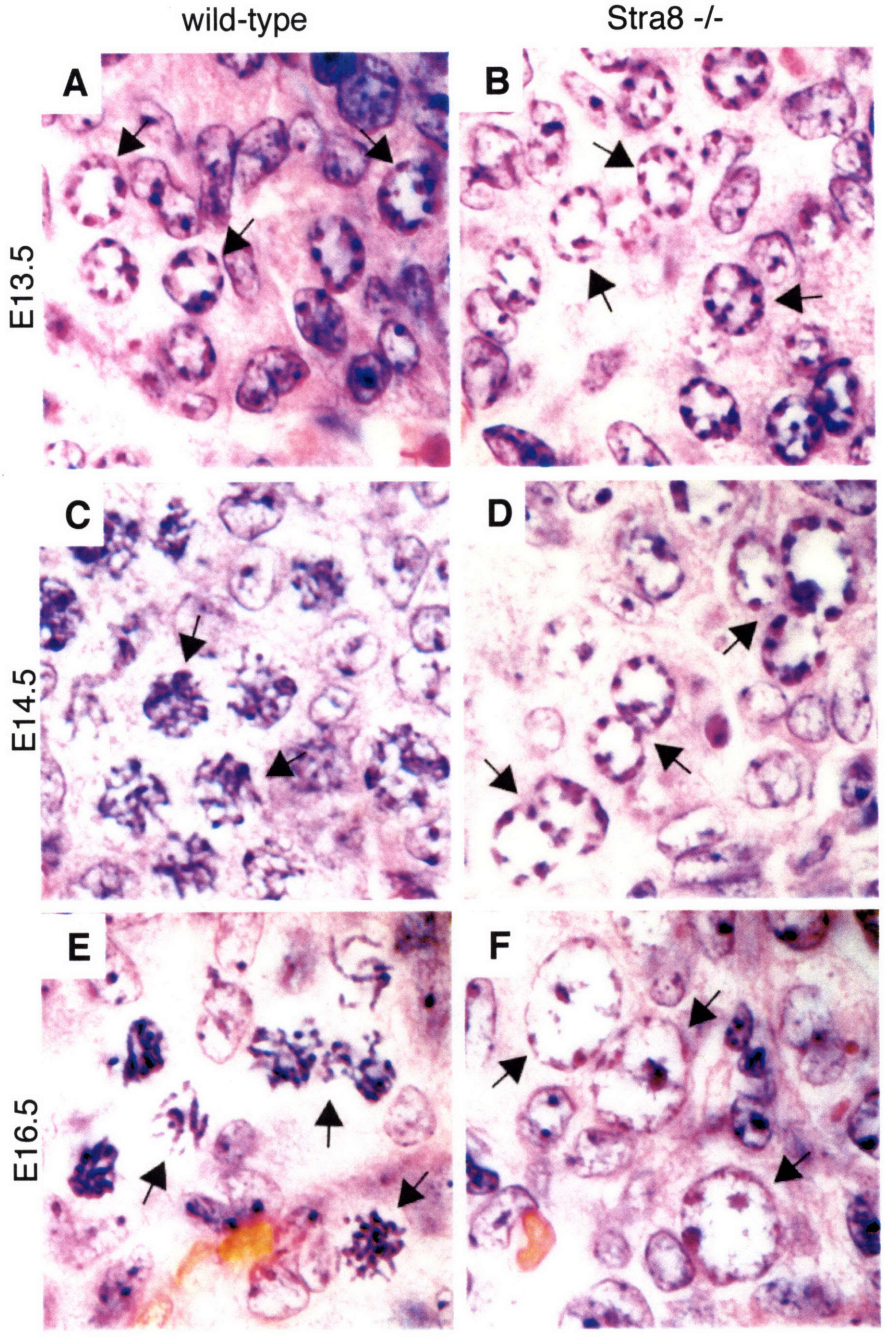
wild-type
Stra8 -/-
A
B
C
D
E
F
E13.5
E14.5
E16.5

deficient germ cells also display this premeiotic morphology at E13.5 (Figure 3B). Interestingly, testicular germ cells exhibit a similar morphology at about this time, which, as some studies have suggested, may be a pivotal period of germ cell sensitivity to extrinsic meiosis-inducing or inhibiting factors that differ between female and male gonads (Devictor et al., 1979; McLaren and Southee, 1997). We conclude that *Stra8* function is not required for germ cells to develop the premeiotic morphology observed in wild-type females at E13.5.

In ovaries of wild-type embryos, germ cells enter meiotic prophase in a spatiotemporal wave that begins at E13.5-E14.5 (Borum, 1961; Bullejos and Koopman, 2004; Hartung and Stahl, 1977; Menke et al., 2003; Speed, 1982; Yao et al., 2003). By E14.5, many germ cells in wild-type ovaries display the thread-like chromosome condensation that defines leptotene, the initial stage of meiotic prophase (Figure 3C). By E16.5, most germ cells in wild-type ovaries exhibit the more advanced nuclear morphologies that characterize the zygotene and pachytene stages of meiotic prophase (Figure 3E). By contrast, the germ cells of *Stra8*-deficient ovaries do not advance beyond the premeiotic morphology observed in wild-type ovaries at E13.5 (Figure 3D and 3F). Instead, *Stra8*-deficient germ cells retain this morphology until at least E16.5, by which point most of their nuclei are enlarged (Figure 3F). (Oocytes with a similar morphology are sometimes observed in age-matched wild-type ovaries, but at much lower frequency.) By birth, *Stra8*-deficient ovaries are severely depleted of germ cells (data not shown). Taken as a whole, these histological findings suggest that, in female embryos, *Stra8*-deficient germ cells develop normally to the brink of meiosis but do not undergo the chromosome condensation indicative of early meiotic prophase.

***Stra8*-deficient female germ cells do not initiate meiotic prophase**

Our histological findings suggested that *Stra8* might be required for female germ cells to enter meiotic prophase. If so, then the chromosomes of *Stra8*-deficient female germ cells should not be decorated with the cohesion or synaptonemal complexes characteristic of meiotic prophase. To test this, we immunostained chromosomes from ovarian germ cells of wild-type and *Stra8*-deficient E15.5 littermates with antibodies to either REC8, a meiotic cohesin (Eijpe et al., 2003; Lee et al., 2003), or SCP3, a synaptonemal complex protein (Moens and Spyropoulos, 1995). As expected, REC8 and SCP3 proteins were found along the lengths of chromosomes in most wild-type oocytes at this time (Figure 4A and 4B). In all *Stra8*-deficient germ cells, REC8 and SCP3 were localized not along the lengths of chromosomes, but in the patterns recently reported in premeiotic germ cells of the embryonic ovary (Figure 4A and 4B)(Prieto et al., 2004). We conclude that *Stra8* is required in female germ cells for meiotic cohesion and synaptonemal complex formation.

If *Stra8* is required for female meiotic prophase, then *Stra8*-deficient cells should not engage in meiotic recombination. Accordingly, we asked whether *Stra8*-deficient female germ cells form DNA double-strand breaks (DSBs), a hallmark of meiotic recombination. When DNA DSBs are formed, cells respond by phosphorylating H2AX, a histone H2A isoform, to yield γ-H2AX (Rogakou et al., 1998). As expected, immunostaining for γ-H2AX revealed the presence of DNA DSBs throughout the ovaries of wild-type embryos at E15.5 (Figure 4C). By contrast, the ovaries of *Stra8*-deficient

Figure 4. Testing ovarian germ cells for molecular markers of meiotic prophase. (**A** and **B**) Immunohistochemical staining for REC8 protein (**A**) or SCP3 protein (**B**) in wild-type and *Stra8*-deficient oocytes. (**C**) Whole-mount immunohistochemical staining for γ-H2AX protein in wild-type and *Stra8*-deficient E15.5 ovaries. (**D**) Whole-mount *in situ* hybridization for *Dmc1* mRNA in wild-type and *Stra8*-deficient E15.5 ovaries. (**E**) RT-PCR analysis of *Spo11* and *Dmc1* transcription in wild-type and *Stra8*-deficient E14.5 ovaries; *β-actin* serves as a control.

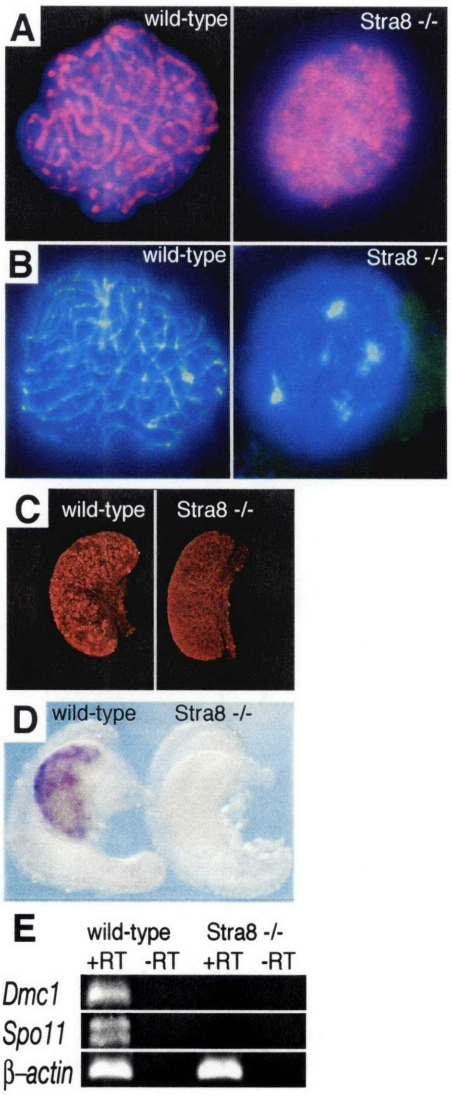
A
wild-type
Stra8 -/-
B
wild-type
Stra8 -/-
C
wild-type
Stra8 -/-
D
wild-type
Stra8 -/-
E
wild-type
Stra8 -/-
+RT
-RT
+RT
-RT
Dmc1
Spo11
β–actin

embryos were negative for γ-H2AX, indicating that DNA DSBs had not formed (Figure 4C).

In additional tests of engagement in meiotic recombination, we asked whether *Stra8*-deficient female germ cells express *Spo11* and *Dmc1*, which are genes required, respectively, to form and to repair meiotic DSBs (Baudat et al., 2000; Pittman et al., 1998; Romanienko and Camerini-Otero, 2000; Yoshida et al., 1998). As previously demonstrated by whole-mount *in situ* hybridization, *Stra8* is expressed shortly before *Dmc1* in wild-type embryonic ovaries (Menke et al., 2003). By this same assay, we found that *Stra8*-deficient germ cells do not express *Dmc1* (Figure 4D), a result confirmed by RT-PCR analysis (Figure 4E). Likewise, *Spo11* was not expressed in *Stra8*-deficient female germ cells (Figure 4E). Taken together, the absence of γ-H2AX staining and the absence of *Spo11* and *Dmc1* expression provide strong evidence that *Stra8*-deficient female germ cells do not undertake meiotic recombination.

Stra8-deficient female germ cells complete the last mitotic division, but do not undergo premeiotic DNA replication

Immediately prior to meiotic prophase, germ cells replicate their DNA and so become 4N. Given the weight of evidence that *Stra8* is required for female germ cells to enter meiotic prophase, the question arises whether *Stra8* is also required for premeiotic DNA replication. Although no markers specific to premeiotic replication are known in mammals, this replication has been shown to occur during the 15 hours preceding meiotic prophase (Crone et al., 1965). By image cytometry, we compared the DNA content of

cells from wild-type and *Stra8*-deficient ovaries at E14.5 and E15.5, when wild-type 4N germ cells should accumulate in meiotic prophase. We first analyzed DNA content in cells of the entire ovary, where germ cells are greatly outnumbered by somatic cells. In wild-type ovaries, the proportion of 4N cells increases from E14.5 (Figure 5A) to E15.5 (Figure 5C), reflecting the increasing number of germ cells that have completed premeiotic replication. By contrast, *Stra8*-deficient ovaries contain few if any 4N cells, and their numbers do not increase (Figure 5B and 5D), implying that *Stra8*-deficient germ cells have not undergone premeiotic replication.

To validate this inference, we used a germ-cell-specific antibody (α-MVH) (Toyooka et al., 2000) to isolate cell populations enriched in germ cells. In wild-type ovaries, a substantial fraction of such cells are 4N at E14.5 (Figure 5E), and the great majority are 4N at E15.5 (Figure 5G). In *Stra8*-deficient ovaries, few such cells are 4N at either E14.5 (Figure 5F) or E15.5 (Figure 5H). Due to the fact that the small population of 4N germ cells found in *Stra8*-deficient ovaries at E14.5 are no longer present at E15.5 we conclude that they are likely to be cells that have yet to finish their last mitosis at E14.5 but have by E15.5. We cannot exclude the possibility that they represent a small percentage of *Stra8*-deficient germ cells that undergo premeiotic DNA replication and then die before E15.5. We conclude that, in female germ cells, *Stra8* is required not only for entry into meiotic prophase, but also for the DNA replication that precedes it.

Figure 5. Histograms of cellular DNA content in embryonic ovaries. (**A** to **D**) All cells from (**A**) wild-type E14.5, (**B**) *Stra8*-deficient E14.5, (**C**) wild-type E15.5, or (**D**) *Stra8*-deficient E15.5 ovary. (**E** to **H**) Germ cells from (**E**) wild-type E14.5, (**F**) *Stra8*-deficient E14.5, (**G**) wild-type E15.5, or (**H**) *Stra8*-deficient E15.5 ovary.

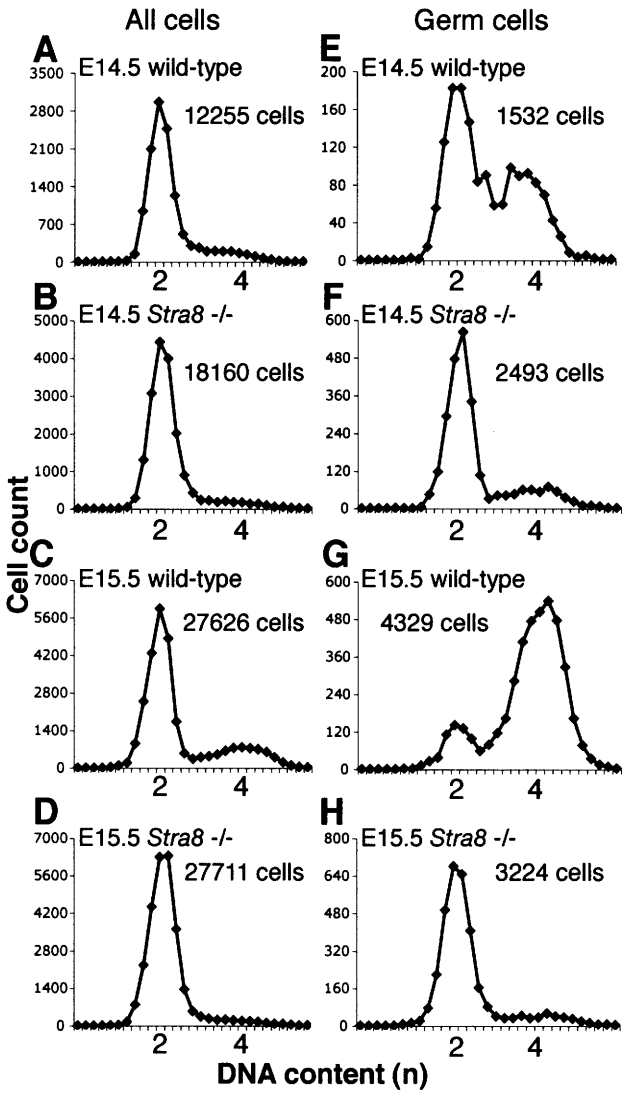
All cells
Germ cells
A
E14.5 wild-type
12255 cells
E
E14.5 wild-type
1532 cells
B
E14.5 Stra8 -/-
18160 cells
F
E14.5 Stra8 -/-
2493 cells
C
E15.5 wild-type
27626 cells
G
E15.5 wild-type
4329 cells
D
E15.5 Stra8 -/-
27711 cells
H
E15.5 Stra8 -/-
3224 cells
Cell count
DNA content (n)

Stra8-deficient male germ cells become apoptotic prior to entry into meiotic prophase

Is *Stra8* also required for male meiosis? In wild-type male mice, spermatogenesis is initiated shortly after birth. Spermatogonia (Figure 6A) undertake a series of mitotic divisions, eventually giving rise to a population of spermatocytes, which undergo meiosis. In wild-type mice of the strain that we employed, spermatocytes first appear 7 or 8 days after birth (Figure 6C) and quickly progress into meiotic prophase (Ashley, 2004; Bellve et al., 1977). In *Stra8*-deficient males, spermatogonial divisions appear to proceed normally (Figure 6B), with premeiotic spermatocytes appearing as expected 7 or 8 days after birth (Figure 6D). These *Stra8*-deficient spermatocytes (Figure 6D) display premeiotic chromatin condensation as in wild-type testes (Figure 6C), but here the development of *Stra8*-deficient spermatocytes appears to cease. While wild-type cells readily progress through leptotene (Figure 6E) and zygotene (Figure 6G) stages of meiotic prophase, most *Stra8*-deficient spermatocytes undergo apoptosis before reaching these stages (Figure 6F and 6H). Admixture with mitotically active spermatogonia precluded our determining whether *Stra8*-deficient spermatocytes replicate their DNA before undergoing apoptosis. Nonetheless, we conclude that male germ cells, like female germ cells, require *Stra8* for early meiotic events prior to prophase.

The _Stra8_ gene appears to have emerged during vertebrate evolution

To address the evolution of the *Stra8* gene we used the mouse *Stra8* cDNA sequence to search available databases electronically for *Stra8* homologs in all species for

Figure 6. Photomicrographs of hematoxylin and eosin-stained sections from wild-type and *Stra8*-deficient testes at 7 or 8 days after birth. In each section, arrows indicate the most advanced spermatogenic cell type; arrowheads indicate apoptotic cells. (**A** and **B**) B-type spermatogonia in wild-type and *Stra8*-deficient testes. (**C** and **D**) Preleptotene spermatocytes in wild-type and *Stra8*-deficient testes. (**E**) Leptotene spermatocytes in wild-type testes. (**F**) Preleptotene spermatocytes in *Stra8*-deficient testes, with no meiotic chromosome condensation. (**G**) Zygotene spermatocytes in wild-type testes. (**H**) Preleptotene spermatocytes and apoptotic spermatocytes in *Stra8*-deficient testes.

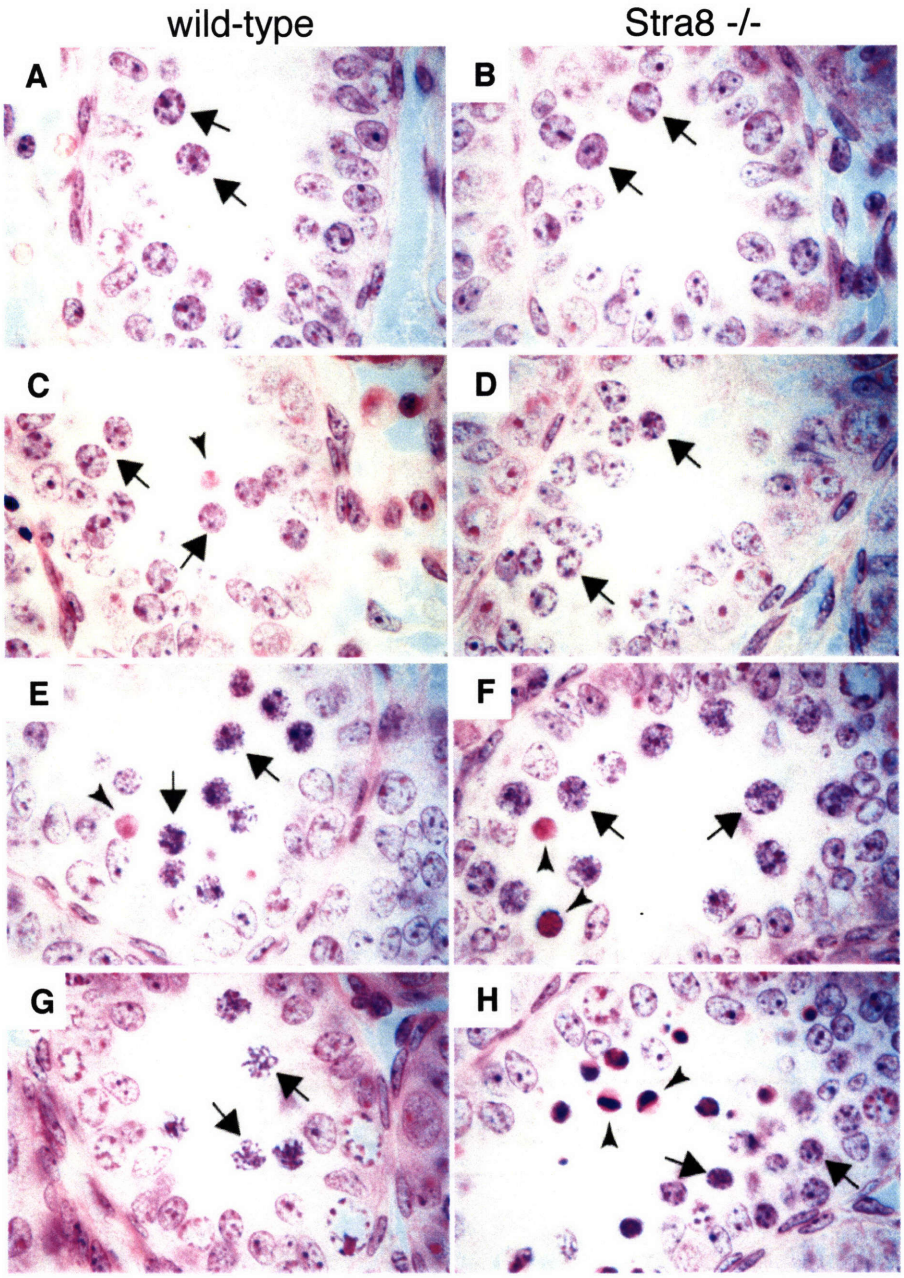
wild-type
Stra8 -/-
A
B
C
D
E
F
G
H

which sequence data are available. From genomic and EST sequence data we have identified predicted *Stra8* orthologs in 9 other vertebrate species (human, chimp, cow, rabbit, rat, dog, chicken, opossum and rainbow trout). A *Stra8* ortholog was not found in any invertebrate genome or in several non-mammalian vertebrate species with abundant genomic sequence data, including pufferfish, zebrafish, medaka and xenopus. Alignment of the proteins encoded by the various *Stra8* orthologs for which we were able to get a full-length sequence (Figure 7) reveals a conserved helix-loop-helix (HLH) domain, usually associated with regulation of developmental cell fate decisions via transcriptional activation and/or repression(Garrell and Campuzano, 1991; Littlewood and Evan, 1995; Massari and Murre, 2000). Additionally, the presence of several highly conserved stretches containing serine, threonine or tyrosine residues (putative phosphorylation sites) is consistent with the previous report that several different phosphorlyated isoforms of *Stra8* can be found in P19 teratocarcinoma cells after exposure to RA(Oulad-Abdelghani et al., 1996).

Figure 7. Alignment of identified STRA8 orthologs. Highly conserved amino acids are highlighted in orange. The black box indicates the conserved helix-loop-helix domain.

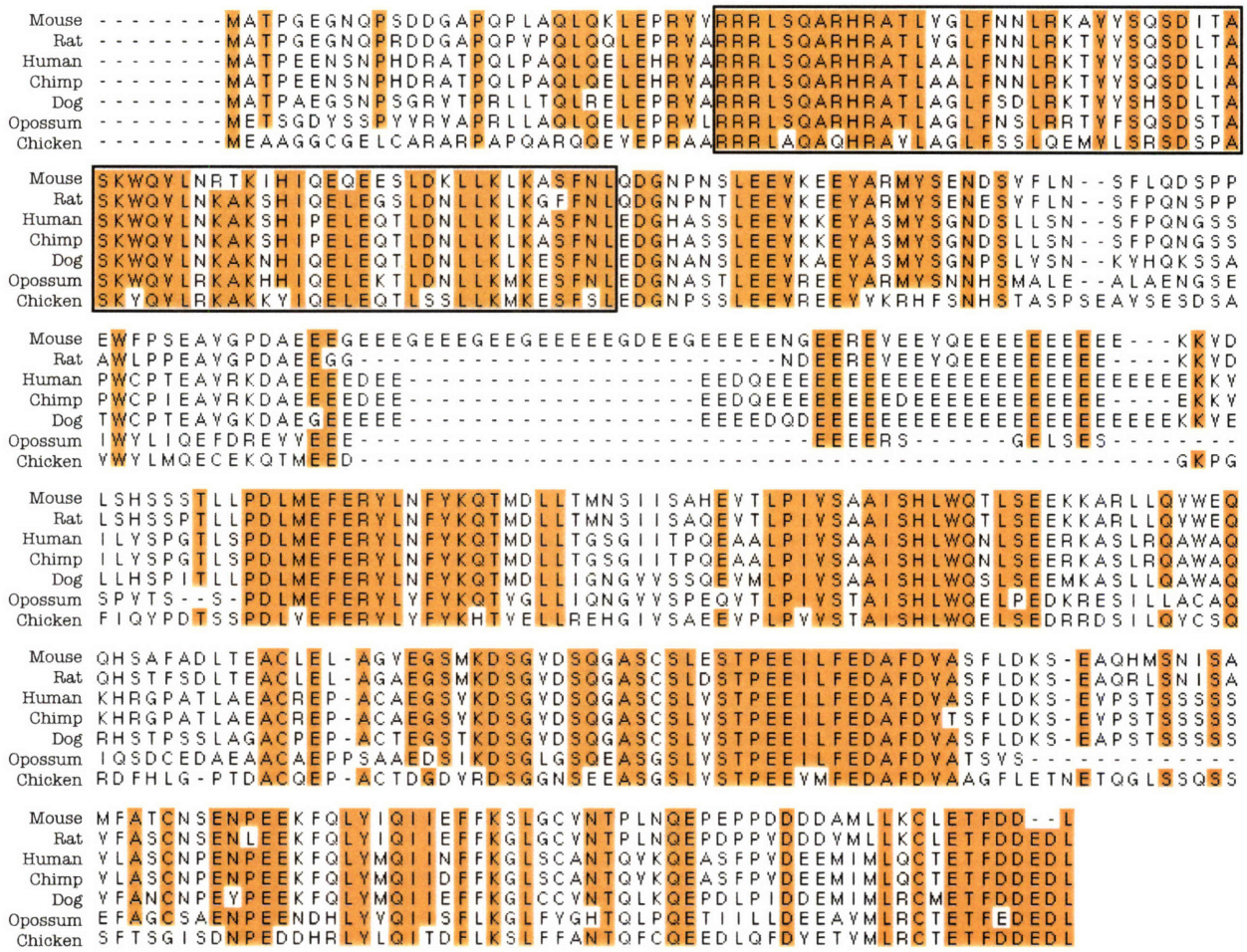
Mouse
Rat
Human
Chimp
Dog
Opossum
Chicken

Discussion

Stra8 defines a key juncture in germ cells' transition from mitosis to meiosis. It functions prior to meiotic prophase and, at least in females, before or during premeiotic replication. Although many other genes are known to be required for vertebrate meiosis, they function during or after meiotic prophase in females and males. For example, germ cells lacking either *Rec8*, *Scp3*, *Dmc1*, or *Spo11* readily progress into meiotic prophase in both females and males (Bannister et al., 2004; Baudat et al., 2000; Pittman et al., 1998; Romanienko and Camerini-Otero, 2000; Xu et al., 2005; Yoshida et al., 1998; Yuan et al., 2002; Yuan et al., 2000); germ cells lacking *Stra8* do not. Since *Stra8* functions before the other known meiotic factors, it might be engaged in regulating the transition or commitment to meiosis in mice.

In mice, germ cells in embryonic ovaries initiate meiosis while those in testes do so only after birth – a difference that must depend on factors governing expression of *Stra8*. In culture, retinoic acid treatment of embryonic carcinoma or embryonic stem cells induces expression of *Stra8* (Oulad-Abdelghani et al., 1996). Similarly, *Stra8* expression in germ cells of embryonic ovaries depends on retinoic acid signaling, while the absence of *Stra8* expression in embryonic testes appears to be caused by sex-specific degradation of retinoic acid in that developing organ (Koubova et al., 2006). We suggest that the dramatic difference in timing of meiotic initiation between mammalian females and males reflects a pivotal regulatory role for *Stra8* and its inducer, retinoic acid.

Materials and Methods

Targeted disruption of the *Stra8* locus

A *Stra8 IRES-LacZ/PGK-Neo* targeting construct was generated using PCR products amplified with Advantage HF2 polymerase (Clontech). All PCR products were sequenced to ensure the absence of point mutations. The v6.5 ES cell line (Rideout et al., 2000) was electroporated with 40 mg of linearized targeting construct DNA, and selection was performed with 300 mg/ml G418 (GIBCO-BRL). ES cell colonies were picked and screened by long distance PCR specific for homologous targeting at the 5' arm. Homologous targeting at the 3' arm was confirmed by Southern blot analysis. Correctly targeted ES cell clones were injected into Balb/c or C57Bl/6 blastocyts and transferred to pseudo-pregnant Swiss Webster females. Germline transmission was obtained with three independent clones.

Primers for PCR genotyping were as follows: p1 (5' AGCTGCAGAAGCTTGAGCCT 3'), p2 (5' AGGTCAGGCTGCTAGGATGC 3'), and p3 (5' TCCGATAGCTTGGCTGCAGGTC 3'). The wild-type allele gives rise to a PCR product of 280 bp. The mutant allele gives rise to a PCR product of 180 bp.

Histology

Dissected tissues were fixed overnight in Bouin's solution, embedded in paraffin, sectioned, and stained with hematoxylin and eosin. Images were obtained with a Nikon

Optipshot 2 microscope and a Kodak DC290 Zoom digital camera and Photoshop 7 (Adobe).

Meiotic chromosome spread preparations

Gonads removed from embryos between E14.5 and E15.5 were separated from mesonephroi and incubated in 50μl of Trypsin-EDTA solution at 37°C for 5 min, followed by a brief wash with PBS. To obtain single cells, digested gonads were repeatedly pipetted and then centrifuged, followed by resuspension in 30 μl of hypotonic solution (0.5% sodium chloride in PBS). Cell suspensions were placed on poly-L-lysine coated slides, which were kept in a humid chamber at room temperature until the cells settled. Cells on the slides were fixed in 2% paraformaldehyde/0.03% SDS solution for 1 hr at room temperature and washed three times in 0.4% Photoflo (Kodak) for 1 min, and air-dried. These slides were stored at ⁻80°C prior to use.

Cell spread immunohistochemistry

For fluorescence immunostaining, slides were removed from storage at ⁻80°C, washed twice in PBS and treated with blocking buffer (3%BSA/0.05%Tween-20/0.05% Triton X-100 in PBS). Cell preparations were then incubated with rabbit α-SCP3 or α-REC8 antibody (1:500, gifts from Christa Heyting, Department of Genetics, Agricultural University, Wageningen, The Netherlands) overnight at 4°C, washed with PBS, and incubated with Texas red or FITC conjugated secondary antibody (1:200, Jackson ImmunoResearch Laboratories) for 1 h at RT. Following extensive washing with PBS, slides were mounted using VECTASHIELD medium with DAPI (Vector Laboratories).

Images were taken using an Olympus BX51TF Fluorescence Microscope with a Spot RT digital camera and Spot version 4.1 software (Diagnostic Instruments).

Whole-mount immunohistochemistry

Whole-mount indirect fluorescent immunohistochemistry was performed as previously described (Albrecht and Eicher, 2001). Mouse monoclonal γ-H2AX antibody (Upstate) was used at a 1:1000 dilution and donkey α-mouse Texas red-conjugated secondary antibody (Jackson) was used at a 1:200 dilution. Images were merged z-stacks taken using a Zeiss LSM 510 meta confocal microscope.

Whole mount in situ hybridizations

Gonads for *in situ* hybridization were collected at E15.5 and fixed in 4% paraformaldehyde at 4°C overnight. Tissues were dehydrated into 100% methanol and stored at -20°C until used. Digoxigenin whole-mount *in situ* hybridizations for *Dmc1* were performed as previously reported (Menke et al., 2003).

RT-PCR

Total RNA was isolated from gonads using an RNA miniprep kit (Qiagen). Total RNA (1 μg) was reverse transcribed with oligo d(T)18N using 1st Strand cDNA Synthesis Kit for RT-PCR (Roche) in a total reaction volume of 20 μl, of which 1 μl was used as a template for PCR with the following primer sets. *Dmc1* primers: *Dmc1*fwd (5' CAGTATGACACTATCCAAAAATGGTATG 3') and *Dmc1*rev (5' CAATCACACACACTCAAAAACAATGTTC 3'). *Spo11* primers: *Spo11*fwd (5'

CTGTTGGCCATGGTGAGAGAGG 3') and *Spo11*rev (5' TCCTTGAATGTTAGTCGGCACAGC 3'). *β-actin* primers: *β-actin*fwd (5' TAAAGACCTCTATGCCAACACAGT 3') and *β-actin*rev (5' CACGATGGAGGGGCCGGACTCATC 3').

Preparation of ovarian single cell suspensions and DNA content analysis

Cell spreads were prepared as described above for meiotic chromosome spread preparations with the exception that cells were not treated with hypotonic solution. Immunostaining with rabbit α-MVH antibody (1:1000, a gift from Toshiaki Noce, Mitsubishi Kagaku Institute of Life Science, Tokyo, Japan) was also performed as described above. Images were captured for each slide in non-overlapping fields, for analysis of as many cells as possible without duplication. DAPI (blue) and MVH (red) images were taken using an Olympus BX51TF Fluorescence Microscope with Spot RT digital camera and Spot version 4.1 software (Diagnostic Instruments).

Each image set was then processed using the software program CellProfiler (http://www.cellprofiler.org (Carpenter et al., 2006)). For each field of view, the DAPI and MVH images were loaded and background fluorescence in the MVH images below an absolute threshold of 0.1 (the dynamic range of incoming images is 0 to 1) was set to 0. The DAPI and MVH images were aligned and nuclei were identified on the DAPI images using local intensity maxima with a maxima suppression neighborhood of 7 and a blur radius of 3. The nuclear edges were determined using a threshold calculated automatically using Otsu's method multiplied by an adjustment factor of 0.7. For this

analysis, objects touching the image border or those with area less than 35 pixels were discarded. Since MVH is a cytoplasmic protein, MVH-positive cells were identified using the nuclei as seeds for the propagate function (Jones et al., 2005), with a regularization factor of 0.05. The perimeter of the MVH-positive region was determined for each cell using a threshold calculated automatically using Otsu's method multiplied by an adjustment factor of 0.8 (6). The intensity of the DAPI and MVH signal was measured for each cell.

Prior to processing, clumped cells and non-cellular artifacts were manually removed from DAPI images (Adobe Photoshop 7.0). The CellProfiler analysis was performed automatically on all image sets to ensure unbiased, consistent results. Measurements collected by CellProfiler were then exported to Excel. As the majority of embryonic gonadal cells are non-replicating somatic cells (with 2N DNA content), we normalized the integrated intensity of DAPI (directly proportional to DNA content) of each cell to the median integrated intensity of DAPI (set to 2N) across the field. Cell data from several gonads at each time point and genotype were pooled and histograms were prepared with cells being sorted by DNA content into 40 bins of 0.2N ranging from 0-8N. Additionally, histograms were generated for germ-cell-enriched populations by binning only those cells with an integrated intensity of MVH above a threshold determined empirically for each dataset.

Acknowledgements

We thank Rudolf Jaenisch for v6.5 ES cells; Alex Bortvin, Terry Hassold and Terry Ashley for advice; Christa Heyting for SCP3 and REC8 antisera; Toshiaki Noce for MVH antisera; and E. Anderson, G. Baltus, M. Capelson, M. Gill, J. Koubova, J. Lange, Y. Lim, J. Mueller and J. Potash for comments on the manuscript.

References

Albrecht, K. H., and Eicher, E. M. (2001). Evidence that Sry is expressed in pre-Sertoli cells and Sertoli and granulosa cells have a common precursor. Dev Biol *240*, 92-107.

Ashley, T. (2004). The mouse "tool box" for meiotic studies. Cytogenet Genome Res *105*, 166-171.

Bannister, L. A., Reinholdt, L. G., Munroe, R. J., and Schimenti, J. C. (2004). Positional cloning and characterization of mouse mei8, a disrupted allelle of the meiotic cohesin Rec8. Genesis *40*, 184-194.

Baudat, F., Manova, K., Yuen, J. P., Jasin, M., and Keeney, S. (2000). Chromosome synapsis defects and sexually dimorphic meiotic progression in mice lacking Spo11. Mol Cell *6*, 989-998.

Bellve, A. R., Cavicchia, J. C., Millette, C. F., O'Brien, D. A., Bhatnagar, Y. M., and Dym, M. (1977). Spermatogenic cells of the prepuberal mouse. Isolation and morphological characterization. J Cell Biol *74*, 68-85.

Borum, K. (1961). Oogenesis in the mouse. A study of the meiotic prophase. Exp Cell Res *24*, 495-507.

Bullejos, M., and Koopman, P. (2004). Germ cells enter meiosis in a rostro-caudal wave during development of the mouse ovary. Mol Reprod Dev *68*, 422-428.

Carpenter, A. E., *et al.* (2006). CellProfiler: image analysis for high throughput microscopy. *in preparation.*

Crone, M., Levy, E., and Peters, H. (1965). The duration of the premeiotic DNA synthesis in mouse oocytes. Exp Cell Res *39*, 678-688.

Devictor, M., Luciani, J. M., and Stahl, A. (1979). [Do male germ cells begin meiosis during fetal life?]. J Genet Hum *27*, 21-28.

Eijpe, M., Offenberg, H., Jessberger, R., Revenkova, E., and Heyting, C. (2003). Meiotic cohesin REC8 marks the axial elements of rat synaptonemal complexes before cohesins SMC1beta and SMC3. J Cell Biol *160*, 657-670.

Garrell, J., and Campuzano, S. (1991). The helix-loop-helix domain: a common motif for bristles, muscles and sex. Bioessays *13*, 493-498.

Hansen, D., Hubbard, E. J., and Schedl, T. (2004). Multi-pathway control of the proliferation versus meiotic development decision in the Caenorhabditis elegans germline. Dev Biol *268*, 342-357.

Hartung, M., and Stahl, A. (1977). Preleptotene chromosome condensation in mouse oogenesis. Cytogenet Cell Genet *18*, 309-319.

Honigberg, S. M., and Purnapatre, K. (2003). Signal pathway integration in the switch from the mitotic cell cycle to meiosis in yeast. J Cell Sci *116*, 2137-2147.

Jones, T. R., A. E. Carpenter, A. E., and Golland, P. (2005). Voronoi-based segmentation of cells on image manifolds. Paper presented at: ICCV Workshop on Computer Vision for Biomedical Image Applications.

Kadyk, L. C., and Kimble, J. (1998). Genetic regulation of entry into meiosis in Caenorhabditis elegans. Development *125*, 1803-1813.

Koubova, J., Menke, D. B., Zhou, Q., Capel, B., Griswold, M. D., and Page, D. C. (2006). Retinoic acid regulates sex-specific timing of meiotic initiation in mice. PNAS *in press*.

Lee, J., Iwai, T., Yokota, T., and Yamashita, M. (2003). Temporally and spatially selective loss of Rec8 protein from meiotic chromosomes during mammalian meiosis. J Cell Sci *116*, 2781-2790.

Littlewood, T. D., and Evan, G. I. (1995). Transcription factors 2: helix-loop-helix. Protein Profile *2*, 621-702.

Massari, M. E., and Murre, C. (2000). Helix-loop-helix proteins: regulators of transcription in eucaryotic organisms. Mol Cell Biol *20*, 429-440.

McLaren, A., and Southee, D. (1997). Entry of mouse embryonic germ cells into meiosis. Dev Biol *187*, 107-113.

Menke, D. B., Koubova, J., and Page, D. C. (2003). Sexual differentiation of germ cells in XX mouse gonads occurs in an anterior-to-posterior wave. Dev Biol *262*, 303-312.

Moens, P. B., and Spyropoulos, B. (1995). Immunocytology of chiasmata and chromosomal disjunction at mouse meiosis. Chromosoma *104*, 175-182.

Oulad-Abdelghani, M., Bouillet, P., Decimo, D., Gansmuller, A., Heyberger, S., Dolle, P., Bronner, S., Lutz, Y., and Chambon, P. (1996). Characterization of a premeiotic germ cell-specific cytoplasmic protein encoded by Stra8, a novel retinoic acid-responsive gene. J Cell Biol *135*, 469-477.

Pittman, D. L., Cobb, J., Schimenti, K. J., Wilson, L. A., Cooper, D. M., Brignull, E., Handel, M. A., and Schimenti, J. C. (1998). Meiotic prophase arrest with failure of chromosome synapsis in mice deficient for Dmc1, a germline-specific RecA homolog. Mol Cell *1*, 697-705.

Prieto, I., Tease, C., Pezzi, N., Buesa, J. M., Ortega, S., Kremer, L., Martinez, A., Martinez, A. C., Hulten, M. A., and Barbero, J. L. (2004). Cohesin component dynamics during meiotic prophase I in mammalian oocytes. Chromosome Res *12*, 197-213.

Rideout, W. M., 3rd, Wakayama, T., Wutz, A., Eggan, K., Jackson-Grusby, L., Dausman, J., Yanagimachi, R., and Jaenisch, R. (2000). Generation of mice from wild-type and targeted ES cells by nuclear cloning. Nat Genet *24*, 109-110.

Rogakou, E. P., Pilch, D. R., Orr, A. H., Ivanova, V. S., and Bonner, W. M. (1998). DNA double-stranded breaks induce histone H2AX phosphorylation on serine 139. J Biol Chem *273*, 5858-5868.

Romanienko, P. J., and Camerini-Otero, R. D. (2000). The mouse Spo11 gene is required for meiotic chromosome synapsis. Mol Cell *6*, 975-987.

Speed, R. M. (1982). Meiosis in the foetal mouse ovary. I. An analysis at the light microscope level using surface-spreading. Chromosoma *85*, 427-437.

Toyooka, Y., Tsunekawa, N., Takahashi, Y., Matsui, Y., Satoh, M., and Noce, T. (2000). Expression and intracellular localization of mouse Vasa-homologue protein during germ cell development. Mech Dev *93*, 139-149.

Xu, H., Beasley, M. D., Warren, W. D., van der Horst, G. T., and McKay, M. J. (2005). Absence of mouse REC8 cohesin promotes synapsis of sister chromatids in meiosis. Dev Cell *8*, 949-961.

Yao, H. H., DiNapoli, L., and Capel, B. (2003). Meiotic germ cells antagonize mesonephric cell migration and testis cord formation in mouse gonads. Development *130*, 5895-5902.

Yoshida, K., Kondoh, G., Matsuda, Y., Habu, T., Nishimune, Y., and Morita, T. (1998). The mouse RecA-like gene Dmc1 is required for homologous chromosome synapsis during meiosis. Mol Cell *1*, 707-718.

Yuan, L., Liu, J. G., Hoja, M. R., Wilbertz, J., Nordqvist, K., and Hoog, C. (2002). Female germ cell aneuploidy and embryo death in mice lacking the meiosis-specific protein SCP3. Science *296*, 1115-1118.

Yuan, L., Liu, J. G., Zhao, J., Brundell, E., Daneholt, B., and Hoog, C. (2000). The murine SCP3 gene is required for synaptonemal complex assembly, chromosome synapsis, and male fertility. Mol Cell *5*, 73-83.

Chapter 4

Spermatogonial Depletion and Testicular Germ Cell Tumor Formation in *Stra8*-deficient Mice

Andrew E. Baltus, Ericka Anderson, Stephanie Schrump,

Dirk G. de Rooij, Terry Hassold and David C. Page

Author Contributions:
AEB conceived of and coordinated all experiments; EA assisted AEB with the study of testicular germ cell tumor formation in the *Stra8*-deficient mice and performed the antibody staining presented in Figure 5. SS and TH performed the meiotic chromosome spreads present in Figure 2A-F. DGD provided invaluable expertise on the morphological characterization of testicular germ cells.

Abstract

We have previously described the premeiotic arrest of *Stra8*-deficient germ cells in embryonic female and juvenile male mice. Our analysis demonstrated a G_1 or early S-phase arrest of premeiotic female germ cells. In the male, we reported apoptosis of *Stra8*-deficient spermatocytes coincident with the earliest appearance of meiotic spermatocytes in their wild type littermates. Here we further address the phenotype of *Stra8*-deficient male germ cells. While most mutant spermatocytes undergo apoptosis prior to initiating meiosis, some instead become arrested at this transition. Although they are never observed to properly condense their chromatin, they do initiate DNA replication, load meiotic cohesins and form synaptonemal complexes, consistent with early meiotic prophase. Nonetheless, *Stra8*-deficient spermatocytes are never observed to initiate meiotic recombination or undergo meiotic synapsis, two additional processes expected during early meiotic prophase. These results indicate that some *Stra8*-deficient spermatocytes are able to progress aberrantly into meiotic prophase, although never progressing beyond an abnormal leptotene/zygotene-like stage. Additionally, we document a progressive depletion of the spermatogonia in *Stra8*-deficient adult testes, indicating a potential role for *Stra8* in the regulation of spermatogonial maintenance, possibly at the level of the stem cells. Interestingly, this germ cell depletion is followed by the formation of testicular germ cell tumors in the *Stra8*-deficient mice. These tumors appear with high frequency around one year of age, indicating a predisposition to testicular germ cell tumor formation in *Stra8*-deficient male mice.

Introduction

We have previously described the phenotype of *Stra8*-deficient germ cells in embryonic female mice, at which time we presented only a brief description of *Stra8*-deficient male germ cells. Although our main focus of study of *Stra8* and likewise *Stra8*-deficient mice has been in the female, the preponderance of literature references for *Stra8* surround its expression during spermatogenesis. To date, no functional characterization of *Stra8* has been reported, however several reports of *Stra8* expression in wild type and mutant mice has generated broad interest in *Stra8*.

Stra8 was first reported in 1995 as being inducible by retinoic acid treatment of P19 cells *in vitro* (Bouillet et al. 1995). The same group further characterized the induction of *Stra8* upon retinoic acid treatment of P19, F9 and ES cells. They also described the expression pattern of *Stra8* in juvenile and adult testes, concluding that *Stra8* is only expressed by the premeiotic (spermatogonia) cells of the testis (Oulad-Abdelghani et al. 1996). Although their report showed that *Stra8* mRNA and STRA8 protein are restricted to premeiotic cells, it also demonstrated that *Stra8* expression is either restricted to specific sub-stages of spermatogonia or is expressed by several stages of spermatogonia within specific tubule stages. This is based on the observation that *Stra8*-positive cells line the basal lamina of many, but not all testicular tubules. They also showed that several distinct phosphorylated isoforms of STRA8 are generated upon induction by retinols *in vitro*, with distinct isoforms present depending on the retinol used for induction (all-trans vs. 9-cis). They also concluded that STRA8 is abundantly cytoplasmic in spermatogonia, by immunohistochemistry, and more definitively by cell fractionation of ectopic STRA8 in COS-1 cells.

Stra8 expression has recently become associated with spermatogonial stem cells. A transgenic mouse line, with a cell surface epitope tag under the control of the *Stra8* promoter, was used to isolate *Stra8*-expressing testicular cells. These "*Stra8*-positive" cells had high levels of expression of stem cell markers *Ep-Cam* (Anderson et al., 1999) and *beta1*- and *alpha6-integrin* (Shinohara et al., 1999) and accounted for ~30,000 cells per testis. When used in spermatogonial transplant experiments this "*Stra8*-positive" cell population demonstrated significant levels of engraftment, indicating enrichment for spermatogonial stem cells (Giuili et al., 2002). Another group reported the isolation of the testicular side population. A side population is all cells from a tissue, identified by flow cytometry, that demonstrate Hoechst 33342 efflux; the side population from several tissues has been demonstrated to be highly enriched for stem cells (summarized in Mogi et al., 2003). It was shown that in addition to demonstrated stem cell activity and expression of known stem cell markers, the testicular side population had high levels of *Stra8* gene expression (Lassalle et al., 2004). Together these experiments demonstrate that *Stra8* expression is correlated with spermatogonial stem cell activity, although it does not demonstrate that *Stra8* is restricted to the stem cell population or that *Stra8* is required for stem cell activity. More recently, using a *Stra8* promoter driven GFP as a marker for spermatogonial stem cells, it was demonstrated that F9 teratocarcinoma cells could be differentiated into spermatogonial stem cells by treatment with retinoic acid followed by selection for *Stra8* expression (Nayernia et al., 2004). Again, these cells were shown to have spermatogonial stem cell activity based on their ability to engraft when transplanted into germ-cell-depleted testes. This result does suggest that retinoic acid may be sufficient to drive F9 cells to differentiate into spermatogonial stem cells in

culture; however, using the retinoic-acid-inducible *Stra8* as a marker to follow this differentiation does not demonstrate a role for *Stra8* in spermatogonial stem cell biology.

Although *Stra8* has recently become highly cited as a marker of either spermatogonial stem cells or as a marker of spermatogonial differentiation, there is no evidence for the role that *Stra8* actually plays during male germ cell development. Here we present data characterizing the early meiotic arrest of the most advanced germ cells within the testes of *Stra8*-deficient mice. Those *Stra8*-deficient spermatocytes that do not rapidly apoptose (as described in the previous chapter) appear to arrest for up to 7 days prior to undergoing apoptosis. During this time they are able to initiate DNA replication and load meiosis-specific cohesin and synaptonemal complex proteins onto their chromosomes. They do not, however, undergo synapsis or initiate meiotic recombination, and therefore *Stra8*-deficient spermatocytes do not properly progress into meiotic prophase. Additionally, we describe the gradual loss of germ cells in the *Stra8*-deficient male testes. This germ cell depletion would be consistent with a requirement for *Stra8* in maintenance of the premeiotic spermatogonial population. Additionally, we report here the formation of testicular germ cell tumors in the *Stra8*-deficient male mice. These tumors form at a high frequency as the mice approach a year of age and demonstrate that *Stra8*-deficiency, which prior to tumor formation results in germ cell depletion, predisposes testicular germ cells to become unregulated in their proliferation.

Results

In the previous chapter we presented that *Stra8*-deficient spermatocytes usually become apoptotic shortly after their appearance, beginning 7-8 days after birth. Here we will present data from further study of the phenotype of *Stra8*-deficient male mice.

Arrest and Accumulation of *Stra8*-deficient Male Germ Cells

Analysis of *Stra8*-deficient male mice between 26 and 30 days old reveals the presence of spermatocytes with abnormal cellular morphology and chromosome condensation inconsistent with meiotic prophase (Figure 1B,D,F). Compared with the number of wild-type tubules that contain preleptotene spermatocytes, *Stra8*-deficient testes contain two to three times as many tubules with preleptotene spermatocytes (based on histological observations – does not indicate similar numbers per tubule) indicating arrest of *Stra8*-deficient spermatocytes. Additionally, these *Stra8*-deficient spermatocytes can be found in tubules that contain type B spermatogonia (immediate spermatocyte precursor) or the next round of preleptotene spermatocytes (Figure 1F). This demonstrates that the *Stra8*-deficient spermatocytes that do not rapidly undergo apoptosis (described in chapter 3) become arrested and remain histologically premeiotic for as long as 7 days, the time it takes for the next round of preleptotene spermatocytes to appear and thus accumulate within the tubules of *Stra8*-deficient males.

Analysis of Meiotic Prophase Markers in *Stra8*-deficient Male Germ Cells

Based on cellular morphology and chromosome condensation, we did not observe any *Stra8*-deficient spermatocytes properly transitioning into meiosis. We did observe spermatocytes that appeared histologically to be arrested with late preleptotene morphology, as if unable to transition into meiotic prophase. We next wanted to

Figure 1. Periodic acid Schiff and hematoxylin stained sections from 26-30 day old wild type and *Stra8*-deficient testes. Wild type spermatocytes are observed to progress from preleptotene (A) into meiotic prophase (C and E) based on chromosome condensation. *Stra8*-deficient spermatocytes appear as expected (B) but fail to properly undergo the meiotic chromosome condensation associated with progression into meiotic prophase (D) and become arrested (marked by an asterisk) indicated by their presence within the lumen of tubules in which the next round of preleptotene spermatocytes are already present (F). Arrowheads indicate spermatocytes in each panel.

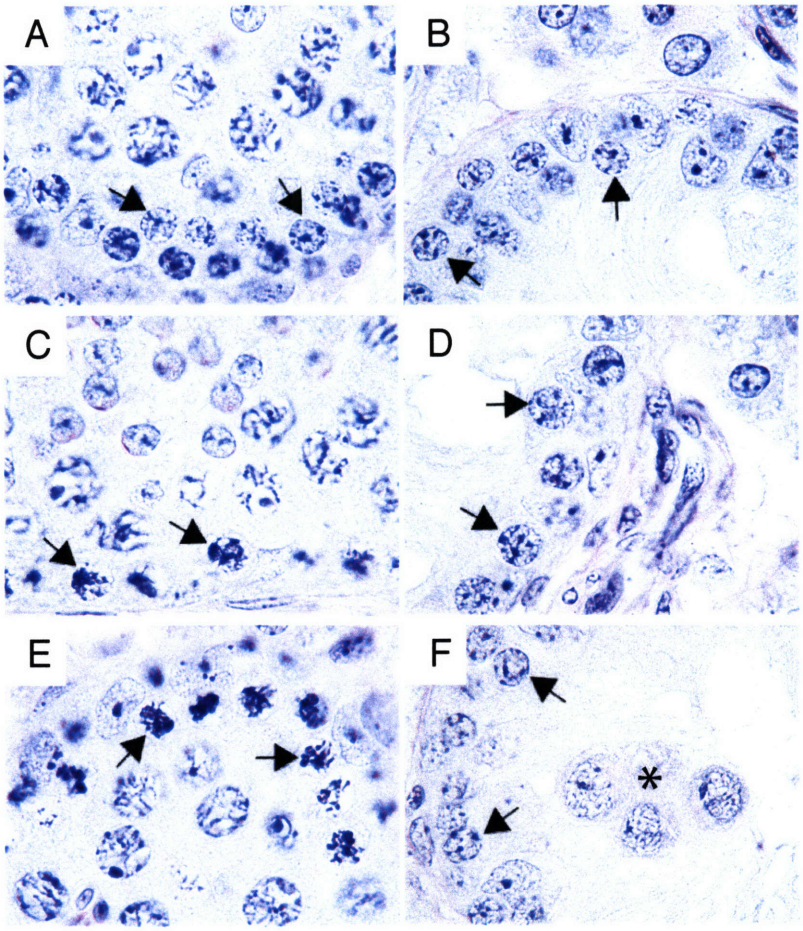
A
B
C
D
E
F

determine if the *Stra8*-deficient spermatocytes were initiating any molecular functions normally associated with meiosis. Using immunostaining on chromosome spreads and testis sections, we analyzed several early meiotic events, including chromosome pairing, synapsis and recombination in *Stra8*-deficient spermatocytes from 24-day-old males. For all surface spreads, we used antibodies against the synaptonemal complex protein, SCP3, to determine the sub-stage of prophase of the cells (see Lynn et al, 2002), as well as to monitor assembly of the lateral/axial elements of the synaptonemal complex. In addition to SCP3, a second antibody was used on all cells: against either STAG3 (a meiosis-specific cohesin sub-unit) to examine establishment of sister chromatid cohesion; SCP1 to assess formation of the transverse element of the synaptonemal complex, a hallmark of synapsis; or RAD51 or MLH1 to monitor early and late events in the recombination pathway, respectively. It is important to note here that any spermatocytes that are not positive for SCP3 could not be identified or quantified in this experiment. Both wild-type and heterozygous males had normal numbers of cells at each of the different sub-stages of prophase, and exhibited normal antibody localization patterns (Figure 2 A, C and E). In contrast, the *Stra8*-deficient spermatocytes had clear defects (Figure 2 B, D and F). We observed an increased number of leptotene/zygotene-like cells, but no evidence of pachytene cells. The early events in cohesion appeared relatively normal, as STAG3 formed linear structures that co-localized with SCP3 in these cells (Figure 2B). SCP3 formed linear aggregates that frequently coalesced to form full-length axial elements, but there was no evidence of synapsis (i.e., SCP1 localization; Figure 2D). There was little evidence of organized localization patterns for either of the two recombination proteins,

Figure 2. Immunohistochemistry on meiotic chromosome spreads and sections from 24-day-old wild type and *Stra8*-deficient testes. All meiotic chromosome spreads are stained for the synaptonemal complex protein SCP3 (red) and an additional marker (green); the meiotic cohesin STAG3 (A and B), the synaptonemal complex protein SCP1 (C and D) or the meiotic recombination protein DMC1 (D and F). Testis sections were stained for γ-H2AX, which marks the sites of DNA double-strand breaks (G and H).

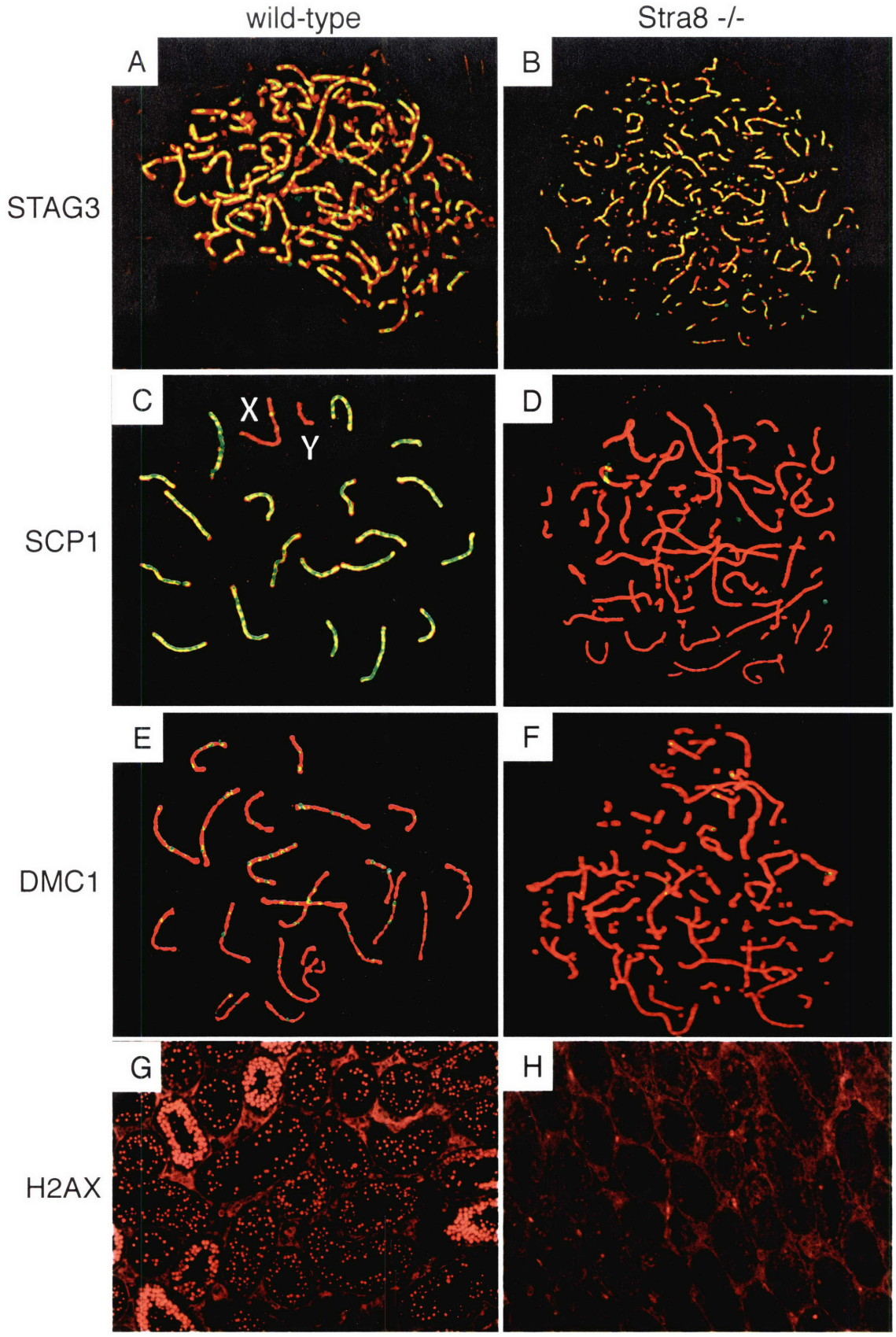
wild-type
Stra8 -/-
A
B
STAG3
C
X
Y
D
SCP1
E
F
DMC1
G
H
H2AX

RAD51 (Figure 2F) and MLH1 (data not shown) indicating a defect in meiotic recombination.

To address further the possibility of meiotic recombination we performed immunostaining for γ-H2AX, an early marker of DNA double-strand breaks, on testis sections from 24-day-old males to assay for meiotic recombination. In wild-type animals γ-H2AX marks the entire nuclei of spermatocytes after the formation of DNA double-strand breaks, becoming restricted to the inactivated X and Y chromosomes in pachytene stage spermatocytes (Figure 2G). *Stra8*-deficient testis sections showed very little γ-H2AX staining (Figure 2H), which confirmed the lack of meiotic recombination as well as the absence of pachytene spermatocytes. The cells that faintly stained for γ-H2AX were generally apoptotic when observed in bright field (data not shown). RT-PCR analysis confirmed that *Stra8*-deficient testes do not express the recombination-initiating gene *Spo11*; further substantiating that meiotic recombination was not properly initiated in these animals (data not shown).

Spermatogonial depletion in *Stra8*-deficient adult testes

As all of our observations of juvenile *Stra8*-deficient males are consistent with a role for *Stra8* around the onset of meiosis, we were somewhat surprised to find a gradual depletion of spermatogonial populations within the tubules of *Stra8*-deficient animals as they aged. Targeted disruption of the meiosis-specific genes *Spo11* or *Dmc1* results in a slightly later meiotic arrest and spermatocyte apoptosis. However, in these mutants, unlike what we observe in *Stra8*-deficient mice, spermatogonia are maintained in normal numbers into adulthood (Yoshida et al., 1998; Pittman et al., 1998; Baudat et al., 2000; Romanienko and Camerini-Otero, 2000). Interestingly, we observe a substantial loss of spermatogonia in *Stra8*-deficient males within 4-6 weeks of birth (Figure 3), with

Figure 3. Hematoxylin and eosin staining of testes sections from *Stra8*-deficient mice. The number of germ cells found within the tubules of Stra8-deficient mice decreases with age from 2 weeks old (A) to 3 weeks old (B) to 6 weeks old (C) and finally to 8 weeks old (D). All panels are 200x.

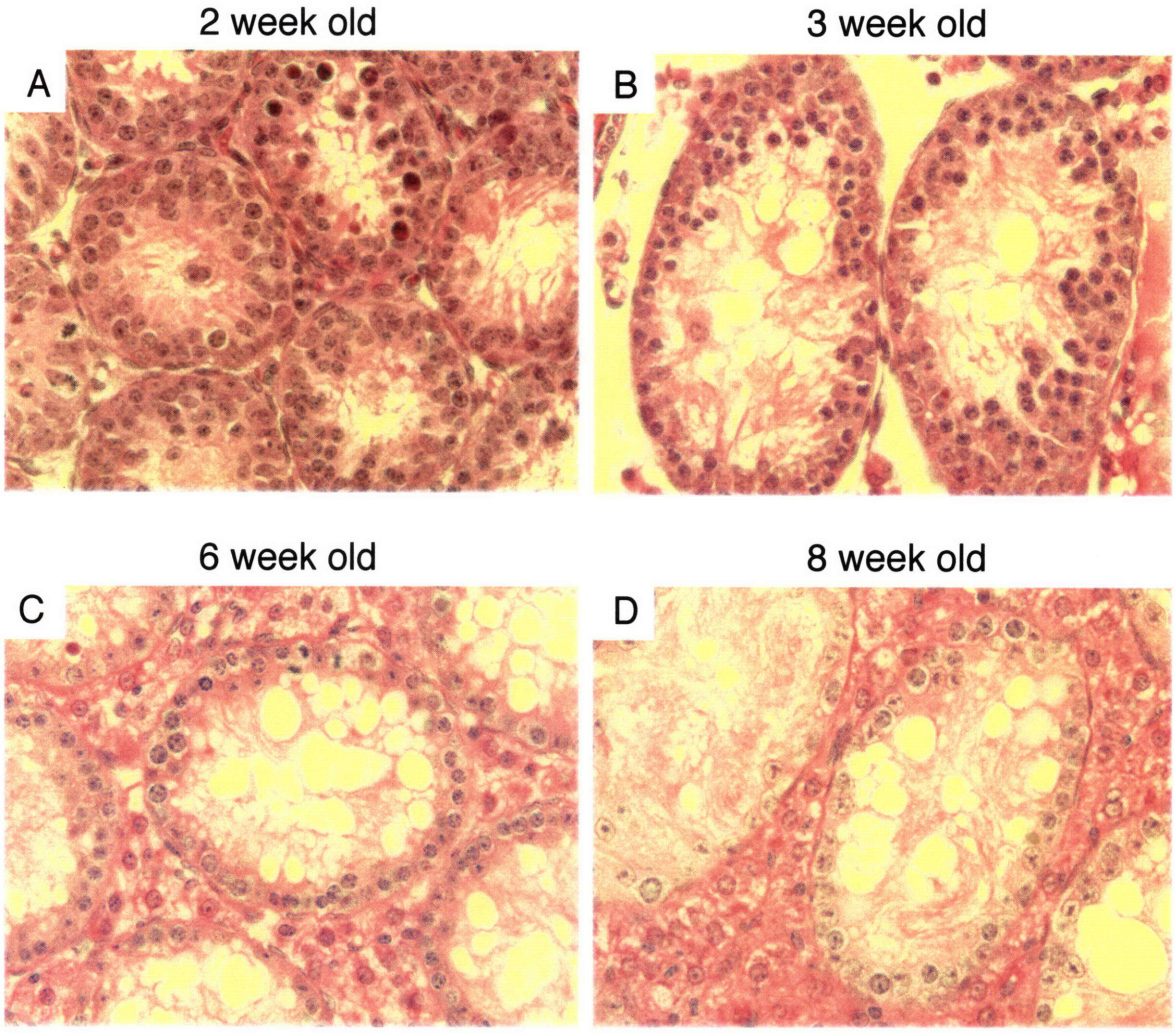
2 week old
A
3 week old
B
6 week old
C
8 week old
D

progressing loss such that by 8-10 weeks of age the testicular tubules appear to contain mostly Sertoli cells with few spermatogonia (Figure 3). In fact, adult *Stra8*-deficient testes weights are consistent with those reported for the spermatogonial depletion mutant *jsd/jsd* (Beamer et al., 1988). This loss of spermatogonia highlights a possible role for *Stra8* in regulation of spermatogonial stem cell activity, which is consistent with the association between *Stra8* expression and spermatogonial stem cell activity.

Testicular germ cell tumors in *Stra8*-deficient adult testes

As mentioned above, *Stra8*-deficient testes become severely germ-cell-depleted by adulthood. However, when we examined the testes of *Stra8*-deficient male mice at 1 year of age or older we observed frequent examples of greatly enlarged testes. Whereas a typical adult testis from a *Stra8*-deficient animal weighs around 20mg, we find testes weighing up to 5g. Histological analysis of these enlarged testes suggested germ cell hyperplasia, based upon the spermatogonia-like morphology of the cells, and was consistent with the seminoma class of testicular germ cell tumors. Further histological analysis of *Stra8*-deficient male mice around 1 year of age revealed that in addition to the large testes containing obvious testicular germ cell tumors, in more than 80% of all testes studied, at least one tubule was filled with proliferating germ cells. An inferred progression is presented in Figure 4. Panels A and B show testis sections from one year old mice prior to formation of germ cell tumors. At the earliest stage of tumor formation we find most tubules to contain very few if any spermatogonia, with one tubule (or a small cluster of tubules) that contains substantial numbers of proliferating germ cells (Figure 4 C and D). At later stages, the proliferating germ cells can be found spreading interstitially throughout the testis, as well as continuing to proliferate within some tubules

(Figure 4 E and F). This transition from tubular to interstitial germ cell appears to correlate with reduced apoptosis. Once the germ cells escape the tubules they appear to spread rapidly throughout the testis resulting in large regions of the testis being nearly devoid of non-germline cells. Eventually the testis loses nearly all tubular structure and appears to be entirely composed of germ cells (Figure 4G). At this time it is common to find increased vasculature (Figure 4H) and lymphocytes (Figure 4G).

Immunohistochemical staining for germ-cell-specific markers confirms that the tumors are composed predominantly of germ cells. Immunostaining for the germ cell marker *Mvh*, which labels spermatogonial and early meiotic spermatocytes within wild-type tubules (Figure 5A), reveals the presence of scattered germ cells within the non-tumorigenic tubules of adult *Stra8*-deficient mice (Figure 5B). This staining also confirms that the cells proliferating within and filling the tubules, as well as those filling the entire testis, are germ cells (Figure C-H). Similar results were observed for immunohistochemistry with the germ-cell-specific gene *Dazl* (data not shown). The germ-cell nature of the tumors was also confirmed by RT-PCR analysis for several germ-cell-specific genes including *Oct4* and *C-kit* (data not shown).

Figure 4. Hematoxylin and eosin staining of testes sections from 1 year old *Stra8*-deficient mice. An inferred progression for the formation of testicular tumors in the *Stra8*-deficient mice is presented at 40x magnification (A,C,E and G) and 100x magnification (B, D, F and H). Prior to tumor formation all tubules remain significantly germ cell depleted (A and B). At the earliest stage of tumor formation a tubule can be observed to be filling with hyperplastic cells which appear germ cell by histology (C and D). Eventually the proliferating cells overload the tubule and are released into the interstitial space of the testis (E and F). Ultimately, the hyperplastic cells expand to the point at which no testicular tubules can be found (G and H) and which time lymphocytes and increased vasculature can often be observed (arrows in G and H respectively).

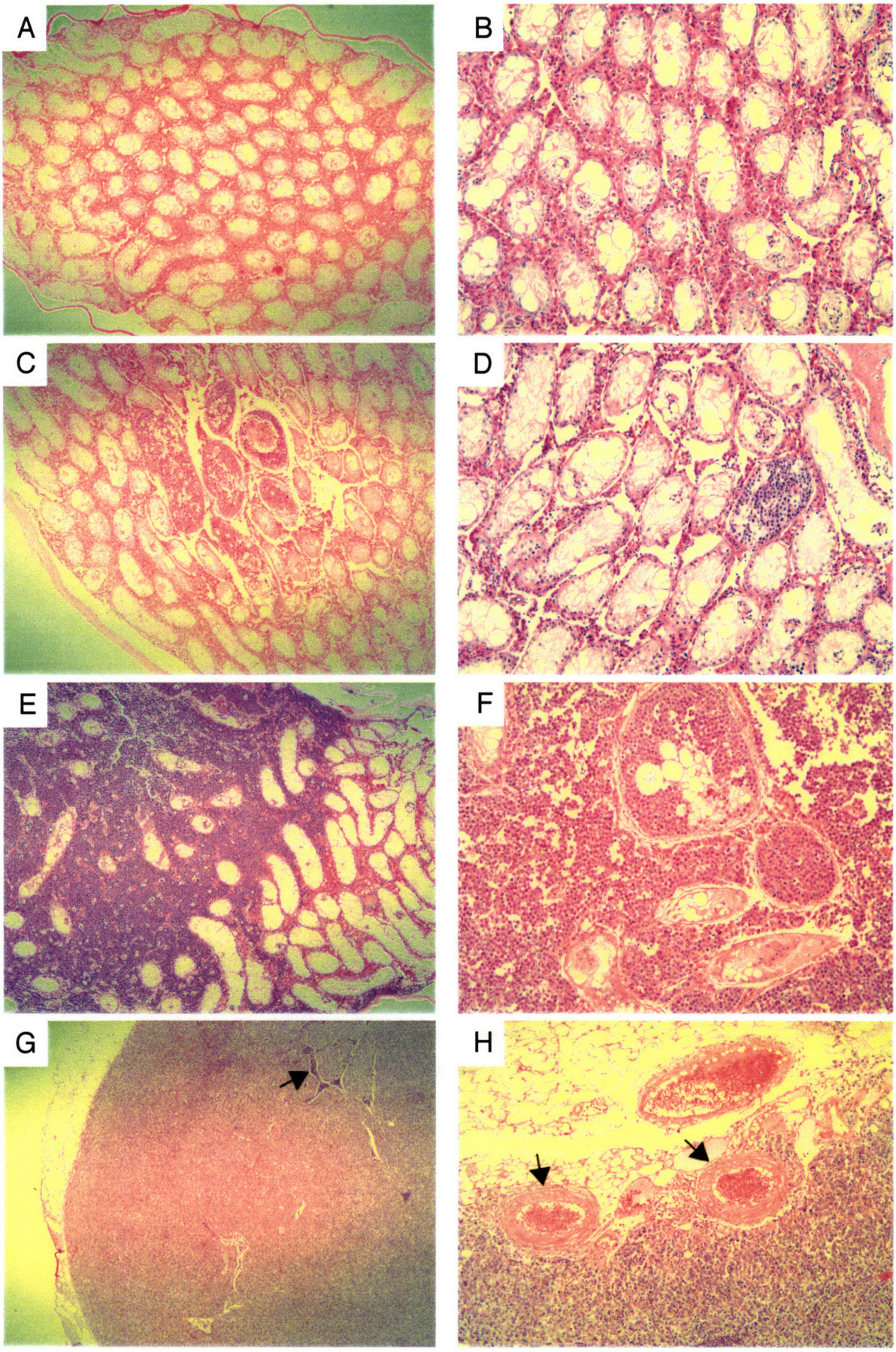
A
B
C
D
E
F
G
H

Figure 5. Immunohistochemistry for the germ cell marker MVH demonstrates that the hyperplastic cells within *Stra8*-deficient testes are germ cells. Staining for MVH on wild type testis sections demonstrates that it stains all premeiotic (spermatogonia) and early meiotic (spermatocytes) germ cells (A). Staining for MVH on *Stra8*-deficient testes sections prior to the appearance of the hyperplastic cells reveals a small number of remaining germ cells (B). Staining on *Stra8*-deficient testes with obvious hyperplasia, however, indicates that the tumors forming in the *Stra8*-deficient testes are composed of germ cells (C and D). Panels A, B and the bottom two images in panels C and D are 200x and the top panels in C and D are 40x.

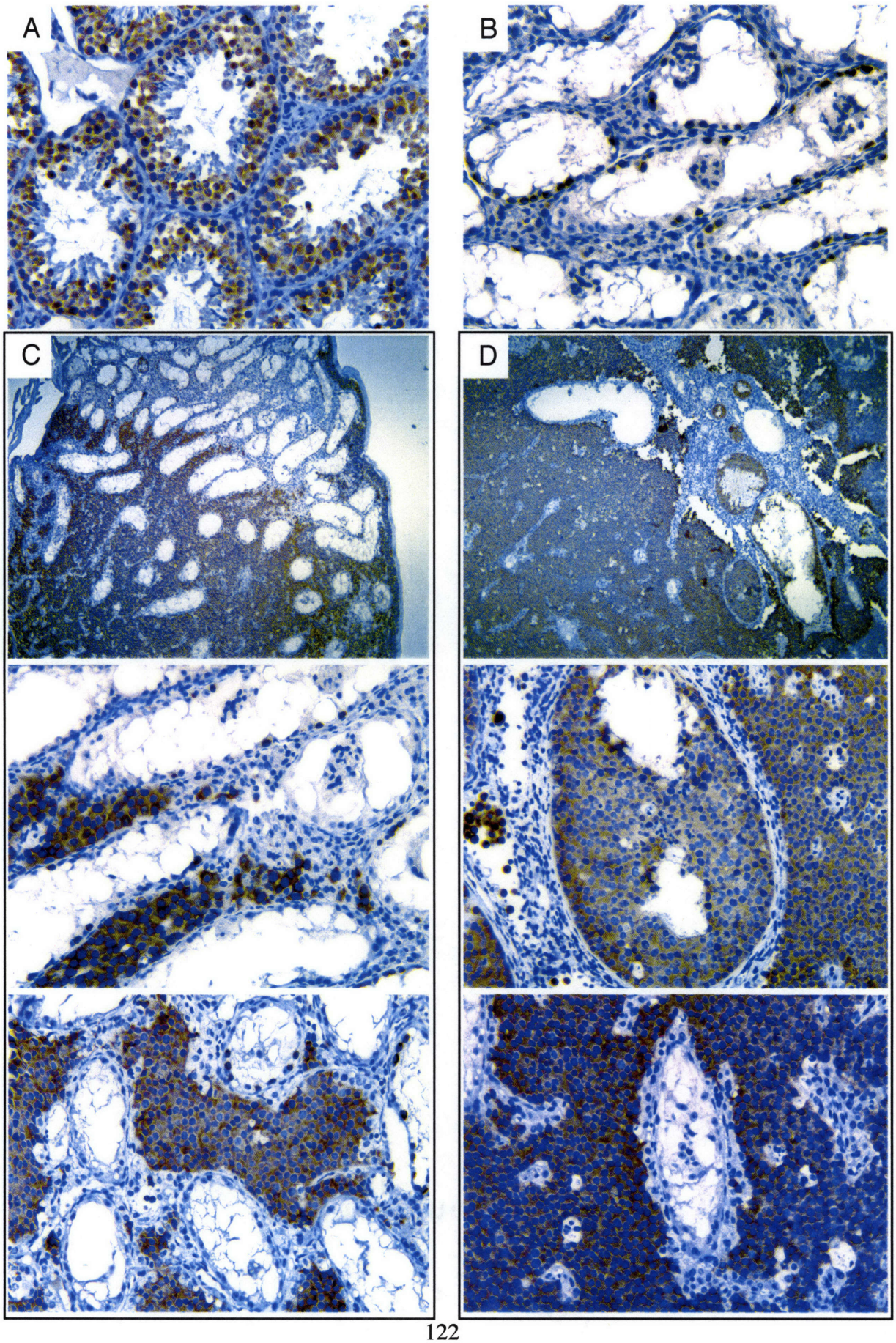
A
B
C
D

Discussion and future directions

We demonstrate here that *Stra8* is required for proper progression through meiotic prophase and proper maintenance of the premeiotic spermatogonial populations in mouse testes. Furthermore, examination of testes from aging *Stra8*-deficient mice reveals that although *Stra8*-deficiency results in substantial germ cell loss, it also strongly predisposes these animals to testicular germ cell tumor formation. The maintenance of a stem cell population within the testis throughout adult life is distinct from the situation in the ovary in which all germ cells enter meiosis embryonically, and where no stem cell has been identified. Therefore, study of *Stra8*-deficient males allows us to explore possible roles for *Stra8* in germ cell biology beyond those that we can observe in the embryonic ovary.

Stra8 is one of several hundred genes with a demonstrated role in the maintenance of male fertility. Interestingly, however, *Stra8* is the only gene that has been shown to be required for the initiation of meiosis. In fact, even the most advanced *Stra8*-deficient spermatocytes arrest earlier than in any other mutant that disrupts meiotic prophase (reviewed in Hassold and Hunt, 2002) (Figure 6). *Stra8* is also the only mouse mutant to result in germ cell depletion followed by testicular germ cell tumor formation, which is similar to the progression of germ cell tumors in humans with cryptorchidism (Mutter, personal communication).

Combined with the observations reported in chapter 3, these results clearly demonstrate that, in the absence of *Stra8,* spermatocytes are not able to progress properly into meiosis. In the *Stra8*-deficient males we do observe cells that appear to have progressed into the early stages of meiotic prophase based on SCP3 and STAG3 protein localization, which we never observed in *Stra8*-deficient females. It is interesting to note here that mutations that specifically disrupt cohesion, synapsis or recombination almost

Figure 6: Chart documenting the degree to which various meiotic mutants are able to progress into meiotic prophase. The extent of normal meiotic progression by both male and female germ cells is marked by dark grey bars and the continuation of light grey bars indicates the further progression of female germ cells beyond that of male germ cells. The degree to which meiosis is completed normally in female germ cells is noted to the right of each bar. *Stra8*-deficient female germ cells arrest stringently prior to meiotic DNA replication which is the earliest stage depicted in this figure, the continuation of the brown bar denotes the degree to which *Stra8*-deficient male germ cells are able to progress further into meiosis than *Stra8*-deficient female germ cells, which is distinct from all other meiotic mutants in which the female germ cells progress further than the male germ cells. Modified from *Chromosome Research* **12**:197-213, 2004 and *Science* **296**:2181-3, 2002.

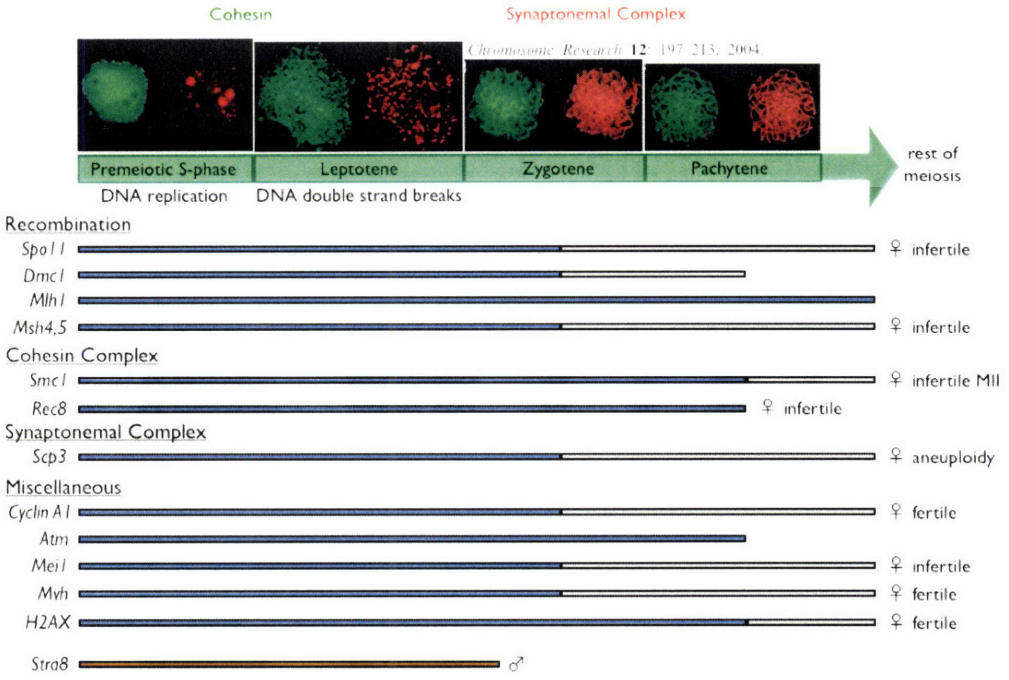
Cohesin
Synaptonemal Complex
Premeiotic S-phase
Leptotene
Zygotene
Pachytene
rest of meiosis
DNA replication
DNA double strand breaks
Recombination
Spo11
Dmc1
Mlh1
Msh4,5
♀ infertile
Cohesin Complex
Smc1
♀ infertile MII
Rec8
♀ infertile
Synaptonemal Complex
Scp3
♀ aneuploidy
Miscellaneous
Cyclin A1
♀ fertile
Atm
Mei1
♀ infertile
Myh
♀ fertile
H2AX
♀ fertile
Stra8
♂

always display a sexually dimorphic phenotype. Usually, mutant male germ cells stringently arrest in zygotene or pachytene of meiotic prophase (likely as the result of a synapsis checkpoint) but female germ cells deficient for these same genes proceed at least as far and usually farther into meiosis, often maintaining at least some level of fertility (Hassold and Hunt, 2002). This is distinct from the *Stra8*-deficient germ cells which progress further into meiotic prophase in the male and arrest very stringently in a premeiotic state in the female. The possibility exists that *Stra8*-deficiency triggers a premeiotic checkpoint in female germ cells that, in contrast to previously identified meiotic-checkpoints, is either more stringent in female germ cells or absent from male germ cells. If this were the case, the arrest prior to meiotic DNA replication in female germ cells and the initial wave of apoptosis by male germ cells likely represents the result of *Stra8*-deficiency, while the prophasic spermatocytes observed in males are the result of these arrested cells pushing past the checkpoint but unable to progress properly into meiosis in the absence of *Stra8*. The ability of *Stra8*-deficient male germ cells to initiate cohesin and synaptonemal complex formation suggests that *Stra8* is not directly required for initiation of these processes but for some process that should have occurred prior to induction of these prophasic events, and therefore prevents advancement through meiotic prophase. It is also possible that male germ cells employ a parallel pathway to *Stra8* that does not exist in the female, such that male germ cells are able to progress farther into meiosis in the absence of *Stra8*.

Although *Stra8* appears unique among spermatogenic mutants, we find an interesting similarity when we compare the *Stra8*-deficient males to wild-type males on a vitamin A-deficient (VAD) diet (a model of retinoic-acid deficiency as vitamin A is an

essential precursor to retinoic acid). When adult rats or mice are fed a VAD diet their spermatogenesis arrests at several steps, including the transition of preleptotene spermatocytes into meiotic prophase (Van Pelt et al., 1995; reviewed in Chung and Wolgemuth, 2004). In fact, under VAD conditions the preleptotene spermatocytes appear arrested in S-phase and have increased levels of apoptosis similar to *Stra8*-deficient spermatocytes. The effect of VAD on spermatogenesis can be rescued with administration of retinoic acid, indicating that it is the inability to produce retinoic acid that results in the spermatogenic defects of VAD animals. Two recent reports demonstrate that under VAD conditions *Stra8* expression is nearly undetectable in the testis. Interestingly, upon treatment with retinoic acid (or vitamin A) *Stra8* expression rises dramatically within a period of less than 12 hours (Koubova et al., 2006; Ghyselinck et al., 2006). Additionally, recent reports demonstrate that *Stra8* is regulated by retinoic acid signaling in embryonic gonads (Koubova et al., 2006; Bowles et al., 2006). These observations further support the idea that at least part of the VAD phenotype may be mediated through *Stra8*.

Because the only phenotype we observe during the first round of spermatogenesis affects the spermatocytes we were surprised to observe that by 2 months of age spermatogonial numbers are substantially reduced. This is in contrast to mutants that disrupt meiotic cohesion, synapsis or recombination in which roughly normal numbers of spermatogonia and spermatocytes are still present in the adult testis (Yoshida et al., 1998; Pittman et al., 1998; Baudat et al., 2000; Romanienko and Camerini-Otero, 2000; Yuan et al., 2000; Bannister et al., 2004). This observation indicates that *Stra8* may play a role in the maintenance of the premeiotic spermatogonia, and possibly directly in regulation of

the stem cells. This would be consistent with the published observations of *Stra8* expression correlating with spermatogonial stem cell activity (Giuili et al., 2002; Lassalle et al., 2004; Nayernia et al., 2004).

Future directions include analysis of whether or not the first *Stra8*-deficient spermatocytes, appearing around 7-8 days after birth, progress into meiotic prophase prior to arrest and apoptosis. This requires additional cell spreads to be done on 8-12 day old males and these experiments are underway. Additionally, it is important to address meiotic DNA replication by *Stra8*-deficient spermatocytes. Without a marker that allows isolation of the preleptotene population, an experiment like the one performed on the *Stra8*-deficient female germ cells (in chapter 3) cannot be performed on the males. BrdU incorporation assays are underway and preliminary observations indicate that at least some *Stra8*-deficient spermatocytes do initiate DNA replication. Additionally, analysis in the male is complicated by the fact that we can only assay spermatocytes that are positive for the marker that we are using and we have no way of determining what fraction of *Stra8*-deficient spermatocytes apoptose at an earlier stage and are thus not analyzed.

In addition to characterizing further the role of *Stra8* during the initiation of meiosis in spermatocytes, it will be interesting to pursue a better understanding of the role *Stra8* may play in spermatogonial stem cell regulation. Although this may require a more complete understanding of the molecular function of *Stra8*, we may currently be able to learn more about *Stra8* via analysis of the testicular germ cell tumors that develop in the *Stra8*-deficient adult testes. If we can gain a better understanding of how *Stra8*-deficient germ cells transition from hypoproliferation to hyperproliferation, we may gain

additional insight into the molecular function of *Stra8*. Additionally, it is important to note that *Stra8*-deficiency appears to be the most reliable and physiologically most relevant model of human seminoma class testicular germ cell tumors. Further study of the testicular germ cell tumors that develop in *Stra8*-deficient animals will hopefully provide insight into testicular germ cell tumor formation in humans.

Materials and Methods

Histology

Dissected tissues were fixed overnight in Bouin's solution, embedded in paraffin or plastic, sectioned, and stained with hematoxylin and eosin or periodic acid Schiff. Images were obtained with an Olympus BX51TF Fluorescence Microscope with a Spot RT digital camera and Spot version 4.1 software (Diagnostic Instruments).

Meiotic chromosome spreads

Testicular tubules were gently teased apart, and the tissue was transferred to freshly prepared buffer solution (containing 30 mM Tris, pH 8.2; 50 mM sucrose; 17 mM citric acid; 5 mM EDTA; 0.5 mM dithiothreitol; and 0.1 mM phenylmethylsulphonyl fluoride, pH 8.2–8.4) and was incubated at room temperature for 45–60 min. Approximately 3–5 mm of the tissue was transferred into 20 μl of 100 mM sucrose for further teasing, and 10 μl of the resultant germ-cell slurry was deposited onto microscope slides coated with a 1% paraformaldehyde solution (pH 9.2; 0.14%–0.20% Triton X [Sigma]) and was incubated overnight in a humid chamber. Slides were air-dried and placed in a 0.04% PhotoFlo solution (Eastman Kodak) for 2 min and then were drained, allowed to air-dry, and immediately processed for immunostaining.

Microscope slides were hydrated in antibody dilution buffer (ADB) (containing 1% normal donkey serum [Jackson ImmunoResearch], 0.3% BSA, and 0.005% Triton X in PBS) for 30 min at room temperature. A total of 60 μl of the primary antibody cocktail—consisting of SCP3 (1:75) and either SCP1 (1:1,000), STAG3 (1:100), RAD51/DMC1 (1:75) (Santa Cruz Biotechnology) in ADB—was overlaid on slides, and the slides were coverslipped and incubated overnight at 37°C in a humid chamber. After

the primary antibody incubation, slides were washed in ADB for 20 min at room temperature, followed by a second wash in ADB at 4°C overnight. Slides were then overlaid with 60 µl of the secondary antibody cocktail (fluorescein donkey anti-rabbit, rhodamine donkey anti-goat [1:100] [Jackson ImmunoResearch] in ADB) for 60 min at 37°C in a humid chamber. Slides were washed three times in PBS for 10 min and then were drained, and mounted in Antifade (BioRad Laboratories). Images were collected using a Zeiss Axiophot epifluorescence microscope (Carl Zeiss) using the Applied Imaging Quips Pathvision System.

Section immunohistochemistry

Testes were fixed in 4% paraformaldehyde overnight and then embedded in paraffin and cut into 5 µm sections. Sections were baked at 65°C for 30min, deparaffinized in zylene 3 times for 5 min each, washed in 100% EtOH twice and rehydrated by washes in 95% EtOH, 85% EtOH and twice in H_2O. Antigen retrieval was performed by microwaving for 15min at 60% power in 0.01M sodium citrate buffer (pH 6.0). Sections were washed twice in H_2O then treated with 3.5M HCl for 10min and then washed twice in PBS. For γ-H2AX staining sections were blocked in 3% donkey serum for 30min, and incubated with primary antibody (2hr at room temp for γ-H2AX at 1:200 for polyclonal and 1:1000 for monoclonal - Upstate), washed in PBS 3 times, and incubated with secondary antibody (donkey anti-mouse RRX or donkey anti-rabbit Texas red at 1:200 – Jackson) for 1hr at room temperature, washed 3 times in PBS, and mounted (Sigma – mounting solution). For Mvh staining tissue sections were treated using M.O.M. Basic Immunodetection kit (Vector) following manufacturer's instructions with anti-MVH antibody (1:1000), a gift from Toshiaki Nove, Mitsubishi Kagaku Instutute of Life

Sciences, Tokyo, Japan. Images were taken using an Olympus BX51TF Fluorescence Microscope with a Spot RT digital camera and Spot version 4.1 software (Diagnostic Instruments).

Acknowlegements

We thank Toshiaki Noce for MVH antisera.

References

Anderson, R., Schaible, K., Heasman, J., and Wylie, C. (1999). Expression of the homophilic adhesion molecule, Ep-CAM, in the mammalian germ line. J Reprod Fertil 116, 379-384.

Bannister, L. A., Reinholdt, L. G., Munroe, R. J., and Schimenti, J. C. (2004). Positional cloning and characterization of mouse mei8, a disrupted allelle of the meiotic cohesin Rec8. Genesis 40, 184-194.

Baudat, F., Manova, K., Yuen, J. P., Jasin, M., and Keeney, S. (2000). Chromosome synapsis defects and sexually dimorphic meiotic progression in mice lacking Spo11. Mol Cell 6, 989-998.

Beamer, W. G., Cunliffe-Beamer, T. L., Shultz, K. L., Langley, S. H., and Roderick, T. H. (1988). Juvenile spermatogonial depletion (jsd): a genetic defect of germ cell proliferation of male mice. Biol Reprod 38, 899-908.

Bouillet, P., Oulad-Abdelghani, M., Vicaire, S., Garnier, J. M., Schuhbaur, B., Dolle, P., and Chambon, P. (1995). Efficient cloning of cDNAs of retinoic acid-responsive genes in P19 embryonal carcinoma cells and characterization of a novel mouse gene, Stra1 (mouse LERK-2/Eplg2). Dev Biol 170, 420-433.

Bowles, J., Knight, D., Smith, C., Wilhelm, D., Richman, J., Mamiya, S., Yashiro, K., Chawengsaksophak, K., Wilson, M. J., Rossant, J., et al. (2006). Retinoid signaling determines germ cell fate in mice. Science 312, 596-600.

Chung, S. S., and Wolgemuth, D. J. (2004). Role of retinoid signaling in the regulation of spermatogenesis. Cytogenet Genome Res 105, 189-202.

Ghyselinck, N. B., Vernet, N., Dennefeld, C., Giese, N., Nau, H., Chambon, P., Viville, S., and Mark, M. (2006). Retinoids and spermatogenesis: Lessons from mutant mice lacking the plasma retinol binding protein. Dev Dyn 235, 1608-1622.

Giuili, G., Tomljenovic, A., Labrecque, N., Oulad-Abdelghani, M., Rassoulzadegan, M., and Cuzin, F. (2002). Murine spermatogonial stem cells: targeted transgene expression and purification in an active state. EMBO Rep 3, 753-759.
Hunt, P. A., and Hassold, T. J. (2002). Sex matters in meiosis. Science 296, 2181-2183.

Koubova, J., Menke, D. B., Zhou, Q., Capel, B., Griswold, M. D., and Page, D. C. (2006). Retinoic acid regulates sex-specific timing of meiotic initiation in mice. Proc Natl Acad Sci U S A 103, 2474-2479.

Lassalle, B., Bastos, H., Louis, J. P., Riou, L., Testart, J., Dutrillaux, B., Fouchet, P., and Allemand, I. (2004). 'Side Population' cells in adult mouse testis express Bcrp1 gene and are enriched in spermatogonia and germinal stem cells. Development 131, 479-487.

Lynn, A., Koehler, K. E., Judis, L., Chan, E. R., Cherry, J. P., Schwartz, S., Seftel, A., Hunt, P. A., and Hassold, T. J. (2002). Covariation of synaptonemal complex length and mammalian meiotic exchange rates. Science 296, 2222-2225.

Mogi, M., Yang, J., Lambert, J. F., Colvin, G. A., Shiojima, I., Skurk, C., Summer, R., Fine, A., Quesenberry, P. J., and Walsh, K. (2003). Akt signaling regulates side population cell phenotype via Bcrp1 translocation. J Biol Chem 278, 39068-39075.

Nayernia, K., Li, M., Jaroszynski, L., Khusainov, R., Wulf, G., Schwandt, I., Korabiowska, M., Michelmann, H. W., Meinhardt, A., and Engel, W. (2004). Stem cell based therapeutical approach of male infertility by teratocarcinoma derived germ cells. Hum Mol Genet 13, 1451-1460.

Oulad-Abdelghani, M., Bouillet, P., Decimo, D., Gansmuller, A., Heyberger, S., Dolle, P., Bronner, S., Lutz, Y., and Chambon, P. (1996). Characterization of a premeiotic germ cell-specific cytoplasmic protein encoded by Stra8, a novel retinoic acid-responsive gene. J Cell Biol 135, 469-477.

Pittman, D. L., Cobb, J., Schimenti, K. J., Wilson, L. A., Cooper, D. M., Brignull, E., Handel, M. A., and Schimenti, J. C. (1998). Meiotic prophase arrest with failure of chromosome synapsis in mice deficient for Dmc1, a germline-specific RecA homolog. Mol Cell 1, 697-705.

Romanienko, P. J., and Camerini-Otero, R. D. (2000). The mouse Spo11 gene is required for meiotic chromosome synapsis. Mol Cell 6, 975-987.

Shinohara, T., Avarbock, M. R., and Brinster, R. L. (1999). beta1- and alpha6-integrin are surface markers on mouse spermatogonial stem cells. Proc Natl Acad Sci U S A 96, 5504-5509.

van Pelt, A. M., van Dissel-Emiliani, F. M., Gaemers, I. C., van der Burg, M. J., Tanke, H. J., and de Rooij, D. G. (1995). Characteristics of A spermatogonia and preleptotene spermatocytes in the vitamin A-deficient rat testis. Biol Reprod 53, 570-578.

Yoshida, K., Kondoh, G., Matsuda, Y., Habu, T., Nishimune, Y., and Morita, T. (1998). The mouse RecA-like gene Dmc1 is required for homologous chromosome synapsis during meiosis. Mol Cell 1, 707-718.

Yuan, L., Liu, J. G., Zhao, J., Brundell, E., Daneholt, B., and Hoog, C. (2000). The murine SCP3 gene is required for synaptonemal complex assembly, chromosome synapsis, and male fertility. Mol Cell 5, 73-83.

Chapter 5

Discussion and Future Directions

Mammalian germ cell development begins in the early embryo and continues well into adulthood. During this period, the germ cells need to navigate properly many developmental decisions. In recent years it has become increasingly clear that throughout their development germ cells are in nearly constant communication with the surrounding somatic cells. At some stages the somatic cells do most of the talking (i.e. specification and sex determination). At others the germ cells do much of the talking (i.e. development). Given the protracted development of mammalian germ cells, from specification to gamete formation, it is no wonder that many questions remain unanswered about the germ cell lineage. In this thesis I have presented both forward and reverse genetic approaches intended to expand upon our current understanding of germ cell development.

Mapping of the gene responsible for spermatogonial depletion in the *jsd/jsd* mouse resulted in the identification of a functional X-to-autosome retroposon that compensates for the inactivation of the X-chromosome during male meiosis. Evolutionary analysis demonstrated that this retroposition of the X-linked *Utp14* gene, required for the production of ribosomes, occurred independently at least four separate times during eutherian evolution. Possibly the most striking observation is that in each instance one, and only one, retroposition occurred and was maintained. This finding directly supports the model that X-to-autosome retropositions provide a mechanism for continued function of X-linked "housekeeping" genes whose inactivation during male meiosis would, at the very least, reduce the fitness of the organism. As more and more eutherian genomes are sequenced it will be interesting to expand upon this study with a

greater sample size and information about the sites of retroposon insertion in species other than the mouse and human.

The targeted disruption of the germ-cell-specific gene *Stra8* results in male and female infertility. Female germ cells appear to arrest in G_1 or early S-phase of the meiotic cell cycle, as they do not undergo meiotic DNA replication or progress into meiotic prophase. *Stra8*-deficient male germ cells are also disrupted during the initiation of meiosis, as evidenced by arrest and apoptosis of early spermatocytes (the male germ cells that undergo the meiotic cell cycle), with the most advanced spermatocytes undergoing aberrant early prophasic events prior to their apoptosis. Additionally the disruption of *Stra8* results in gradual loss of the premeiotic spermatogonial populations, possibly the result of misregulation of spermatogonial stem cell divisions. In older animals the germ cells, which appear hypoproliferative during much of the adult life, frequently become hyperporliferative resulting in the formation of testicular germ cell tumors.

The observations presented in this thesis demonstrate that the embryonic ovary makes an ideal test tube for the study of mammalian germ cells as they transition into meiosis, while the adult testis is complicated by the dependence of each stage upon the continued progression of the others. In addition to the precise arrest of *Stra8*-deficient germ cells within the embryonic ovary, recent publications demonstrating regulation of *Stra8* expression by retinoic acid in the embryonic gonad allow a more complete model of the process at this time (Bowles et al., 2006; Koubova et al., 2006) (Figure 1). These reports demonstrate that endogenous retinoic acid, acting via retinoic acid receptors, induces *Stra8* expression in the germ cells of the embryonic ovary. This observation is

Figure 1: (A) Model depicting the role of retinoic acid in the induction of meiosis via *Stra8* in germ cells of embryonic ovaries while *Cyp26b1* breaks down retinoic acid in embryonic testes, thereby blocking meiotic initiation. Meiosis is, however, induced in the adult testis and this is also believed to require retinoic acid. (B) Cartoon depicting the cell cycle transition from mitosis to meiosis including the regulation of meiotic initiation in mammals as well as that of yeasts.

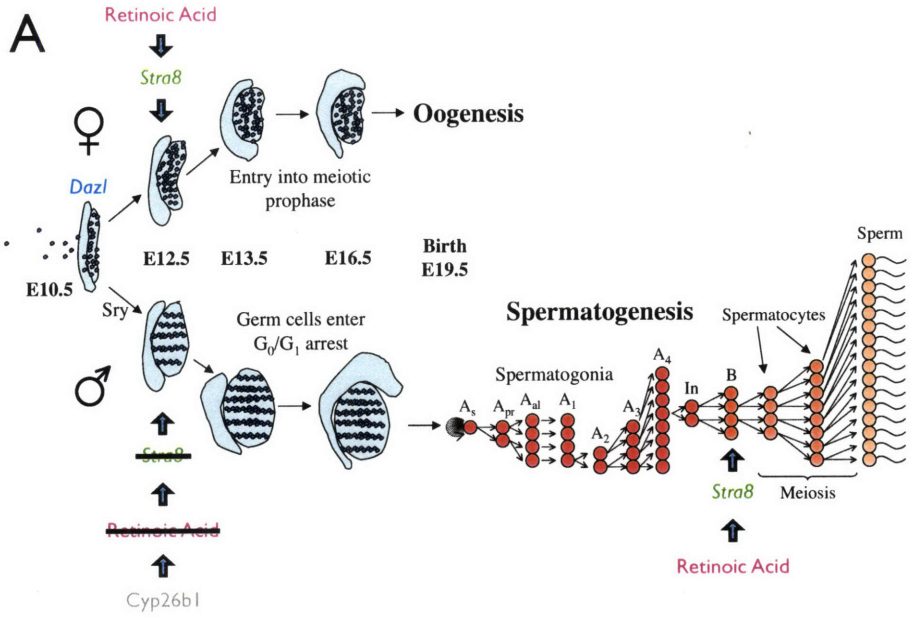
A
Retinoic Acid
Stra8
Oogenesis
Dazl
Entry into meiotic prophase
E10.5
E12.5
E13.5
E16.5
Birth
E19.5
Sry
Germ cells enter
G0/G1 arrest
Spermatogenesis
Spermatogonia
Spermatocytes
Sperm
In
B
Meiosis
Stra8
Retinoic Acid
Cyp26b1

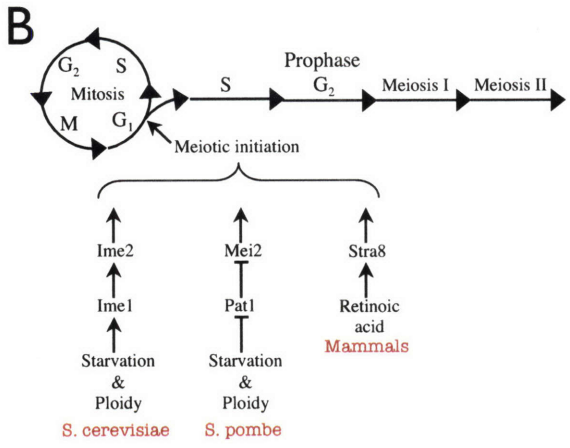
B
G2
S
Mitosis
M
G1
Prophase
S
G2
Meiosis I
Meiosis II
Meiotic initiation
Ime2
Ime1
Starvation & Ploidy
S. cerevisiae
Mei2
Pat1
Starvation & Ploidy
S. pombe
Stra8
Retinoic acid
Mammals

consistent with the previous report that the *Stra8* promoter contains consensus retinoic-acid-receptor-binding elements (Oulad-Abdelghani et al., 1996). Within a broader developmental context these reports also demonstrated that it is the specific activity of a cytochrome p450 protein *Cyp26B1* that actively degrades retinoic acid in the testis, thus preventing the germ cells within the embryonic testis from receiving the retinoic acid signal and entering meiosis at this time. Inhibition of *Cyp26B1* within the embryonic testis, by targeted disruption or chemical inhibition, results in *Stra8* expression by male embryonic germ cells. Together with these observations the results presented in this thesis indicate a regulatory pathway required for the initiation of meiosis by embryonic female germ cells, and the active inhibition of this process within the embryonic testis.

An interesting question that remains is why only germ cells express *Stra8* upon retinoic acid induction, when many other developmental processes including hindbrain and lung development require retinoic acid signaling, but do not require or even express *Stra8*? The answer to this may come from another line of research in our lab, the study of the *Dazl*-deficient mice. As previously mentioned, ovarian germ cells deficient for *Dazl* do not down-regulate markers of pluripotency (*Oct4* and *Dppa3/Stella*) or up-regulate *Stra8* or markers of meiosis (*Dmc1*, γH2AX and SCP3). The lack of meiotic markers would be consistent with the absence of *Stra8*, however *Stra8*-deficient germ cells down-regulate pluripotency markers, as expected (Lin and Koubova, personal communication). These observations indicate that *Dazl* may be required to prime the germ cells so that they are capable of responding to the retinoic acid signal by expressing *Stra8*.

An additional question still exists as to how similar this regulation is in the adult testis compared to the embryonic ovary. *Dazl*, *Stra8* and retinoic acid have all been shown to be required for proper spermatogenesis. Additionally, reduced *Stra8* expression in testes from mice fed a vitamin A-deficient diet (thus blocking retinoic acid production) followed by significant up regulation of *Stra8* expression upon re-admission of vitamin A indicates a direct role for retinoic acid is *Stra8* expression in the testis (Ghyselinck et al., 2006; Koubova et al., 2006). It is also possible, if not likely, that in addition to meiotic initiation these factors could act together to regulate other stages of spermatogenesis.

Future Directions

Stra8 Knockout Analysis

Stra8 provides a new point of entry for study of mammalian germ cell development. Although we have determined that *Stra8* is required for meiotic initiation, there is more that we can learn from the *Stra8* knockout. Further analysis of *Stra8*-deficient mice should provide greater insight into the molecular nature of meiotic initiation in male and female mice.

The results presented in this thesis demonstrate that *Stra8*-deficient female germ cells appear to be arrested in G_1 or very early S-phase of the meiotic cell cycle. It has been shown from study of invertebrate organisms, particularly yeast, that the transition from mitosis into meiosis requires inhibition of the mitotic cell cycle along with activation of the meiotic cell cycle during G_1. Interestingly, retinoic acid has been shown to affect directly expression of cell cycle regulatory genes of the G_1 phase of mitosis (Chung and Wolgemuth, 2004). Given the model that retinoic acid functions via *Stra8* to initiate the meiotic cell cycle during G_1, we would expect that the *Stra8*-deficient oogonia

would be arrested in G_1. To address this it will be necessary to determine the status of the cell cycle regulatory factors in *Stra8*-deficient germ cells. It is interesting to note here that observation of gonadal germ cell proliferation in the rat demonstrated that both male and female germ cells arrest in G_1 prior to the initiation of meiosis by the female germ cells (Wartenberg et al., 1998). It is possible that this brief period of arrest is observed in rats but not in mice due to the rats' longer gestation period, and therefore longer period between PGC entry into the gonad and meiotic initiation. It is therefore compelling to propose that in all mammals the germ cells of the male and female complete their last mitotic division and then by an as-yet-unknown mechanism (possibly involving *Dazl*) arrest in G_1 becoming competent for induction of meiosis. It is during this window that the cells are able to respond to retinoic acid and induce *Stra8*, but because the window is so short in mice we do not observe the mitotic arrest in females. Further support for this hypothesis comes from the observation that both male and female germ cells express *Scp3* mRNA and generate SCP3 protein, the levels of which rise in the female and drop off in the male around the time of germ cell sex determination (Di Carlo et al., 2000). In addition to a candidate approach for the study of cell cycle regulators in the *Stra8* knockout, it will be interesting to perform microarray analysis of the *Stra8*-deficient mice. This method could help characterize the cell cycle status of these cells, as well as give insight into the immediate downstream consequences of *Stra8*-deficiency on the transcriptome of the germ cells.

Continued Analysis of the Role of *Stra8* During Spermatogenesis

Additional experiments are currently underway to characterize more accurately the arrest point of the *Stra8*-deficient preleptotene spermatocytes. These include additional cell spreads on the first wave of preleptotene spermatocytes to determine how

far these cells initially progress towards meiosis, as much of our current analysis was done on cells that may have been in a prolonged arrest. Additionally, we are trying to work out a technique for quantifying the DNA content of the *Stra8*-deficient spermatocytes. Again, we have preliminary evidence that some preleptotene spermatocytes do undergo DNA replication. It will, however, be necessary to address the ability of the earliest spermatocytes to replicate their DNA prior to undergoing apoptosis. Additionally, as with the female germ cells, it will be important to determine the cell cycle status of the *Stra8*-deficient spermatocytes.

Some of the most interesting questions about the *Stra8*-deficient males may be some of the most difficult to address. With mounting circumstantial evidence that *Stra8* may be required for spermatogonial stem cell regulation as well as for the initiation of meiosis, it will be important to address this with the *Stra8*-deficient mice. This is complicated by the fact that the preleptotene arrest results in high levels of apoptosis and absence of all meiotic and post-meiotic stages of germ cell within the tubules. Due to the cross-talk between several stages of germ cell and a single Sertoli cell, there is risk for secondary effects on earlier stages of spermatogenesis via disruption of the Sertoli cell by later stage spermatogenic failure. As a result it may be very difficult to determine what phenotypes are the direct result of *Stra8*-deficiency and which are secondary. Also, there are several defined stages of premeiotic spermatogonia based on histology and morphology, but there exist few if any markers that are well enough characterized and reliable enough to differentiate these stages.

Testicular Germ Cell Tumors in Adult *Stra8*-deficient Male Mice

Despite the difficulties outlined above, the transition from germ cell depletion to germ cell hyperplasia in *Stra8*-deficient mice is one that appears unique among male

fertility mutants. This may indicate that *Stra8* is required for proper regulation of spermatogonial stem cells. We now must ask why *Stra8*-deficiency predisposes germ cells toward the formation of germ cell tumors and what is the presumptive secondary event that drives this transformation? In an attempt to address this question, microarrays were performed comparing the pre-tumorigenic *Stra8*-deficient adult testis with *Stra8*-deficient testes in which the hyperlastic germ cells have enlarged the testis several fold. Analysis of this data set is underway, but the identification of several thousand significantly affected genes makes interpretation difficult at this time. This list does in fact confirm a significant reduction in the levels of somatic gene expression, as would be expected, and significantly increased expression levels of spermatogonia specific genes including *Oct4*, *Mvh* and *Dazl*, confirming the germ cell nature of the tumor cells.

In addition to addressing how and why the *Stra8*-deficient germ cells become tumorigenic, we are also currently trying to determine to what degree these tumors make a good model for human testicular germ cell tumor formation. Based on cell morphology, these tumors appear to be of the seminoma class, one in which no good mouse model currently exists. Additionally, the germ cell loss, followed by germ cell tumor formation is consistent with testicular germ cell tumor formation in patients suffering from chryptorchidism (Mutter, personal communication). Additionally, we find that several genes commonly upregulated in human testicular germ cell tumors, including *Pim1*, *Pim2*, *Vav2*, *Ret*, *Ccnd2*, *Cdc25B*, *Klf4* and *MycN*, are also upregulated in the *Stra8*-deficient tumors (Okada et al., 2003). This further supports the conclusion that *Stra8*-deficiency makes a good model for human seminoma class testicular germ cell tumors.

Molecular Function of STRA8

To understand the precise role of *Stra8* in germ cell development we will need to gain insight into the molecular function of the STRA8 protein. As has been mentioned previously in this thesis, STRA8 does not belong to an obvious protein family within the mouse genome nor is it conserved outside of vertebrates. The only similarity that is shared with other genes is a conserved basic helix-loop-helix (bHLH) domain. Several hundred bHLH proteins have been identified in organisms ranging from yeast to humans. Evidence from characterized bHLH proteins is that they, as a class, function as transcriptional regulators, often controlling key developmental transitions (Garrell and Campuzano, 1991; Littlewood and Evan, 1995; Massari and Murre, 2000). Other than the bHLH domain, STRA8 shows no similarity with any other sequence from vertebrates or invertebrates. An obvious question is whether or not STRA8 is a transcription factor. Previous reports indicate that STRA8 is an abundantly cytoplasmic protein, which would be at odds with a role as a transcriptional regulator. Observation of a STRA8-GFP fusion protein, transfected into an immortalized spermatogonial cell line, demonstrates that STRA8 can translocate from the cytoplasm to the nucleus by an unknown mechanism (Hu, personal communication). Further characterization of STRA8's subcellular localization is needed to answer this question. Additionally it would be important to address experimentally the possibility that STRA8 is a transcription factor. As bHLH proteins usually function as dimers it will be important to demonstrate if STRA8 homodimerizes or, by protein interaction studies, binds other bHLH proteins.

This leads to the next direction: identification of STRA8-interacting partners. A traditional Gal4-UAS based yeast two-hybrid screen was initiated with STRA8, however the full-length protein, as well as several smaller fragments of STRA8 including the

bHLH domain alone, self-activated in the screen. A cytoplasmic yeast two-hybrid screen, in which full-length STRA8 can be used without self-activation, is underway. Additionally, IP-mass spec analysis should be performed to identify STRA8 interacting partners. This approach is limited by the need for a suitable STRA8 antibody and appropriately purified starting material. If STRA8 functions transiently in a small population of ovarian or testicular germ cells, as appears to be the case, a purification method may be required to acquire adequate starting material.

Characterization of STRA8's molecular function(s) may be necessary before we can address many of the remaining questions about the role of STRA8 in germ cell development. Additionally, as STRA8 is the only factor known to function in germ cells during the transition from mitosis to meiosis, understanding STRA8 function will provide additional insight into this developmentally important transition.

References

Bowles, J., Knight, D., Smith, C., Wilhelm, D., Richman, J., Mamiya, S., Yashiro, K., Chawengsaksophak, K., Wilson, M. J., Rossant, J., *et al.* (2006). Retinoid signaling determines germ cell fate in mice. Science *312*, 596-600.

Chung, S. S., and Wolgemuth, D. J. (2004). Role of retinoid signaling in the regulation of spermatogenesis. Cytogenet Genome Res *105*, 189-202.

Di Carlo, A. D., Travia, G., and De Felici, M. (2000). The meiotic specific synaptonemal complex protein SCP3 is expressed by female and male primordial germ cells of the mouse embryo. Int J Dev Biol *44*, 241-244.

Garrell, J., and Campuzano, S. (1991). The helix-loop-helix domain: a common motif for bristles, muscles and sex. Bioessays *13*, 493-498.

Ghyselinck, N. B., Vernet, N., Dennefeld, C., Giese, N., Nau, H., Chambon, P., Viville, S., and Mark, M. (2006). Retinoids and spermatogenesis: Lessons from mutant mice lacking the plasma retinol binding protein. Dev Dyn *235*, 1608-1622.

Koubova, J., Menke, D. B., Zhou, Q., Capel, B., Griswold, M. D., and Page, D. C. (2006). Retinoic acid regulates sex-specific timing of meiotic initiation in mice. Proc Natl Acad Sci U S A *103*, 2474-2479.

Littlewood, T. D., and Evan, G. I. (1995). Transcription factors 2: helix-loop-helix. Protein Profile *2*, 621-702.

Massari, M. E., and Murre, C. (2000). Helix-loop-helix proteins: regulators of transcription in eucaryotic organisms. Mol Cell Biol *20*, 429-440.

Okada, K., Katagiri, T., Tsunoda, T., Mizutani, Y., Suzuki, Y., Kamada, M., Fujioka, T., Shuin, T., Miki, T., and Nakamura, Y. (2003). Analysis of gene-expression profiles in testicular seminomas using a genome-wide cDNA microarray. Int J Oncol *23*, 1615-1635.

Oulad-Abdelghani, M., Bouillet, P., Decimo, D., Gansmuller, A., Heyberger, S., Dolle, P., Bronner, S., Lutz, Y., and Chambon, P. (1996). Characterization of a premeiotic germ cell-specific cytoplasmic protein encoded by Stra8, a novel retinoic acid-responsive gene. J Cell Biol *135*, 469-477.

Wartenberg, H., Hilscher, B., and Hilscher, W. (1998). Germ cell kinetics during early ovarian differentiation: an analysis of the oogonial cell cycle and the subsequent changes in oocyte development during the onset of meiosis in the rat. Microsc Res Tech *40*, 377-397.

Appendix 1

Do Follicle Formation and Oocyte Growth Occur Independently of Meiotic Progression?

Andrew E. Baltus and David C. Page

Introduction

In the previous chapters I have presented the phenotype of *Stra8*-deficient embryonic female and adult male mice. Characterization of these animals has demonstrated that *Stra8* is required for initiation of meiosis in both sexes, though we do observe some cells with aberrant early meiotic progression in the males. Here I present analysis of a small number of follicles that are found in *Stra8*-deficient female mice between the time of birth and the first ovulation (approximately 24 days after birth). Beyond this point, we never observe follicles in these animals.

In this appendix I present data that indicates that the follicles we observe in the *Stra8*-deficient female mice do not contain normal meiotic oocytes. When isolated from the follicles, these oocyte-like cells are often found to be non-spherical, unlike wild type oocytes. They do not consistently produce polar bodies when cultured and are often parthenogenic upon isolation from the ovary. Additionally, *Stra8*-deficient oocyte-like cells frequently display assembled spindles at the time of isolation from the ovary, which is inconsistent with the expected meiotic arrest observed in wild type oocytes. I also show that these oocyte-like cells have not progressed properly through meiotic prophase, specifically that they have not initiated meiotic recombination.

Results

As presented in a previous chapter, *Stra8*-deficiency blocks the ability of female germ cells to initiate meiosis. Specifically, we found that in the absence of *Stra8* the germ cells were unable to undergo meiotic DNA replication. However, although we never observed meiotic cells within embryonic ovaries of *Stra8*-deficient female mice, we do observe the presence of a small number of follicles in the ovaries of juvenile mice. In *Stra8*-deficient females up to 30 days old, we observe a small number of follicles (less than 20) by histological analysis. After this time, no follicles are found. Comparison of the follicles found in *Stra8*-deficient and wild-type littermate animals that are 5 days old (Figure 1A and 1B), 8 days old (Figure 1C and 1D), and 21 days old (Figure 1E and 1F) demonstrates that the *Stra8*-deficient follicles develop as a cohort that mature at the same rate as the first cohort of follicles in wild-type ovaries. Additionally, the *Stra8*-deficient oocyte-like cells within the follicles appear histologically normal by comparison with the wild-type oocytes.

To characterize further these oocyte-like cells found in the ovaries of *Stra8*-deficient mice, I isolated oocytes from follicles of *Stra8*-deficient and wild-type littermates from 21-23 days after birth. The oocytes isolated from wild-type ovaries were extremely uniform in size and shape and formed polar bodies with high efficiency after culture, whereas the oocyte-like cells isolated from *Stra8*-deficient ovaries were widely variable in diameter and less uniformly spherical than wild-type oocytes (Figure 2A and 2B). Few of the Stra8-deficient oocyte-like cells formed polar bodies, and those that did often appeared abnormal (Figure 2B). It was also common to find *Stra8*-deficient oocyte-like cells that appeared parthenogenic, as they were clearly multicellular upon

Figure 1: H&E staining of wild type (A,C and E) and *Stra8*-deficient follicles (B,D and F) from 5 day old (A and B), 8 day old (C and D), and 21 day old (E and F) female mice.

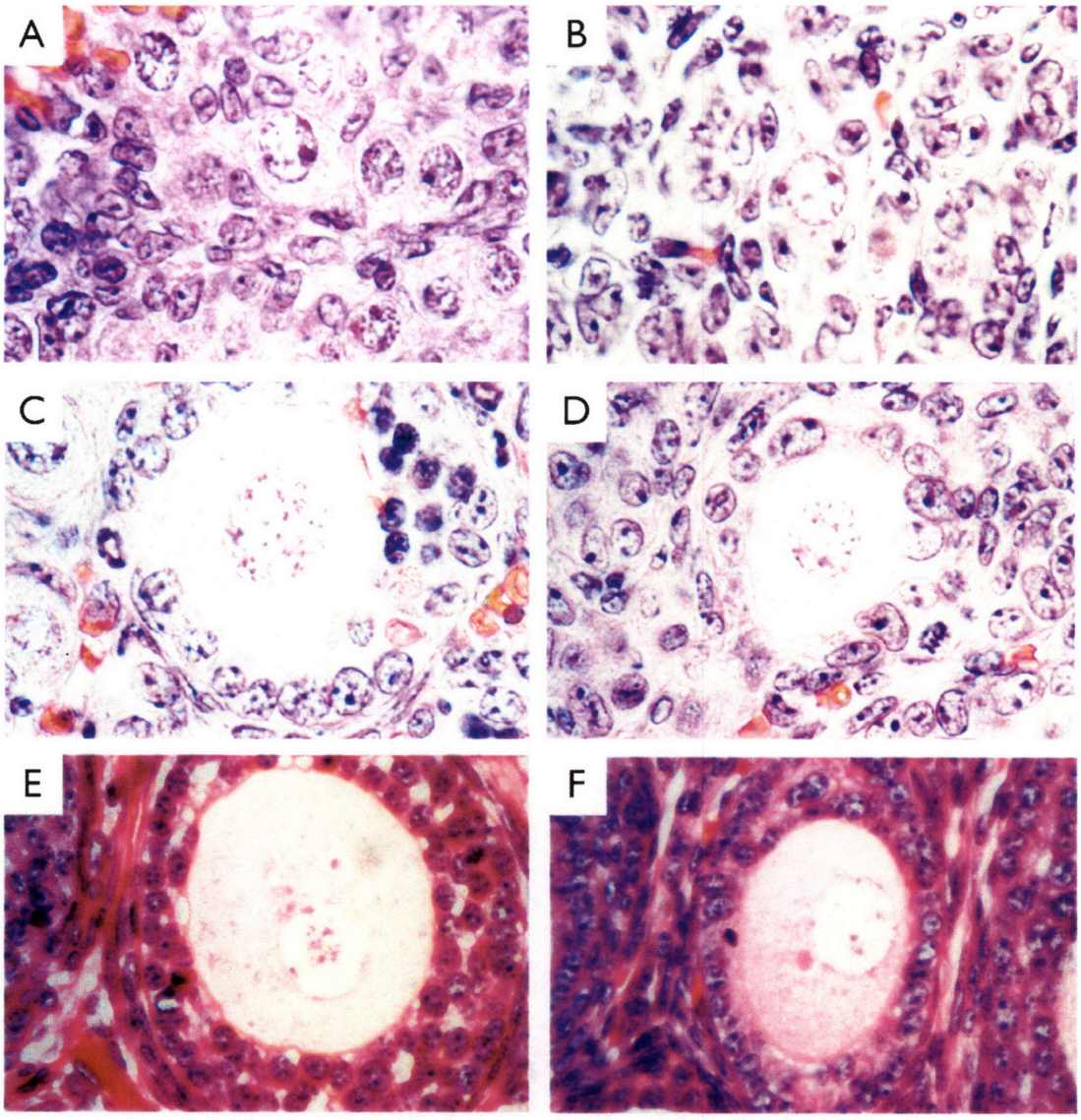
A
B
C
D
E
F

Figure 2: (A) Oocytes isolated from 21-day-old wild-type females and cultured for 18 hours. Note the uniform morphology and the polar bodies. (B) Oocyte-like cells isolated from 21-day-old *Stra8*-deficient females and cultured for 18 hours. Note the less uniform size and shape, the predominant absence of polar bodies and the parthenote in the upper right corner. (C and D) Immunohistochemistry for β-tubulin (green) and DNA (blue) on wild-type oocytes (C) and *Stra8*-deficient oocyte-like cells (D) isolated from 21-day-old ovaries.

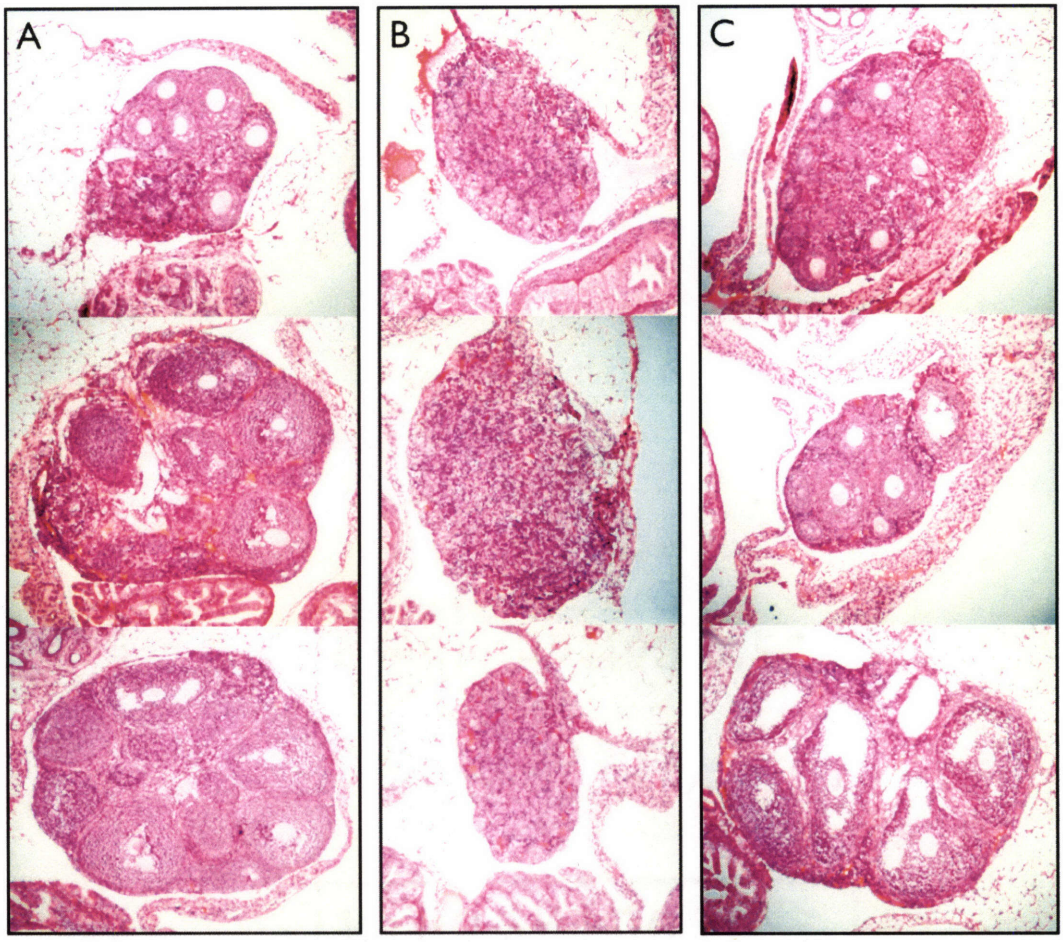
A
B
C

isolation from the ovary (Figure 2B). Additionally, when immunostained for β-tubulin, *Stra8*-deficient oocyte-like cells were often found to have their chromosomes condensed and aligned on spindles, whereas the wild type oocytes remained arrested in meiosis I and did not have assembled spindles or condensed chromatin (Figure 2C and 2D). These observations demonstrated that there was something wrong with oocyte-like cells found in *Stra8*-deficient ovaries, including improper meiotic progression.

In an attempt to determine if the *Stra8*-deficient oocyte-like cells, unlike the majority of *Stra8*-deficient female germ cells, initiate and progress through meiotic prophase, I set up an epistasis experiment in which the targeted *Stra8* allele was crossed with the *Dmc1*-deficiency allele. As *Dmc1* is required to repair DNA double-strand breaks during meiotic recombination, *Dmc1*-deficiency results in complete loss of embryonic female germ cells because they are unable to repair the DNA double-strand breaks formed by the meiotic recombination protein SPO11 (Pittman et al., 1998; Yoshida et al., 1998). If the *Stra8*-deficient, oocyte-like cells progressed properly through meiotic prophase then DNA double-strand breaks would be formed. In the absence of *Dmc1*, these cells would be lost prior to follicle formation, as is observed in the *Dmc1*-deficient female mice. *Stra8*/*Dmc1* double heterozygous mice were intercrossed and their offspring were genotyped. Histology was performed on ovaries from mice that were either wild-type at both loci; *Stra8*-deficient; *Dmc1*-deficient; or deficient for both *Stra8* and *Dmc1*. If the *Stra8*-deficient oocyte-like cells properly undergo meiotic prophase in the absence of *Stra8* we would expect them to be lost in the double knockout. Conversely, if the double knockout ovaries contain similar numbers of

follicles to the *Stra8* knockout, it would demonstrate that even though they are capable of initiating follicle formation, the *Stra8*-deficient oocyte-like cells have not undergone meiotic prophase. The results of the experiment are presented in Figure 3. As we previously reported, a small population of maturing follicles was found in *Stra8*-deficient ovaries (Figure 3A). Also, consistent with previous reports, no follicles were observed in *Dmc1*-deficient ovaries (Figure 3B). The double knockout ovaries contained similar numbers of maturing follicles as we find in ovaries deficient for *Stra8* alone (Figure 3C).

Figure 3: H&E staining of ovaries from 21-day-old females. (A) *Stra8*-deficient. (B) *Dmc1*-deficient. (C) *Stra8* and *Dmc1*-deficient.

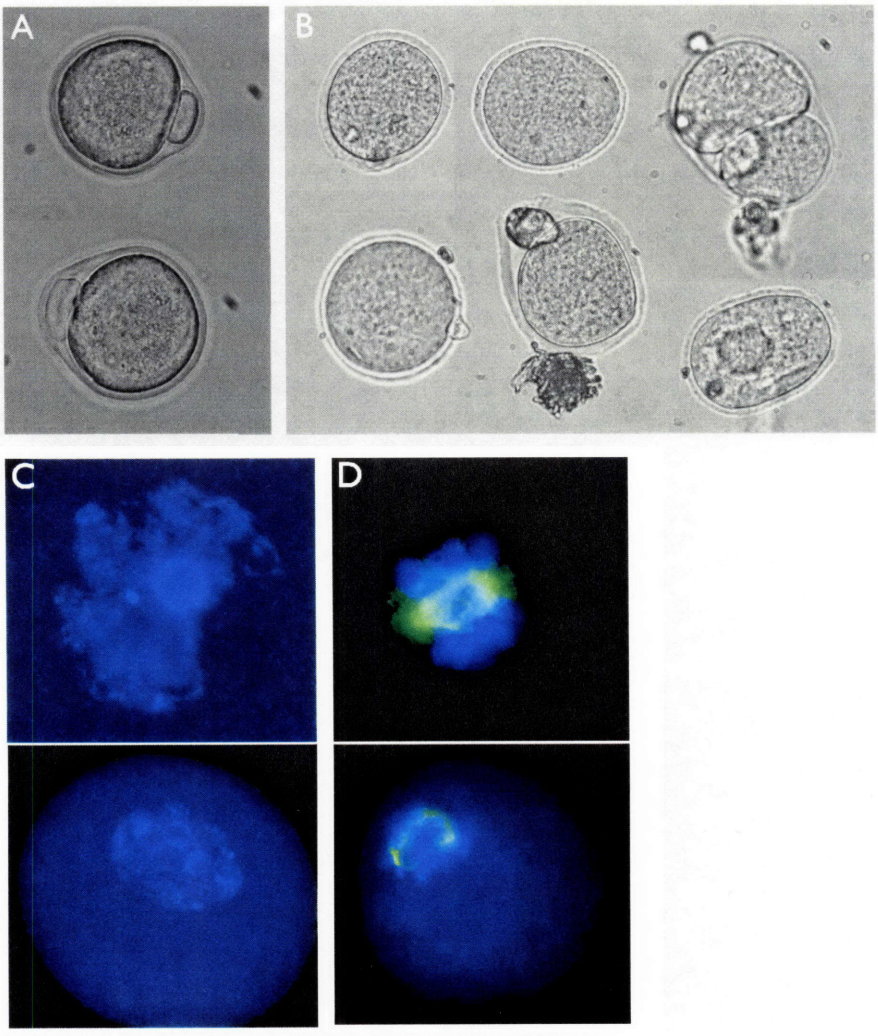
A
B
C
D

Discussion and future directions

It is commonly believed that follicle formation and maturation of the oocyte-follicle complex are coordinated with the meiotic cell cycle. Here I demonstrate that by several methods the oocyte-like cells found within follicles in *Stra8*-deficient female mice are not progressing normally through meiosis. Analysis of mice deficient for both *Stra8* and *Dmc1* demonstrates that the *Stra8*-defcient oocyte-like cells have not undergone meiotic recombination, which is consistent with our finding that *Stra8*-deficient female germ cells are unable to initiate meiotic prophase. Additionally, although they appear very similar histologically to wild-type oocytes, they are aberrant in size, shape and show defects in cell cycle regulation. Although the data provided here do not definitively prove that the *Stra8*-deficient oocyte-like cells have not initiated meiosis, these results provide interesting preliminary observations that it may be possible to uncouple meiosis from follicle formation and oocyte maturation.

As we find that *Stra8*-deficient embryonic female germ cells do not undergo meiotic DNA replication, it is possible that these oocyte-like cells are still 2N. I have been trying to address this, but there are far too few of these cells for most methods to work. I have been currently optimizing immunostaining conditions to label these oocyte-like cells with the CREST antisera, which marks the centromere. In this way I could count the number of chromosomes per cell with a 2N cell containing 40 and a 4N cell containing 80. Unfortunately, I have yet to get the antibody staining to work and may need to acquire a fresh antibody sample.

It will be important to gain a better understanding of the cell cycle status of these oocyte-like cells within the ovaries of *Stra8*-deficient female mice. If they have not initiated meiosis, their ability to mature similarly to oocytes and to drive follicle

formation will provide substantial insight into the development of the ovary. It is interesting to note here that a follow-up study of the recently reported ability to generate oocytes from ES cells in culture (Hubner et al., 2003; Kehler et al., 2005) has shown that the cells within the follicles are not oocytes as they are not in meiosis (Novak et al., 2006). Combined with other recent observation where follicles are observed to form around stem cells of non-germline origin (Couzin, 2005; Dyce et al., 2006; Johnson et al., 2005), which have never been shown to be fertilizable, it might not be that surprising that premeiotic germ cells would be sufficient to induce follicle formation.

References

Couzin, J. (2005). Stem cells. Another route to oocytes? Science *309*, 1983.

Dyce, P. W., Wen, L., and Li, J. (2006). In vitro germline potential of stem cells derived from fetal porcine skin. Nat Cell Biol *8*, 384-390.

Hubner, K., Fuhrmann, G., Christenson, L. K., Kehler, J., Reinbold, R., De La Fuente, R., Wood, J., Strauss, J. F., 3rd, Boiani, M., and Scholer, H. R. (2003). Derivation of oocytes from mouse embryonic stem cells. Science *300*, 1251-1256.

Johnson, J., Bagley, J., Skaznik-Wikiel, M., Lee, H. J., Adams, G. B., Niikura, Y., Tschudy, K. S., Tilly, J. C., Cortes, M. L., Forkert, R., *et al.* (2005). Oocyte generation in adult mammalian ovaries by putative germ cells in bone marrow and peripheral blood. Cell *122*, 303-315.

Kehler, J., Hubner, K., Garrett, S., and Scholer, H. R. (2005). Generating oocytes and sperm from embryonic stem cells. Semin Reprod Med *23*, 222-233.

Novak, I., Lightfoot, D. A., Wang, H., Eriksson, A., Mahdy, E., and Hoog, C. (2006). Mouse embryonic stem cells form follicle-like ovarian structures but do not progress through meiosis. Stem Cells.

Pittman, D. L., Cobb, J., Schimenti, K. J., Wilson, L. A., Cooper, D. M., Brignull, E., Handel, M. A., and Schimenti, J. C. (1998). Meiotic prophase arrest with failure of chromosome synapsis in mice deficient for Dmc1, a germline-specific RecA homolog. Mol Cell *1*, 697-705.

Yoshida, K., Kondoh, G., Matsuda, Y., Habu, T., Nishimune, Y., and Morita, T. (1998). The mouse RecA-like gene Dmc1 is required for homologous chromosome synapsis during meiosis. Mol Cell *1*, 707-718.

Appendix 2

Generation and Initial Characterization of a Doxycycline-inducible *Stra8* Mouse

Andrew E. Baltus, Ericka Anderson,
Mary L. Goodheart, and David C. Page

Author contributions:
AEB initiated and performed all experiments with the following support; MLG injected the ES cells into blastocysts. EA assisted with doxycycline treatment and measurement of body weights.

Introduction

The previously described characterization of the *Stra8* knockout demonstrated a requirement for *Stra8* during the transition from mitosis to meiosis in both male and female mice as well as a possible role in the regulation of spermatogonial stem cells. Because we know very little about the molecular function of *Stra8* and because its expression is very tightly regulated during both male and female germ cell development, we wanted to test the possibility that *Stra8* could, if mis-expressed, induce other cells within the animal to develop abnormally, or possibly even initiate meiosis. To test this, we generated a transgenic mouse in which *Stra8* could be induced by administration of doxycycline. Ectopic expression of *Stra8* results in a reversible wasting phenotype in adult animals and, depending on timing and dosage, disrupts embryonic development.

Results

Taking advantage of a preexisting ES cell line for generation of doxycycline-inducible mice (Hochedlinger et al., 2005), we inserted the full-length Stra8 cDNA into the targeting plasmid and co-transfected it and a vector encoding the FlpE recombinase into genetically modified ES cells such that the targeting vector would be inserted downstream of the *Collagen1A* (*Col1A*) locus as depicted in Figure 1A. Figure 1B shows the resulting structure of the *Col1A* locus following proper insertion. Additionally, these ES cells contain a gene encoding the rtTA transactivator under the ubiquitous Rosa26 promoter (Figure 2C). Cells carrying these two loci will constitutively generate rtTA, which in the presence of its cofactor doxycycline is sufficient to drive transcription of the *Stra8* gene from the *Col1A* locus (Figure 1). After transfection, 5 independent ES cell lines were isolated based on hygromyocin-resistance. DNA extracted from these cell lines was positive by PCR for proper insertion of the *Stra8*-containing plasmid into the *Col1A* locus (Figure 2).

Prior to blastocyst injection, we wanted to verify that the cells would function properly, and express *Stra8* from the *Col1A* locus. To test this, we added doxycycline to the ES cells and assayed by RT-PCR for induction of the Stra8 cDNA from the *Col1A* locus. Figure 3 shows the results of this RT-PCR analysis demonstrating that the two targeted ES cell lines have significantly induced *Stra8* expression when treated with doxycycline, whereas un-targeted ES cells did not. Based on these results, ES cells from these two lines were injected into blastocyts and chimeras were generated. Several high-percentage chimeras sired litters with offspring carrying both modified loci. Mice

Figure 1. Generation of the doxycycline-inducible *Stra8* ES cells. (A) The targeting event resulting in insertion of the doxycycline-inducible *Stra8* cDNA into the *Col1A* locus. (B) The resulting targeted *Col1A* locus. (C) The *Rosa26* locus from the same ES cells which produces the rtTA transactivator which, in the presence of doxycycline, will induce expression of the *Stra8* cDNA.

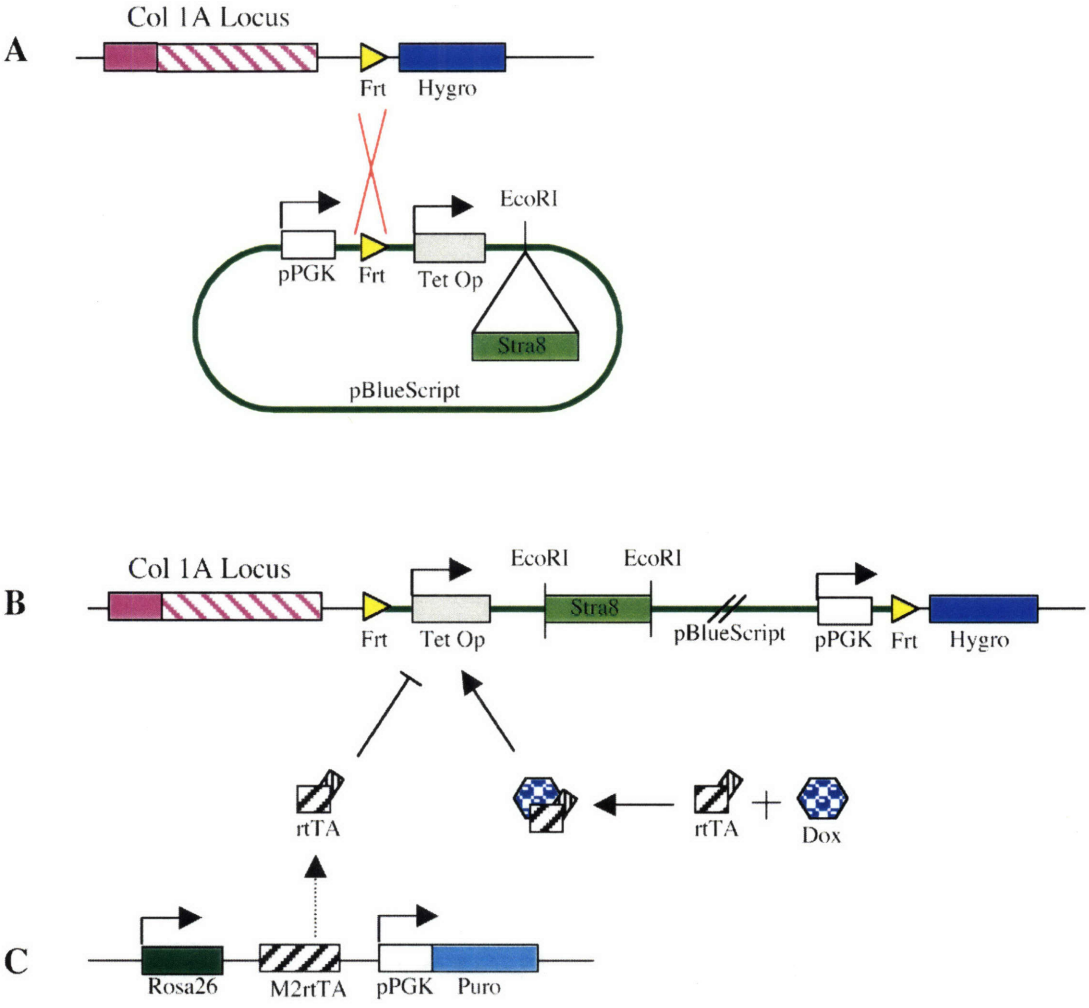
A
Col 1A Locus
Frt
Hygro
EcoRI
pPGK
Frt
Tet Op
Stra8
pBlueScript
B
Col 1A Locus
EcoRI
EcoRI
Frt
Tet Op
Stra8
pBlueScript
pPGK
Frt
Hygro
rtTA
rtTA
Dox
C
Rosa26
M2rtTA
pPGK
Puro

Figure 2. PCR analysis demonstrating proper targeting of the *Stra8* cDNA into the *Col1A* locus of two independent ES cell lines.

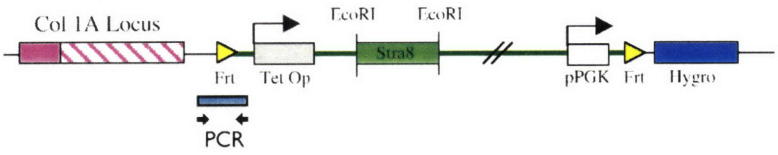
Col 1A Locus
EcoRI
EcoRI
Stra8
Frt
Tet Op
pPGK
Frt
Hygro
PCR

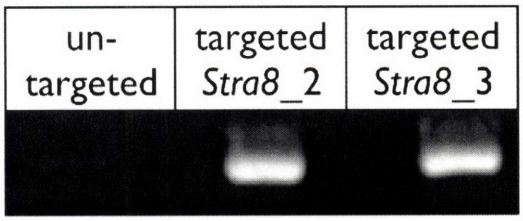
un-targeted
targeted Stra8_2
targeted Stra8_3

Figure 3. RT-PCR analysis demonstrating that the properly targeted ES cells respond to doxycycline by expressing the *Stra8* cDNA from the *Col1A* locus.

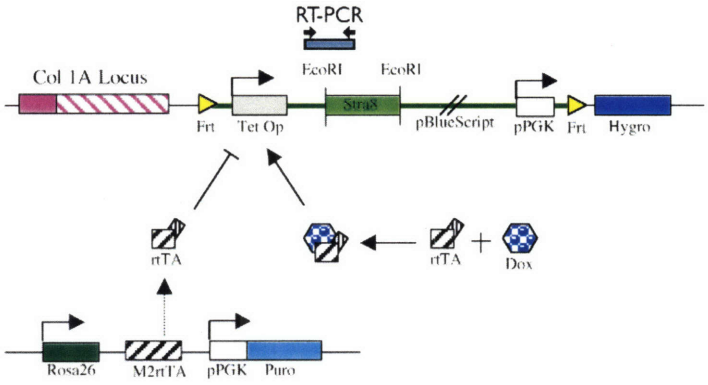

Cell line	un-targetted				*Stra8*_2				*Stra8*_3			
Dox	-		+		-		+		-		+	
RT	+	-	+	-	+	-	+	-	+	-	+	-
Stra8												
Actin												

H_2O	
Stra8	*Actin*

heterozygous or homozygous for both loci displayed no phenotype and sired normal sized litters.

The first experiment that we attempted was to turn on *Stra8* within the germ cells of embryonic male mice during the time that embryonic female germ cells express *Stra8* and enter meiosis. The hypothesis was to test if *Stra8* alone was sufficient to drive male germ cells into meiosis at this time. This was largely based on the idea that we do not know of any molecular difference between male and female germ cells prior to the induction of *Stra8* by retinoic acid in the embryonic ovary. Unfortunately, around this time our lab and the Jaenisch lab demonstrated that this doxycycline-inducible system could not induce transgenic expression within the germline. During these experiments, it became apparent that if the pregnant female carried both the modified *Col1A* and *Rosa26* loci that the pregnancy would be terminated even if the pups did not express *Stra8*. We then mated double homozygous males to wild-type females to observe specifically the effect of ectopic *Stra8* expression in the pups. The *Stra8*-positive pups only survived until birth, but looked grossly normal at this time. Pups that were exposed to doxycycline, but do not carry both loci, develop normally, indicating that doxycycline does not affect development of the mice at these times and dosages.

To address the possibility that Stra8 can function outside of the germline of an adult animal, we provided 4-8 week old adult mice carrying both targeted loci with water containing various concentrations of doxycycline between 200ug/ml and 5mg/ml. When adult animals carrying both loci are given doxycycline we observe a very severe wasting phenotype. The Stra8-induced animals demonstrate a significant loss of body mass (Figure 4) that begins within days of the initial treatment. Additionally, this loss of body

Figure 4. Measurements of body weight of doxycycline-inducible *Stra8* ectopic mice. Graphed as % starting body weight. Red lines indicate control animals. Black lines indicate doxycycline-inducible mice. Asterisks indicate lethality. The black dashed line marks the point at which doxycycline was removed and replaced from the diet. (A) Mice on 500μg/ml doxycycline. (B) Mice on 2mg/ml doxycycline. (C) Mice on 4mg/ml doxycycline.

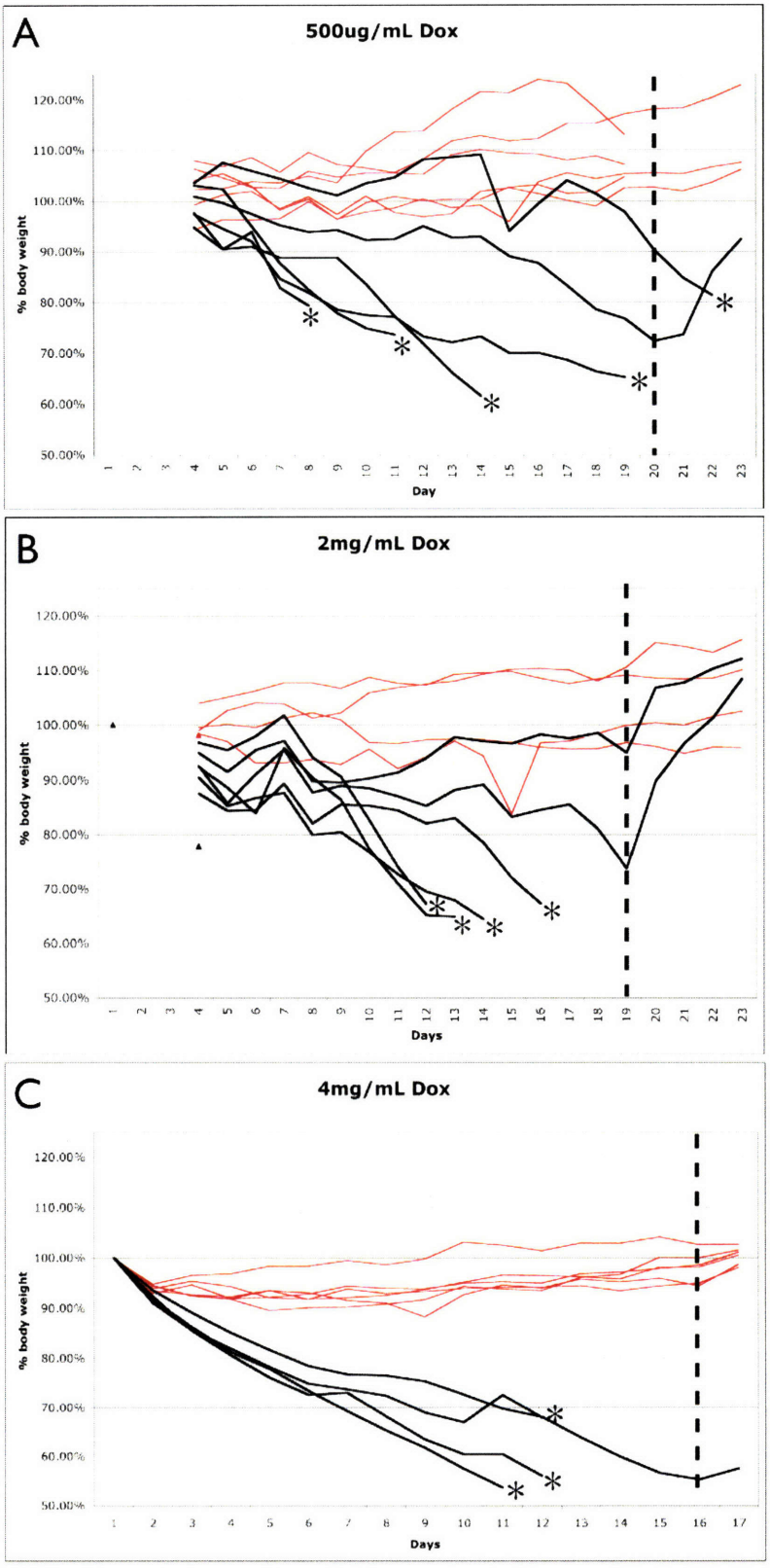
A
500ug/mL Dox
% body weight
120.00%
110.00%
100.00%
90.00%
80.00%
70.00%
60.00%
50.00%
1 2 3 4 5 6 7 8 9 10 11 12 13 14 15 16 17 18 19 20 21 22 23
Day
B
2mg/mL Dox
% body weight
120.00%
110.00%
100.00%
90.00%
80.00%
70.00%
60.00%
50.00%
1 2 3 4 5 6 7 8 9 10 11 12 13 14 15 16 17 18 19 20 21 22 23
Days
C
4mg/mL Dox
% body weight
120.00%
110.00%
100.00%
90.00%
80.00%
70.00%
60.00%
50.00%
1 2 3 4 5 6 7 8 9 10 11 12 13 14 15 16 17
Days

mass is completely reversible, such that an animal that may have lost more than 25% of its body mass will return to its normal body weight within 3-4 days if the doxycyline treatment is stopped (Figure 4). Many of the animals initially tested died during the treatment period. The point of death was not associated with a specific body weight or percentage loss of body mass, however, it usually occurred in mice that had lost more than 30% of body mass and were usually under 20g of total body mass. Additionally, the mice remained active and social during the duration of the experiment and did not demonstrate any signs of discomfort. It is also interesting to note that the rate at which body mass was lost appears to be dose dependent. Mice on lower dosages of doxycycline lost body mass more gradually than those on the higher dosages (Figure 4). We also observed greater lethality among animals that were homozygous at both loci compared to those that were heterozygous at one or both. It is also important to note that the time from initial dosage to the first lethality and the frequency of lethality did not appear to depend on dosage. This might indicate that the lethality may be distinct from the loss of body mass. Tissue samples from the treated animals do not appear histologically abnormal compared to non-*Stra8*-expressing cage-mates.

To address further the loss of body mass, we wanted to examine the effect of ectopic *Stra8* expression in older, larger transgenic animals. For this experiment, we used the high-percentage chimeras that founded the colony, which were over a year old. Additionally, we hoped that this chimeric analysis of ectopic mice might reveal a phenotype that would have been hard to observe otherwise (Hochedlinger et al., 2005). We placed 5 high-percentage (85-100%) chimeras on 4mg/ml doxycycline and monitored their body weight. As with the younger animals, they displayed significant loss of body

mass within the first few days (Figure 5). Most dropped 10-15% body weight, while one animal (the largest in the study, at 65g starting weight) dropped nearly 40% of his body weight. However, unlike the younger animals, the weight loss in these animals seemed to level out, showing little fluctuation in body weight over the remainder of a 3-month period on doxycycline. Additionally, we did not observe any lethality during this 3-month period. The only consistent morphological difference that we found in these mice compared to wild-type animals was reduced body fat, and enlarged hearts. The enlarged heart is histologically normal and appears to be the result of an increased heart rate, which itself may be a secondary effect. We occasionally observe a hunchback phenotype in the animals, which may indicate reduced or weakened muscle mass, as well as occasionally finding patches of balding skin. We are currently aging double homozygous animals so that we can repeat this experiment with larger numbers of animals so that we can determine which effects are most prevalent.

Figure 5. Measurement of body weight of doxycycline-inducible *Stra8* ectopic chimeras on 4mg/ml doxycycline. Graphed as body weight (top) and % of starting body weight (bottom).

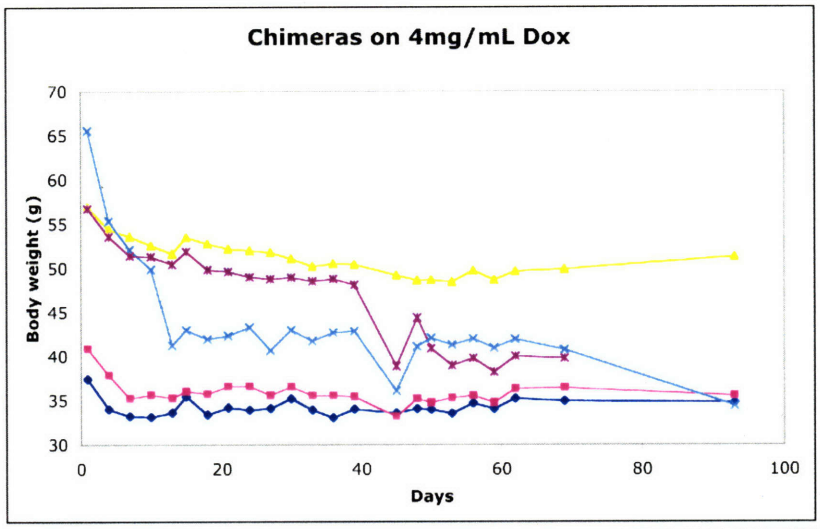
Chimeras on 4mg/mL Dox
Body weight (g)
70
65
60
55
50
45
40
35
30
0
20
40
60
80
100
Days

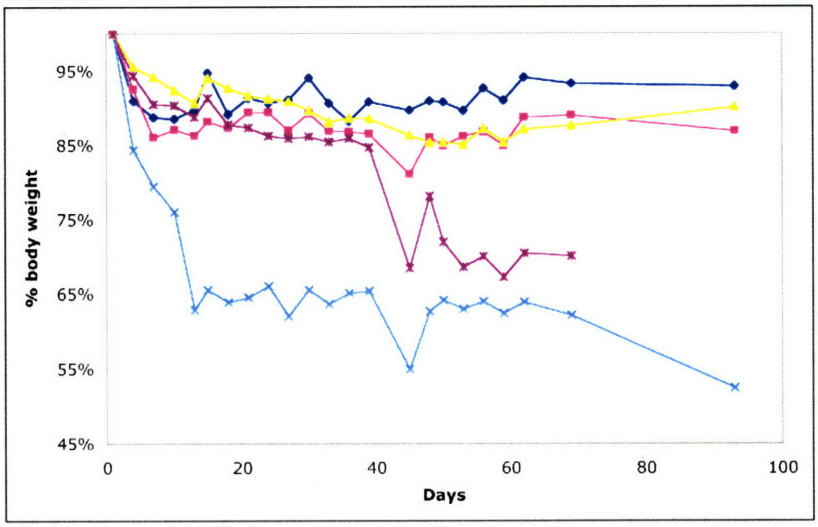
% body weight
95%
85%
75%
65%
55%
45%
0
20
40
60
80
100
Days

Discussion and future directions

These observations demonstrate that ectopic expression of *Stra8* is capable of perturbing non-germ cell functions of both embryonic and adult mice. Because the phenotype of *Stra8*-ectopic adult animals appears to be metabolic and because we have not found any specific organ damage by histology, it may prove difficult to determine in what cells *Stra8* is functioning in the doxycycline-inducible mice. We find it particularly interesting that the wasting appears to be completely reversible upon removal of doxycycline from the animals' diet. This suggests that the *Stra8*-dependent perturbation does not permanently damage the cells in which it is acting. This again demonstrates how difficult it may be to determine the site of function, but the fact that we observe mostly a weight-loss phenotype which appears to be, at least initially, restricted to the fat merits further analysis.

Future experiments will include observing larger numbers of animals on doxycycline and having experts in specific organ pathology examine the tissues from these mice, in the hope that they will see something that we have not. Additionally, follow-up experiments on the embryonic lethality of ectopic *Stra8* expression may help to determine which specific tissues are affected and may also direct our analysis in the adult. However, it is equally likely that different tissues are being affected in the embryonic and adult animals.

Reference

Hochedlinger, K., Yamada, Y., Beard, C., and Jaenisch, R. (2005). Ectopic expression of Oct-4 blocks progenitor-cell differentiation and causes dysplasia in epithelial tissues. *Cell* 121, p465-77.